UNIVERSITY OF OKLAHOMA

GRADUATE COLLEGE

IMPROVING THE QUALITY OF LAMINATES IN LIQUID COMPOSITE MOLDING USING MAGNETIC COMPACTION: EXPERIMENTS AND PROCESS MODEL

A DISSERTATION

SUBMITTED TO THE GRADUATE FACULTY

in partial fulfillment of the requirements for the

Degree of

DOCTOR OF PHILOSOPHY

By

MEHRAD AMIRKHOSRAVI
Norman, Oklahoma
2019

IMPROVING THE QUALITY OF LAMINATES IN LIQUID COMPOSITE MOLDING USING MAGNETIC COMPACTION: EXPERIMENTS AND PROCESS MODEL

A DISSERTATION APPROVED FOR THE
SCHOOL OF AEROSPACE AND MECHANICAL ENGINEERING

BY

Dr. M. Cengiz Altan, Chair

Dr. Zahed Siddique

Dr. Mrinal C. Saha

Dr. Yingtao Liu

Dr. Shivakumar Raman

Dedicated to

My beloved and gorgeous wife, Maya

My wonderful mother, Majera

Acknowledgments

I would like to express my deepest thanks and appreciation for my advisor, Prof. M. Cengiz Altan for his consistent support, invaluable mentorship, and insightful advice throughout my PhD career. I would also like to thank all members of my committee, Prof. Shivakumar Raman, Prof. Zahed Siddique, Prof. Mrinal C. Saha, and Prof. Yingtao Liu, for all their support and encouragement.

I am grateful for the financial support of Graduate Research Assistantship provided by Prof. M. Cengiz Altan, Jim and Bee Close scholarship, and the Gallogly College of Engineering Dissertation Excellence Award. I would also like to thank all the staff and professors from the School of Aerospace and Mechanical Engineering who have contributed to this work directly or indirectly.

I would also like to express my thanks and appreciation to former lab members, particularly Drs. Maya Pishvar, M. Akif Yalcinkaya, Youssef K. Hamidi, and Gorkem E. Guloglu for all the collaborations and help they provided. My gratefulness extends to my friends for giving me a lot of help and emotional support throughout my studies.

Also, I would like to thank my mother, Nazanin (Majera) Akhavan Deilami, my brother, Sina Amirkhosravi, and the rest of my family for all the unconditional love and support they have given me. I appreciate the many sacrifices my mother has made to enable me to achieve this goal. I also want to take this chance to thank my deceased father, Mehrdad Amirkhosravi, who I wish could be here to share this accomplishment. I greatly appreciate my parent in-laws (Hossein Pishvar and Kobra Ghamkhari Tarigheh) for their endless support of my endeavors.

Most importantly, I would like to express my gratitude to my beloved wife, Maya Pishvar, a soul mate in my life who understands me more than anyone else. She has made my life vibrant and fruitful. Without her unending love, encouragement, and support, the completion of this dissertation would not have been possible. I have been so lucky to have her accompany me through this journey, fulfilling the goals we have set.

Table of Contents

List of Tables

List of Figures

Abstract

Despite the extensive use of liquid composite molding (LCM) processes such as wet lay-up vacuum bagging (WLVB) and vacuum assisted resin transfer molding (VARTM) in composite manufacturing, they have two major drawbacks. First, the fiber volume fraction of the composite parts made by LCM is lower than those made under an elevated pressure using either autoclave or hot press, leading to lower mechanical properties. Second, the process induced defects in LCM parts are quite high, which may significantly reduce the mechanical performance and environmental durability of composites. The focus of this dissertation is to tackle the important problems encountered with WLVB and VARTM to improve the quality of molded parts.

The first part of this dissertation introduces a novel technique, magnet assisted composite manufacturing (MACM), to improve the quality of WLVB laminates. In this technique, the composite lay-up is sandwiched between a magnetic tool plate and a set of Neodymium-Iron-Boron (NdFeB) permanent magnets during cure. The details and effectiveness of MACM process are investigated by fabricating of E-glass/epoxy composite laminates with and without magnetic pressure and comparing their void content and morphology, fiber volume fraction, and mechanical properties. The results clearly show that the quality of composite laminates is significantly improved in the presence of magnetic consolidation pressure, where the fiber volume fraction increases by more than 50% to almost 30% and process-induced voids decrease to less than 3%. As a result, the flexural strength and modulus of the parts are enhanced by approximately 60% and 50% to ~245 MPa and ~10 GPa, respectively.

The second part of the dissertation extends the application of the MACM technique to fabricate high-quality VARTM laminates. In VARTM, unlike the WLVB process, the preform impregnation takes place under vacuum, which results in different mechanisms of void formation and different ranges of fiber content. Thus, enhancing VARTM is quite different than enhancing the WLVB process which provides the motivation to investigate the effectiveness of utilizing MACM in VARTM. In this regard, thin (i.e. 6-ply), as well as moderately thick (i.e. 12- and 18-ply) E-glass/epoxy laminates are fabricated by applying MACM either before or after infusion. The results prove the effectiveness of MACM in fabricating high-quality VARTM laminates where a fiber volume fraction of more than 50% and void content of less than 1% is achieved. In addition, a transient magnetic consolidation model is developed, predicting the final thickness and fiber volume fraction of the VARTM/MACM parts.

The third part of this dissertation introduces a novel technique of compacting dry fibrous reinforcement to control the resin flow rate, thus eliminating the void formation in VARTM parts. In this technique, the fibrous preform is compacted by either stationary or moving magnets prior to resin infusion. As a result, the pore size between the fabric layers and permeability are reduced, and the filling rate of resin into preform decreases. The results show that in the absence of magnetic pressure, the void content could be up to 5.7%, much higher than 0.1-0.8% voids in the laminates made by 0.2 MPa magnetic compaction. In addition, moving magnets with a smaller footprint over a larger vacuum bag surface is a feasible approach to apply compaction pressure on medium to large parts, thus dramatically decreasing their void content to below 1%.

CHAPTER 1. Introduction

1.1. Motivation

Fiber reinforced polymer (FRP) composites have been extensively used in a wide variety of applications, ranging from aircraft components [1-3] to automotive parts [4, 5] to even sporting goods [6] due to their high specific strength and modulus. Although a number of molding processes for manufacturing FRP composites are well-established, these processes can still be improved by either reducing the production cost or by increasing the quality and properties of the molded parts. Among these processes, wet lay-up/vacuum bagging (WLVB) and vacuum assisted resin transfer molding (VARTM) are two common, liquid composite molding techniques for manufacturing medium to large composite products at low cost. The following sections explain the advantages and drawbacks associated with WLVB and VARTM and review the processing techniques proposed in the literature for improving the quality of WLVB and VARTM laminates.

1.2. Fabrication of High-Quality Wet Lay-up Vacuum Bag (WLVB) Composite Laminates

Wet lay-up/vacuum bagging (WLVB) is the simplest method for manufacturing of a wide variety of FRP composite parts from small to very large. The easy processing and cost-effectiveness of wet lay-up process in the fabrication of large and complex parts have led this method to be extensively used in the manufacture and repair of civil infrastructure, aerospace structures, wind turbine blades, marine hulls, bridge decks, and housing components [7-17]. In WLVB process, plies of the dry fibrous preform are laid on the mold, layer by layer at a time, then liquid resin is introduced to each individual

layer by hand. Usually, rollers and brushes are used to enhance the wetting and reduce possible air pockets trapped inside the preform. The vacuum bag is placed over the lay-up and sealed to the mold. Finally, the vacuum is drawn to remove excess resin and air trapped between the layers.

Despite the advantages and widespread use of WLVB processes for the manufacture and repair of medium to large parts, the maximum consolidation pressure in this process is limited to the atmospheric pressure (i.e. 0.1 MPa). This low consolidation pressure generated by the vacuum leads to composite parts with a lower fiber volume fraction and higher void content compared to those fabricated under higher pressure (i.e. 0.2-0.7 MPa) [18]. It is also well established that the low fiber volume fraction leads to lower mechanical properties of the fabricated composite laminates. At the same time, the presence of the voids in the parts may cause premature failure and reduce the mechanical performance of the composites. Therefore, the structural performance and load carrying capability of the parts fabricated or repaired by WLVB need to be improved.

To improve the quality of laminates made by WLVB process, several studies have proposed different ways of applying external pressure on the vacuum bag lay-up. For example, Abraham et al. [18] used an autoclave to apply high consolidation pressure (i.e. 1.2 MPa) on the wet lay-up vacuum bag to fabricate high-quality E-glass/epoxy laminates. They reported that by applying autoclave pressure the high-quality laminates with a high fiber volume fraction (~64%) and low void content (~1.6%) were fabricated. Francucci et al. [19] also demonstrated when a consolidation pressure of 1.26 MPa is applied by a hydraulic press on the wet lay-up vacuum bag, the

fiber volume fraction of flax/epoxy laminates can be improved by 37% to almost 60% compared to the parts made by WLVB process without external pressure. They also reported that in the presence of external pressure, the surface porosity of the parts decreased by 90% from 29.5 to 3.2%. Although autoclave and hot press can significantly enhance the quality of WLVB laminates, these processes require high capital investment and energy consumption. Therefore, the composite industry often faces a trade-off between the quality of composite parts and production costs. In addition, the size of the autoclave chamber and hydraulic press limit the size of the fabricated parts, thus preventing the broader use of these methods. Therefore, the development of alternative, low-cost techniques to apply high consolidation pressure for manufacturing large composite parts is of particular interest to the composite community.

In this dissertation, the magnet assisted composite manufacturing (MACM) technique is introduced to improve the quality of WLVB laminates. In this technique, Neodymium Iron Boron (NdFeB) permanent magnets are used to produce sufficiently high consolidation pressure in WLVB process. The NdFeB magnets are low-cost, light-weight, and available in various shapes (i.e. such as disk, cylinder, sphere, block, rings, donuts). For example, $2.54 \times 2.54 \times 1.27$ cm^3, N52-NdFeB magnet is only 60 g and can generate up to 0.6 MPa compaction pressure. The NdFeB magnets are also durable such that they only lose 2% of their magnetic properties after 10 years of service. In addition to these significant properties, using permanent magnets as a source of external pressure offers unique processing capabilities where one can apply non-uniform and local compaction pressure at any time during the fabrication of composite materials.

1.3. Fabrication of High-Quality Vacuum Assisted Resin Transfer Molding (VARTM) Composite Laminates

Vacuum assisted resin transfer molding (VARTM) is one of the most commonly practiced manufacturing processes for composites due to relatively simple tooling and equipment, and thus, low production cost. In VARTM, unlike WLVB process, the resin is infused into the reinforcing material under vacuum. The VARTM is a cleaner and safer molding process than WLVB because it reduces the worker contact with liquid resin and produces less resin waste. In addition, the resin infusion under vacuum makes the VARTM process less labor-intensive compared to the WLVB. As a result, although more complicated tooling is required, VARTM is often preferred to produce higher quality, large composite parts. However, despite extensive use of VARTM process in the energy, marine, and infrastructure industries [20-22], this process has some major drawbacks. First, the fiber volume fractions of VARTM laminates are still lower than that in the parts made by autoclave and resin transfer molding processes because the consolidation pressure in conventional VARTM is limited to the atmospheric pressure (i.e. 0.1 MPa) [18, 23]. Second, the VARTM process induces non-uniformity in the thickness and fiber volume fraction of laminates, leading to spatial variations in laminate properties. These variations are due to non-uniform resin pressure from inlet to outlet during infusion and thus different levels of compaction along with the composite lay-up [24-28]. Third, resin flow during impregnation causes flow-induced defects such as voids in the final part. It is well-known that the presence of voids significantly deteriorates the mechanical performance and environmental durability of composite materials. Fourth, long filling time in conventional VARTM processes due to low

injection pressure of 0.1 MPa (i.e. vacuum pressure) is of great concern for the fabrication of large composite parts. Therefore, fabricating high-quality, large VARTM laminates with enhanced mechanical properties is clearly of interest for various industrial applications. Accordingly, several variants of the VARTM process are developed to overcome the shortcomings of conventional VARTM.

To this end, the focus of several studies was on developing new techniques to improve the infusion time of VARTM process [29-32]. For example, Seemann Composites Resin Infusion Molding Process (SCRIMP) [33] is developed to reduce the filling time of the VARTM process by placing the distribution medium on the stack of fiber reinforcement. However, the presence of a distribution medium on the preforms in SCRIMP process adversely affects the surface quality of the composite part. Fast Remotely Actuated Channeling (FASTRAC) [34] process is also developed to improve the resin infusion process and reduce the filling time. In FASTRAC, a specific double vacuum bag along with non-contact tooling are used to create distribution flow paths for increasing the filling rate. In addition, the surface quality of the laminate is better than the SCRIMP laminates since there is no direct contact between the tooling and the surface of the laminate. Although SCRIMP and FASTRAC mostly solve the slow filling of VARTM process, the consolidation pressure in both processes is limited to the atmospheric pressure (i.e. 0.1 MPa), resulting in a composite part with low fiber volume fraction and high void content.

In the literature, there are also several studies on the use of additional external pressure to improve the quality of VARTM laminates. For example, vacuum enhanced resin infusion technology (VERITy) technique is developed by Verma et al. [35] in

which the additional external pressure is applied on the VARTM lay-up in an autoclave. The laminates made by VERITy method resulted in the fiber volume fraction of more than 60% and void content of less than 2%. Garofalo et al. also developed another technique that applied external pressure on the VARTM lay-up using a press instead of the autoclave. This technique was named specialized elastomeric tooling for resin infusion (SETRI) [36]. The results showed that the SETRI method was capable of fabricating high-quality VARTM laminates with almost 70% fiber volume fraction and less than 1% void content. However, autoclave and hot press are costly pieces of equipment and are very expensive to operate and maintain which altogether increase the final cost per cured part. In another study, Yalcinkaya et al. [37] modified a conventional VARTM process by external pressurization of heated mold. The results demonstrated that the quality of VARTM laminates was considerably improved using a pressurized VARTM where the fiber volume fraction was more than 60% and void content was less than 1%. Recently, Yalcinkaya et al. [38] developed a novel manufacturing technique, Pressurized Infusion (PI), to address the mentioned shortcomings of VARTM process altogether. In PI molding, excessive external pressure is applied on the vacuum bag lay-up using the air pressure chamber, improving the quality of composite laminate. In addition, the injection takes place at a higher pressure than conventional VARTM to reduce the mold filling time. They showed that by pressurizing the inlet reservoir (i.e. up to 0.2 MPa), the fill time decreased by almost 50%. Despite the advantages of PI molding, the application of this method for fabrication of large composite parts requires more complicated tooling (i.e. pressure chamber and pressurized reservoir) than conventional VARTM.

However, conducting experiments to understand the relationship between important processing parameters and quality of fabricated parts, may be very time consuming and costly. For this reason, the modeling of the filling and post-filling stage in liquid composite molding processes has been the focus of many research efforts over the last few decades and considerable progress has been made [39-47]. Depending on the edge constraints and dimension ratio, resin flow can take place in different directions. It can be parallel, normal, or both parallel and normal to the laminate plate as shown in Fig. 1 [48]. In all models, the resin flow is caused by vacuum pressure, positive injection pressure, and/or a possible compression force. Several studies modeled the resin flow based on consolidation theory and flow through a porous medium [49-51]. The consolidation theory was first introduced in 1920s by Terzaghi [52] in soil mechanics and was used in the composite field by Gutowski et al. [50] and Dave et al. [51] later in 1980s. According to the consolidation theory, the total applied force on the porous medium is carried by the hydrostatic force due to resin pressure and spring-like force of the fiber reinforcement. However, some previous studies assume that the total applied force is just carried by resin [53, 54]. Loos and Springer conducted one of those studies in which they simulated one-dimensional consolidation and resin flow without considering the elastic effects of fibers [49]. In all the mentioned studies a constant compression force is considered to cause resin flow. However, the magnetic force used in the MACM technique depends exponentially on the laminate thickness. Therefore, a transient consolidation model that can predict the final thickness and fiber volume fraction of laminate under magnetic compaction pressure can be of interest for broader use of the MACM technique.

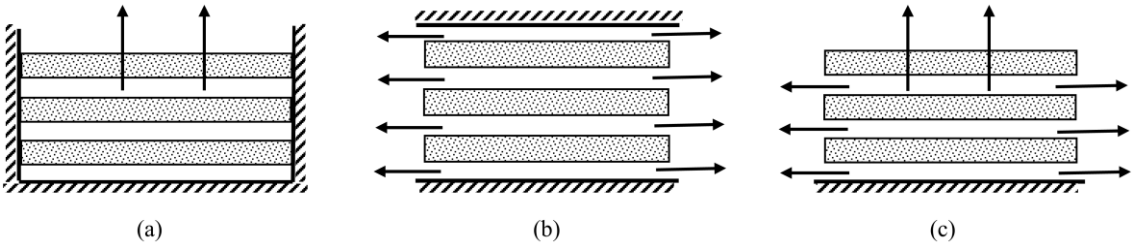

Figure 1. (a) 1-D resin flow normal to the laminate plate, (b) 1-D resin flow parallel to the laminate plate, and (c) 2-D resin flow both parallel and normal to the laminate plate.

In this dissertation, the use of MACM technique to fabricate high-quality VARTM laminates is investigated. It is also shown that using permanent magnets as a source of external pressure results in the flexibility of applying external pressure at different times in VARTM, i.e. either before or after infusion, each of which offers unique processing advantages. In addition, a transient consolidation model is developed which allows for the prediction of the temporal changes in magnetic consolidation pressure, laminate thickness, and thus the fiber volume fraction. The consolidation model is then used to investigate the effect of different process parameters such as the magnet type, resin viscosity, and fabric type on the final laminate thickness and fiber volume fraction.

1.4. Reduction of Voids in Medium to Large VARTM Parts by Magnetic Compaction of Dry Preforms

As mentioned earlier, VARTM process is widely used for the fabrication of medium to large, complex composite parts, mainly due to the ease of the process and lower tooling cost. However, the process induced defects in the VARTM process is one remaining challenge, limiting the wider use of this process. Among all the defects identified in VARTM, voids are the most common ones. Voids, i.e. air bubbles inside

the composite, range from a few microns to several hundred microns and are formed as a result of an imperfection in the manufacturing process.

It is well established that the presence of voids, even in small amounts, is detrimental to the mechanical behavior of fiber reinforced polymer composites [55-65]. These adverse effects would be even more pronounced in the matrix-dominated properties such as compressive strength [66-70], interlaminar shear strength [71-75], and fatigue tolerance [76-78]. For example, Tang et al. [48] reported that by increasing void content from 5% to 12% the longitudinal compressive strength of T300/976 laminates reduced by 43%. Liu et al. [79] found that increased void volume fraction from 0.6% to 3.1% in T700/TDE85 carbon fiber reinforced epoxy laminates caused approximately 40% reduction in interlaminar shear strength. In another study, it was shown that with every 1% increase in void content of flax/epoxy laminates the interlaminar shear strength was reduced by 11.2% [80]. Sisodia et al. [57] investigated the effect of voids on fatigue behavior of carbon fiber and found that for the laminates with 0.8-5% void content, the fatigue life degraded by two orders of magnitude. They also reported that the fatigue life of the laminates with 20% void content degraded even more, i.e. by three orders of magnitude. Moreover, on one hand, voids have effects on hygrothermal properties of FRP composites and on the other hand, the hygrothermal conditioning in the presence of voids have even more detrimental effects on mechanical performance. For instance, it is reported in a number of studies that the rate and equilibrium level of moisture absorption depend on the void content of the composite laminate [81, 82]. Moreover, according to the literature, the moisture inside the FRP composites adversely affects their mechanical performance possibly due to the matrix

plasticization or fiber/resin interface degradation [83-85]. For instance, Allred [86] investigated the effect of temperature and moisture content on the mechanical properties of kevlar/epoxy laminates. He observed that the flexural strength of saturated laminates was 35-40% lower than dry laminates at 21 ℃. He also reported the higher strength loss of 60-70% for the saturated specimens at a higher temperature of 150 ℃ compared to dry specimens. Therefore, to produce reliable composite parts with long service life, it is of great importance to avoid the formation of voids during fabrication.

In VARTM, voids are formed primarily during resin mixing, fiber impregnation, and the curing stage by various reasons: non-uniform distribution of permeability in the fiber tows and spaces in between the fiber tows, absorbed moisture, volatiles expelled during cure, and leakage in the sealing of the mold [21, 87-89]. In addition, the filling rate plays an important role in the formation of voids. For instance, it is observed that the fast filling in the fabrication of random mat composites increases the risk of void entrapment [90]. In contrast, very slow impregnation of fabric may cause incomplete mold filling, resulting in the formation of voids and dry spots. Therefore, controlling the resin flow rate during infusion can be helpful in the reduction or total elimination of voids in the VARTM composites [91, 92].

The formation and removal of voids have been studied for a number of years, leading to several well-understood void formation phenomena governed by the resin flow [93-97]. In this regard, many researchers introduce different processing techniques to control the filling rate for the fabrication of VARTM laminates with low void contents (i.e. <1%). These processing techniques include using localized induction heating [98-102], vacuum-induced preform relaxation (VIPR) process [103, 104],

pressure difference control [105], dual pressure controlled and heated VARTM [106]. Among these techniques, Johnson et al. [98] used induction heating to reduce the resin viscosity at localized low permeability regions of preforms, thus achieving complete and void-free preform saturation. Bender et al. [105] monitored the pressure difference between inlet and outlet to control the resin flow rate. They used a fuzzy logic controller to receive feedback from the weight of infused resin or flow position sensors for adjusting the pressure difference. Alms et al. [104] used VIPR process to manipulate the filling pattern using a relatively small vacuum chamber placed and sealed on top of the vacuum bag lay-up. Kedari et al. [106] utilized a dual pressure control setup to separately control the injection and vent pressure in the VARTM process. They also reported that having high mold temperature, reduced inlet pressure, and high vacuum led to the VARTM parts with low void content. However, due to the additional tooling complexity as well as processing limitation inherent in the abovementioned techniques, there is still a need for the development of new techniques for controlling the flow rate in the VARTM process.

In this dissertation, an innovative technique of using magnetic compaction for reducing the process induced voids in the VARTM process is introduced. This technique involves manipulation of the preform permeability and controlling the resin flow rate through magnetic compaction of fibrous preform before resin infusion. The compaction of the fabrics was performed by placing a set of Neodymium Iron Boron (NdFeB) permanent magnets on a vacuum bag lay-up. It is important to emphasize that the magnets were removed after the compaction was achieved, and thus the infusion took place without any external compaction pressure. In addition to stationary

placement of permanent magnets on the lay-up, sliding a set of magnets over the vacuum bag is explored for the fabrication of much larger parts.

1.5. Outline of the Dissertation

This dissertation constitutes a comprehensive study for developing innovative manufacturing techniques to improve the quality of FRP composites made by liquid composite molding such as wet lay-up vacuum bagging and vacuum assisted resin transfer molding. The novel, robust, and cost-effective manufacturing techniques outlined in this dissertation focus on the use of compaction pressures generated by high-power, permanent magnets.

In chapter 2, a novel fabrication method, magnet assisted composite manufacturing (MACM), for enhancing the quality of wet lay-up vacuum bag laminates is described. In this chapter, the application of MACM technique for improving the WLVB process is examined through the fabrication of 6-ply random mat E-glass/epoxy laminates. In this regard, the lay-up sealed by the vacuum bag is sandwiched between NdFeB magnets and a magnetic tool plate. The mechanical properties, void and fiber volume fractions, and the composite microstructure of the parts made with and without magnetic compaction are compared with each other. In addition, the effect of time and duration of applying magnetic pressure on the quality of laminates are investigated.

Chapter 3 extends the use of MACM technique in vacuum assisted resin transfer molding (VARTM) processes. This chapter discusses the effectiveness of MACM to fabricate high-quality VARTM laminates using both experimental and modeling approaches. Furthermore, the effects of applying magnetic compaction after or before infusion on the filling time and overall quality of final parts are investigated. In this

chapter, a variety of fabrication scenarios is used to evaluate the performance of MACM for thin (6 plies) as well as moderately thick (12 and 18 plies) VARTM laminates. In the modeling section of this chapter, a transient consolidation model that can predict the time-dependent magnetic pressure applied on the laminate, as well as the changes in resin pressure, laminate thickness, and fiber volume fraction during fabrication is developed, and the values obtained are compared with the experimental results. The consolidation model is then used to demonstrate the effects of critical process parameters such as the magnet type, resin viscosity, and fabric type on the evolution of laminate thickness.

Chapter 4 further explores the effectiveness of using magnetic compaction pressure to substantially reduce the process-induced voids in VARTM laminates. In this technique, the compaction pressure is applied on the dry fibrous preform using different sets of permanent magnets. Subsequently, magnets are removed, and infusion takes place into the compacted lay-up. In this chapter, the effectiveness of using either stationary or moving magnets for the fabrication of small to large parts is investigated. Furthermore, the performance of the proposed method for fabrication of thin (6 plies) as well as moderately thick (12 and 18 plies) E-glass/epoxy laminates is studied. Finally, the experimental results including void and fiber content, microstructural analysis, and flexural properties of the laminates manufactured by the proposed technique are presented and compared with those obtained from laminates cured by conventional VARTM.

CHAPTER 2. Improving Laminate Quality in Wet Lay-up/Vacuum Bag Processes by Magnet Assisted Composite Manufacturing (MACM)

A novel method, Magnet Assisted Composite Manufacturing (MACM), which utilizes a magnetic compressive pressure, is proposed to improve laminate quality in wet lay-up/vacuum bag (WLVB) processes. This paper first describes the salient features of MACM/WLVB process, and then demonstrates the effectiveness of this process by investigating the void content and mechanical properties of random mat E-glass/epoxy composite laminates. During cure, high-power, N52 Neodymium permanent magnets are placed on the vacuum bag to apply sufficiently high consolidation pressure. Thus, laminate quality successfully improved such that fiber volume fraction increased more than 55% from 17% to 27% and void content decreased by 53% to under 2% compared to the laminates made without magnetic pressure. The flexural strength and modulus were also substantially improved by 60% and 46% to 253.5 MPa and 9.9 GPa, respectively. The effect of time and duration of applying magnetic pressure on the quality of the part were also investigated. The lowest void content of under 2% and 21% increase in fiber volume fraction were observed by only applying magnetic pressure 15 min at the start of the vacuum in WLVB process.

2.1. Introduction

The widespread use of fiber reinforced polymer (FRP) composites in marine, automotive, defense, energy, and other industrial applications comes from their high specific strength and stiffness. However, a major challenge associated with the composite materials is to reduce the manufacturing and tooling cost while minimizing

microstructural defects and achieving high structural quality, thus leading longer service life. Despite the availability of various manufacturing options, the cost effectiveness of the wet lay-up process for large structural parts has led this method to be extensively used in the marine industry [107-109], automotive industry [110, 111], repair of aerospace structures [112, 113], and strengthening and retrofitting of the civil infrastructure [114, 115]. In this process, plies of a fibrous mat or preform, wetted by a liquid resin, are applied manually on the mold until the desired laminate thickness is achieved. The impregnation of the fabric is usually carried out by rollers to enhance the wetting and to reduce possible air pockets trapped inside the fiber tows. The extensive use of the wet lay-up process results from the low cost of raw materials, minimal tooling cost, and ease of application. However, the emission of volatiles may be a concern in such open-mold processes [116, 117]. Another limitation of this method is the low fiber volume fraction and high void content that lead to the lower mechanical properties compared to the laminates fabricated in autoclaves or by closed-mold processes [118, 119]. The wet lay-up process with the addition of vacuum bagging can prevent the emission of volatiles and also produce better quality parts under vacuum pressure up to 0.1 MPa [120].

Wet lay-up/vacuum bag (WLVB) process is also widely utilized in repairing composite structures used in aerospace, marine, and energy industries. In common scarf repairs, the WLVB is often used to apply the vacuum bag pressure that helps bond the repair patch to the surface of the damaged component. However, in most cases, the mechanical properties of the repair patch are significantly lower than the original undamaged part, primarily due to the inability to apply sufficiently high pressure during

cure. Thus, extra plies are added to the patch to reach the desired structural stiffness and load carrying capability [121]. However, increasing the thickness of the repair patch enhances its bending stiffness which may cause premature failure at the edges of repair under high bending loads [122]. The properties and the quality of the repair patch can be improved by increasing the fiber volume fraction and reducing the void content which may be possible by applying the magnet assisted composite manufacturing as described in this chapter.

The maximum compaction pressure applied by vacuum in WLVB process is 0.1 MPa, which results in a fiber volume fraction far below the levels achievable under a higher pressure, and a high void volume fraction, possibly 10% or higher [123]. Specifically, non-woven fabrics that are mostly used in WLVB applications have lower planar density compared to other types such as woven and multi-axial warp knitted fabrics, which leads to low fiber volume fraction of 14 to 30% in the laminates [124, 125]. Also, environmental conditions such as high humidity and thermal cycling may adversely affect the durability of composites made by WLVB due to high void content [126]. Stringer [17] demonstrated that by only using a vacuum bag, a minimum void volume fraction of 1.5 to 1.7% could be achieved if the vacuum is applied when the resin viscosity is between 7.5 and 16.5 Pa s. Regardless of the resin type, a higher void content is observed when the viscosity is outside of this optimal range. Abraham et al. [18] reported significant improvement of properties when the WLBV assembly is placed in an autoclave and 1.2 MPa consolidation pressure is applied before cure. This high level of consolidation pressure was shown to yield a low cured-ply thickness of 0.116 mm for 12-ply plain weave E-glass fabric and result in a

high fiber volume fraction of 63.9% at a relatively low void volume fraction of 1.57%. Nevertheless, autoclaves are usually large and expensive pieces of equipment. In addition, most autoclaves are labor intensive to operate and consume excessive energy, particularly during long cure cycles [127], and thus leading to a higher cost per cured part.

Accordingly, a cost-effective, robust method to apply sufficiently high compaction pressure during WLVB process will likely yield significant benefits, and possibly lead to increased use of composites. Towards this goal, Ziegenbein and Colton [128] proposed utilization of a magnetic clamping device to apply consolidation pressure to the composite laminates. The electromagnets used in this device apply clamping pressure on a rubber membrane containing iron particles. The maximum achievable compression pressure was reported to be 0.1 MPa using actively cooled electromagnets, which is not high enough to sufficiently consolidate laminates. Moreover, the performance of this device to fabricate composite laminates was not evaluated.

Utilizing high-power permanent magnets to generate the necessary consolidation pressure during WLVB process can be a feasible solution. Using permanent magnets has additional benefits such as low operating cost without any cooling needs. Strong permanent magnetic materials that can generate high compressive pressure include Neodymium Iron Boron (also known as NdFeB), SmCo, Alnico, Ceramic (Ferrite), and Flexible (Rubber). Neodymium Iron Boron magnets, first developed in 1982 by General Motors and Sumitomo Special Metals, are the strongest permanent magnets

commercially available with the highest energy products of 160-400 kJ/m^3 and maximum compressive pressure of 0.8 MPa [129].

In this chapter, an innovative manufacturing technique, magnet assisted composite manufacturing (MACM), is introduced for improving the WLVB process. This method does not require complicated tooling for fabrication and may be easily adopted by the composites industry. The application of MACM to enhance WLVB is validated by fabricating 6-ply, E-glass/epoxy laminates which are placed between the NdFeB magnets and a ferrous tool plate, and compacted by the magnetic force during cure. The void content and morphology, fiber volume fraction, and flexural properties of the laminates produced by MACM/WLVB are compared with the properties obtained without the magnetic compression.

The favorable results presented in this chapter demonstrate the feasiblity of using magnetic compaction to apply tailored, spatially nonuniform pressure on composite laminates to improve their properties and quality. By using MACM, it is possible to fabricate much larger parts and compact curved surfaces by slowly moving the magnets over the vacuum bag with minimal tooling and cost. These extensions, as well as other applications of MACM in conjunction with VARTM and autoclave cure at elevated temperatures, will be addressed in subsequent studies.

2.2. Materials and Experimental Details

2.2.1. Neodymium Permanent Magnets

A set of N52 Neodymium magnets, the strongest permanent magnets commercially available, was used to apply consolidation pressure transverse to the composite laminate. Block-shaped N52 NdFeB magnets (KJ Magnetics) with

dimensions 2.54 (length) × 2.54 (width) × and 1.27 (thickness) cm^3 were chosen in this work because of their high maximum energy product of 393.6 kJ/m^3 at room temperature (20ºC). These magnets have been magnetized through-the-thickness and coated by nickel-copper-nickel to stabilize against oxidation. The temperature increase degrades the magnetic properties of NdFeB magnets such that the maximum energy product of N52 NdFeB magnet decreases reversibly by 20% when the temperature increases from room temperature to its maximum operating temperature of 80ºC. Above 80ºC, a dramatic and irreversible drop in maximum energy product is expected. Thus, to maintain maximum magnetic properties and compaction pressure, the magnets were used at room temperature. A maximum magnetic pressure of 0.64 MPa can be generated when magnets are sandwiched between two steel plates at room temperature. However, the magnetic compressive pressure is also influenced by the gap between the magnet and the bottom tool plate (i.e. lay-up thickness). Fig. 2 illustrates the exponential reduction of the magnetic pressure as a function of the distance from the tool plate. The magnetic force is measured by the mechanical test set up, Com-Ten® 705TN, while the magnet is slowly moved towards the tool plate. The dependence of magnetic pressure on the distance from the tool plate is then calculated by dividing the force by the base area of the magnet. Fig. 2 also shows the magnetic pressure determined from the data provided by the supplier, which corroborates the exponential reduction of pressure with separation distance. Hence, the thickness of the lay-up that separates the magnets and the tool plate determines the compaction pressure, which is likely to increase as the gap is reduced during consolidation, resin out-flow, and cure. The cured thickness of 3-ply, E-glass random mat laminate with a planar mat density of

0.450 kg/m^2 manufactured by wet lay-up was reported to be 2.4 mm [130]. Also, 8-ply, E-glass chopped-strand random mat laminate with a planar mat density of 0.462 kg/m^2 had a cured thickness of 4.96 mm [125]. Considering these thicknesses, an N52-2.54 × 2.54 × 1.27 cm^3 magnet can generate the maximum pressure of 0.25 MPa (37 psi) and 0.14 MPa (20 psi) for 3 and 8 plies respectively. Thus, sufficiently high compressive pressures (≈20 psi or greater) can be produced for consolidating up to 8 plies using these magnets. In this work, the initial and final lay-up thicknesses for 6-ply, random mat laminates manufactured by MACM/WLVB were 3.7 and 2.5 mm respectively. Using these numbers, the initial and final compressive pressure applied during cure can be estimated to be 0.22 MPa (32 psi) to 0.29 MPa (42 psi) as shown in Fig. 2.

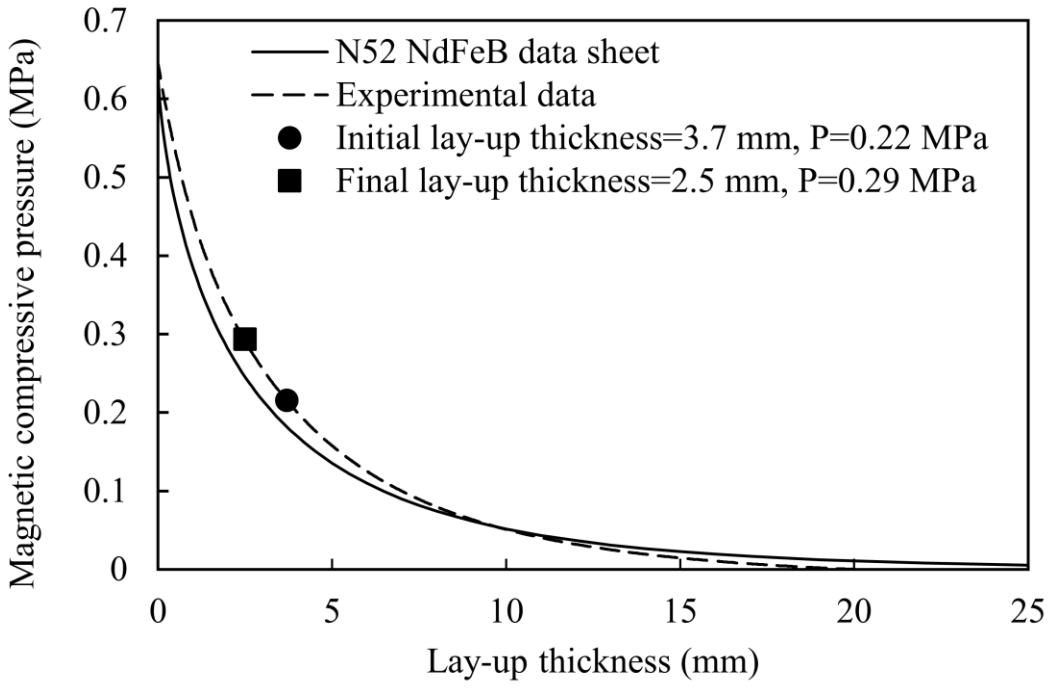

Figure 2. Variation of magnetic compressive pressure with lay-up thickness for a NdFeB, N52-2.54 × 2.54 × 1.27 cm^3 magnet sandwiched between two steel plates.

It is worth noting that the magnetic field generated by the N52 Neodymium magnets is expected to be approximately 0.5 T, which is not high enough to generate any discernable changes in the molecular structure and properties of the epoxy. Hence, all improvements reported in this work are due to magnetic compressive pressure applied on the vacuum bag lay-up.

2.2.2. Composite Constituents

Randomly oriented chopped strand glass fiber preform with a planar density of 0.228 kg/m^2 (Fiberglast part #248) was used as the reinforcing fiber bed. The epoxy system was Part A: EPON 862 Resin (Diglycidyl Ether of Bisphenol F) and Part B: Cycloaliphatic Amine EPIKURE Curing Agent 3300 (Miller-Stephenson Chemical Co.). The EPON 862 has a viscosity of 2.5-4.5 Pa s, and EPIKURE 3300 has a viscosity of 0.012-0.019 Pa s at room temperature. EPON 862/EPIKURE 3300 resin system, with the gel time of 115 min for 100 g of mixed resin, is suitable for this work because of its moderately low viscosity and cross-linking at room temperature. In particular, considering the maximum operating temperature of 80ºC for N52 NdFeB magnets, a resin system that cures at room temperature is needed.

2.2.3. Experimental Plan and Fabrication Process

Nine NdFeB, N52-2.54 × 2.54 × 1.27 cm3 magnets placed on a 1.6 mm-thick, 15.24 × 15.24 cm^2 magnetic steel plate are utilized to generate the magnetic compressive pressure on top of the vacuum bag, which is sandwiched between the magnets and a 5.6 mm-thick, 38.1 × 25.4 cm^2 magnetic bottom tool plate. The configuration of magnets on the top steel plate and the compressive pressure applied on the vacuum bag by the magnets are shown in Fig. 3 and Fig. 4, respectively.

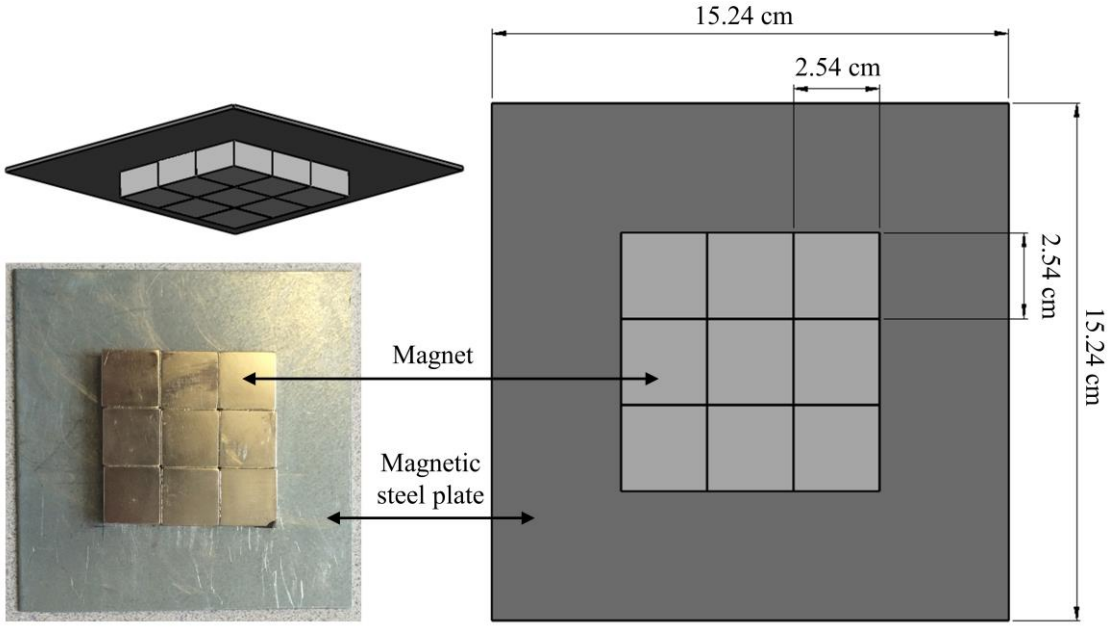

Figure 3. Configuration of nine NdFeB, N52-2.54 × 2.54 × 1.27 cm^3 magnets used to apply consolidation pressure.

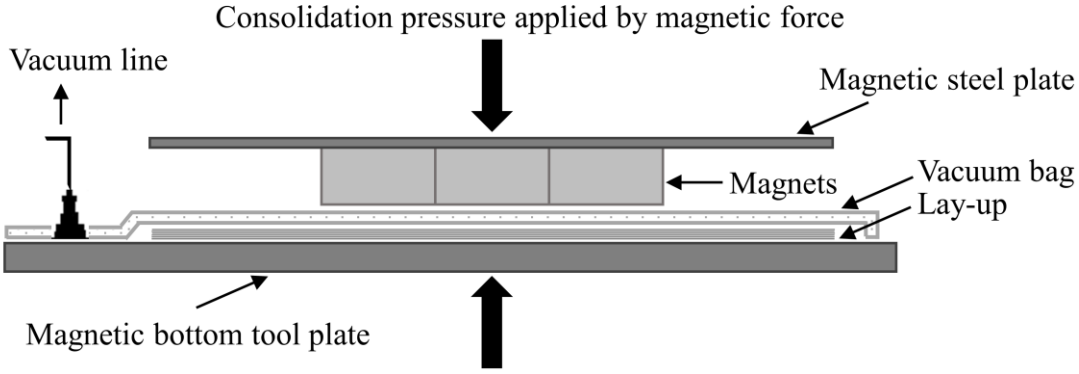

Figure 4. Application of magnetic consolidation pressure on the composite lay-up in the vacuum bag.

The fabrication procedure, in brief, is as follows: Six layers of the randomly-oriented, chopped E-glass fiber mats were cut into 15.24 × 15.24 cm^2 (6" × 6") squares. First, Part A: EPON 862 Resin and Part B: EPIKURE Curing Agent 3300 were mixed using 4:1 weight ratio at room temperature utilizing a mechanical stirrer at 200 rpm for

10 min. Then, a degassing process was carried out using a sonication bath for 20 min to remove bubbles. Afterward, the wet lay-up was prepared by applying one coat of resin and one ply of dry fiber mat on the steel mold, while a roller was used to press and squeeze excess resin after each ply was placed. A small amount of additional resin was also poured on top of the fiber mat, and squeegees were used to make the fiber bed fully saturated. This process was repeated for all six plies. A perforated release film (22.86 × 22.86 cm^2), a layer of polyester tape around the perimeter of the perforated release film, a 0.3 mm-thick aluminum caul plate (15.24 × 15.24 cm^2), and two plies of breather/bleeder were placed onto the fiber bed as illustrated in Fig. 5. Then, lay-up was sealed within a vacuum bag. The cure schedule of the E-glass/epoxy laminate is depicted in Fig. 6. The lay-up assembly was prepared in 60 min (up to point A shown in Fig. 6), and a vacuum at 95 kPa absolute pressure was applied for 180 min during the cure. After room temperature curing for 240 min (until point D shown in Fig. 6), the laminates were demolded and subsequently postcured in the oven for 90 min at 82°C (180°F) plus 90 min at 150°C (302°F) as shown in Fig. 6.

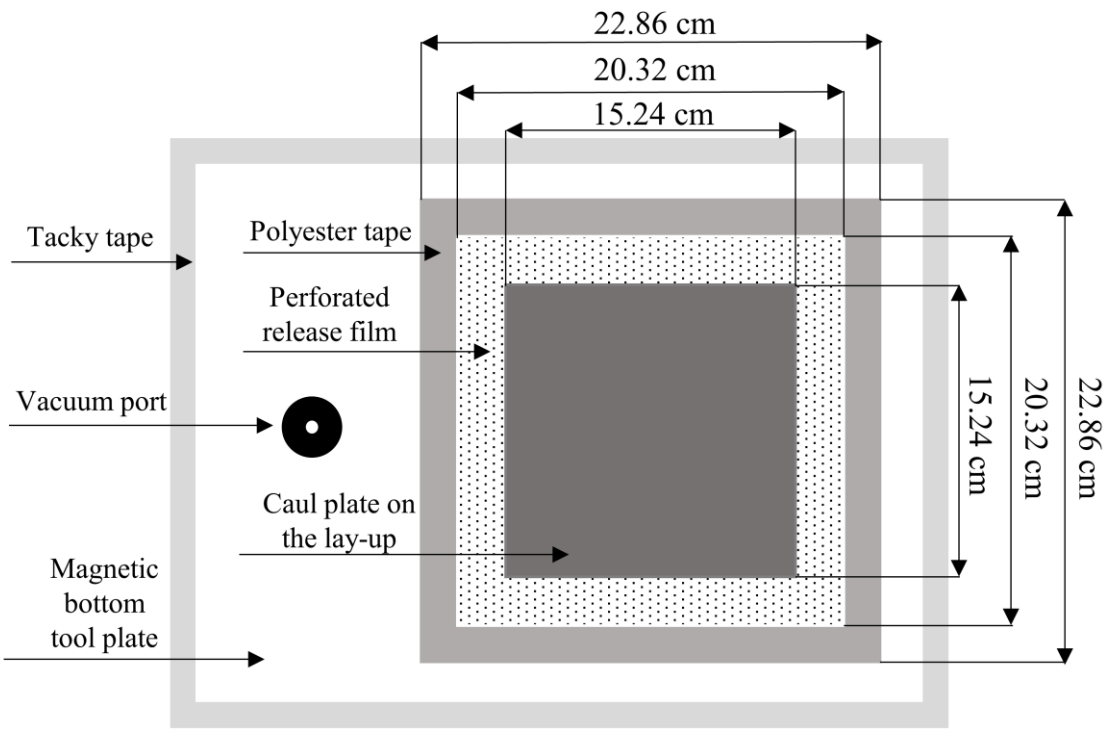

Figure 5. Schematic of the wet lay-up/vacuum bag assembly on the magnetic bottom tool plate used in fabricating the laminates.

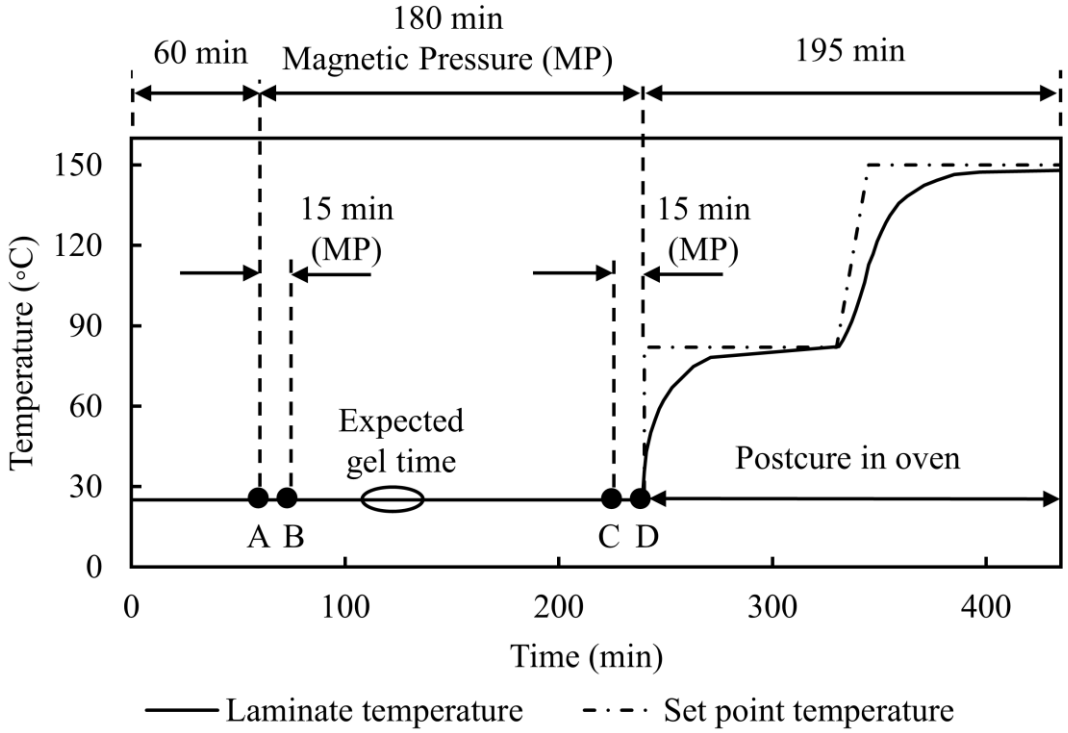

Figure 6. Temperature profile of the random mat E-glass/EPON 862-EPIKURE 3300 used to manufacture laminates (Scenario M-T0: WLVB without magnets, Scenario M-T180: WLVB/MACM with applying magnets from points A to D, Scenario M-T15S: WLVB/MACM with applying magnets from points A to B, and Scenario M-T15E: WLVB/MACM with applying magnets from points C to D).

In this work, 6-ply random mat E-glass/EPON 862-EPIKURE 3300 laminates (15.24×15.24 cm^2) were fabricated under the four scenarios shown in Table 1. For each fabrication scenario, two laminates were fabricated under identical conditions to assess the repeatability of the process.

Table 1. Four fabrication scenarios used in the manufacturing of 6-ply random mat E-glass/EPON 862-EPIKURE 3300 laminates. Detailed illustration of the cure cycle is shown in Fig. 6.

Fabrication scenario		Manufacturing process
1	M-T0	Wet lay-up/vacuum bag (WLVB) process, without external pressure
2	M-T180	Magnets applied for 180 min throughout the vacuum
3	M-T15S	Magnets applied for 15 min at the start of the vacuum
4	M-T15E	Magnets applied for 15 min at the end of the vacuum

In the first scenario, M-T0, the laminates were fabricated by WLVB process without external pressure. Thus, the composite laminate is only compacted by the vacuum pressure. Scenario 2, M-T180, was investigated to demonstrate the effectiveness of the MACM and how this method could improve the conventional WLVB methods. In this scenario, all steps were similar to the first scenario except the application of magnetic consolidation pressure throughout the vacuum (i.e., 180 min from point A to D shown in Fig. 6). Scenarios 3 and 4 were considered to assess the effect of applying magnetic consolidation pressure only for a finite amount of time (i.e., 15 min) at different stages of the cure, where the resin viscosity would be substantially different. In the third scenario, M-T15S, the magnets were applied for 15 min at the start of the vacuum (i.e., 15 min from point A to B shown in Fig. 6) where the resin viscosity was at its minimum level after lay-up preparation. To investigate the effectiveness of applying magnetic pressure after gelation of the resin, the fourth scenario, M-T15E is defined. In this scenario, considering the 110 min expected gel time at room temperature, magnets were only used for 15 min at the end of the vacuum before demolding the laminate (i.e., 15 min from point C to D shown in Fig. 6).

In this work, all the composite samples used in the characterization of void and fiber volume fractions and mechanical properties were taken from an area directly under the magnets to avoid possible edge effects and ascertain the effects of the magnetic consolidation more accurately.

Debulking, a method of applying and releasing vacuum to increase fiber nesting, fiber volume fraction and to remove voids, is also considered as a viable method to improve the wet lay-up laminate quality. To achieve this goal, two additional laminates (i.e., referred to as scenario M-T0D) were manufactured using wet lay-up/vacuum bagging coupled with debulking. After a similar preparation of the lay-up, the resin-saturated fiber bed went through three repeated vacuum-relaxation cycles for a debulking phase. In each cycle, the relaxation phase took 2 min, followed by vacuum for 5 min.

Results show that the properties of these M-T0D laminates did not improve compared to M-T0, where the fiber volume fraction, mechanical properties, and void content of M-T0D remained within the experimental uncertainty of the M-T0 results. Hence, the M-T0D laminate results were not included as a separate fabrication scenario in this work.

2.2.4. Resin Burn-Off and Thermogravimetric Analysis (TGA)

In order to determine the fiber volume fraction and void content, resin burn-off method is frequently utilized to remove the matrix from the laminate [131]. This method is commonly used for glass fiber polymer composites because the epoxy matrix burns at 500-600℃ while the glass fiber can resist being oxidized at this temperature [132]. However, the sizing of the fibers may also become degraded, and the fibers lose

weight during the removal of the resin at high temperatures. Therefore, thermogravimetric analysis (TGA) was used to determine the amount of mass loss of the fibers when they are exposed to high temperatures during burn-off. The heat rates and thermal conditions in TGA tests were the same as the furnace conditions used in the resin burn-off tests. During the TGA runs, approximately a 5.46% fiber mass loss was observed at 600°C, which may be due to the loss of organic sizing from the fiber surface. This small but important mass loss percentage from fibers was accounted for in the calculation of void and fiber volume fraction of the laminates.

2.2.5. Void and Fiber Volume Fraction Measurement

From each laminate, three 20.32 × 6.35 mm^2 rectangular specimens were cut to measure the void and fiber volume fraction according to ASTM D3171-15. Void and fiber volume fraction were obtained using the following equations.

$$v_{matrix} = \frac{\rho_{composite}}{\rho_{matrix}}\left(\frac{w_{composite} - w_{fiber}}{w_{composite}}\right) \quad (1)$$

$$v_{fiber} = \frac{\rho_{composite}}{\rho_{fiber}}\left(\frac{w_{fiber}}{w_{composite}}\right) \quad (2)$$

where, v_{matrix} is resin volume fraction, v_{fiber} is fiber volume fraction, ρ is density, and w is sample weight.

$$v_{void} = 1 - (v_{matrix} + v_{fiber}) \quad (3)$$

where, v_{void} is void volume fraction.

The density of composite specimen, matrix, and fiber need to be measured separately to calculate the void and fiber volume fraction accurately. The density of each composite sample was measured using suspension method. For this purpose, a solution of Cargill Labs heavy liquid with a density of 2.49 g/cm^3 diluted with water

was used [133]. Similarly, the density of cured matrix was determined using the void-free epoxy specimens that were prepared under the same cure conditions. The density of glass fibers was measured by a nitrogen pycnometer. The density of fiber and matrix were obtained to be 2.47 ± 0.004 g/cm^3 and 1.17 ± 0.003 g/cm^3, respectively. The weight fraction of fiber and matrix for each specimen were calculated using resin burn-off method according to ASTM D2584-11.

2.2.6. Characterization of Mechanical Properties

Flexural properties of composite laminates were determined by the three-point bending test performed using Com-Ten® 705TN, at a crosshead speed of 2 mm/min in accordance with ASTM D7264/D7264M-15. A span to depth ratio of 16:1 was used. The specimen width and thickness were 63.5 mm and 12.7 mm (2.5" × 0.5"), respectively. Seven samples were cut by a diamond saw from two manufactured laminates. The flexural strength, σ, and the flexural modulus, E, were calculated from the Eqs. (4) and (5), respectively.

$$\sigma = \frac{3PL}{2bh^2} \tag{4}$$

$$E = \frac{L^3 m}{4bh^3} \tag{5}$$

where, P is applied force, L is support span length, b and h are the width and thickness of the composite specimen, and m is the slope of the load-deflection curve.

2.2.7. SEM: Sample Preparation and Image Analysis

A detailed image analysis either by an optical microscope or a scanning electron microscope (SEM) is considered to be among the most accurate methods to identify each void in the composite and assess the void morphology such as voids size, area, and

other geometrical features. In this work, all analysis of the composite microstructure was performed by the scanning electron microscopy by imaging the through-the-thickness surface of 17.5 mm-long composites samples obtained from four different scenarios. The SEM samples were carefully polished using grit sizes from 15 μm to 1.9 μm and followed by gold sputter coating to prevent sample charging. The Tescan VEGA-II XMU scanning electron microscopy was utilized for imaging of 4.7 mm × 3.2 mm through-the-thickness cross-sectional area from the cured specimens at 35X and 150X magnifications. Four SEM images were taken at 35X magnification to cover the whole length of each sample. These low magnification images were used to identify the larger voids, while the smaller voids were characterized using the higher magnification images. SEM images were analyzed with ImageJ software to characterize the void location, size, and morphology. In this work, all voids were identified manually in ImageJ software because automatic image thresholding may lead to higher experimental uncertainty in recognition of the shape and size of microvoids [134]. The equivalent diameter and roundness of the voids are measured to investigate void size distribution and shape morphology.

The equivalent diameter, D_{eq}, presents a diameter of a circle with the area equal to the area of the voids and is given by

$$D_{eq} = \sqrt{\frac{4A}{\pi}} \tag{6}$$

where, A is the measured area of the void.

Voids are classified in the following three different categories based on their equivalent diameter: small voids ($D_{eq} \leqslant 50$ µm), medium voids (50 µm $\leqslant D_{eq} < 100$ µm), and large voids ($D_{eq} \geqslant 100$ µm).

The roundness, *R*, given by Eq. (7) below, varies from 0 to 1 and characterizes the extent of void elongation.

$$R = \frac{4A}{\pi {d_{max}}^2} \tag{7}$$

where *A* is the area and d_{max} is the maximum diameter of the void.

The roundness of a perfect circle is one, so the voids with roundness more than 0.9 ($0.9 < R \leqslant 1$) are considered as the circular voids. By considering an ellipse where the major radius is four times the minor radius, the roundness will be 0.25, so the roundness between 0.25 and 0.9 is assumed for the elliptical voids. Finally, the voids with the roundness less than 0.25 are determined as highly elongated voids. In order to assess the effect of magnetic compressive force on void elongation, the relative percent contributions of each void shape to total void content for each composite samples were explored.

2.3. Results and Discussion

2.3.1. Magnetic Pressure and Resin Pressure during Consolidation

To validate and complement the measurement of the magnetic pressure as explained in section 2.2.1 and shown in Fig. 2, thin pressure films (Fujifilm Prescale) were used to assess the spatial variation of the magnetic pressure on composite laminates. Multiple experiments were carried out by placing different pressure films on the bottom tool plate, covering the entire 15.24 x 15.24 cm^2 area of the composite laminate.

Fig. 7 shows a scanned image of a pressure film recovered after the fabrication of an M-T180 laminate. The high color intensity of the films directly correlates with the high-pressure areas and can be used to estimate the absolute pressure levels with ± 15% uncertainty.

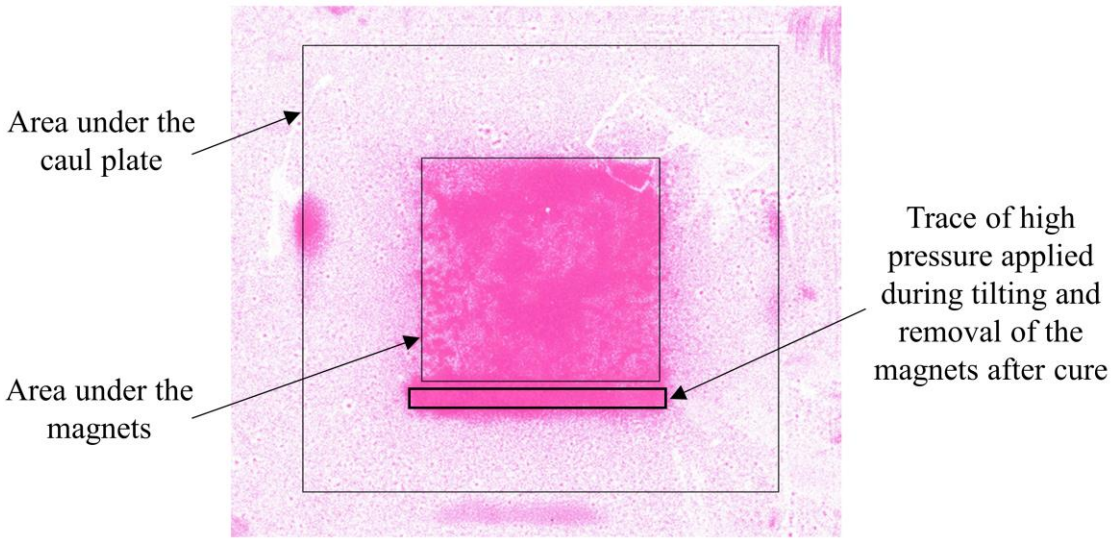

Figure 7. Image of a thin pressure film placed on the tool plate during fabrication of an M-T180 composite laminate.

Based on the image analysis of the pressure films, the area directly under the magnets was subjected to a uniform absolute pressure of 0.37 to 0.39 MPa. This value is consistent with the value of 0.29 MPa (corresponding to the final lay-up thickness) given in Fig. 2 plus the approximately 0.09 - 0.10 MPa pressure due to the vacuum. In addition, a very sharp pressure drop to 0.08 MPa (absolute) is observed in regions that are not directly under the magnets, indicating vacuum as the primary source of compaction pressure in these regions. The sharp drop in pressure also indicates that a 0.3 mm-thick aluminum caul plate placed under the magnets did not distribute the compaction pressure over a larger area on the composite surface. If needed, a stiffer caul plate can be used to enlarge the compaction area of the magnets. However, if the

magnetic force is distributed over a larger area, a proportionally lower compaction pressure will be generated.

As the magnets are applied on the laminate, the resin pressure is expected to increase and, depending on the permeability of the fiber bed, resin viscosity and rate of resin outflow, reach a maximum level. Considering that the final laminate thickness, as well as the formation and growth of the voids during cure, are dependent on the resin pressure, the temporal change of resin pressure is important.

In separate fabrication experiments, a pressure transducer was installed on the bottom tool plate to directly measure the resin pressure. During compaction, the thickness of the lay-up was determined using a digital thickness gage to correlate the variation in resin pressure and magnetic compaction pressure with the lay-up thickness. Fig. 8 shows the variation of resin pressure, magnetic compaction pressure, and the lay-up thickness after the application of the magnets. Fig. 8 indicates an initial sharp rise in resin pressure, reaching a peak at slightly under 20 s after the magnets are applied. This rapid increase in resin pressure promotes higher resin outflow rate, increases fiber volume fraction, and reduces void content. The resin pressure then starts decreasing and reaches the steady value of zero gage pressure within minutes of applying the magnets. Clearly, when the resin pressure returns to its steady value, all the magnetic compaction pressure is carried by the fiber bed, thus resulting in a thinner laminate. During this process, the lay-up is compacted during the first few minutes, reaching a steady thickness value. The lay-up thickness correlates with the magnetic compaction pressure such that, as the gap between the magnets and the tool plate is decreased during the first few minutes, the compaction pressure is increased as shown in Fig. 8.

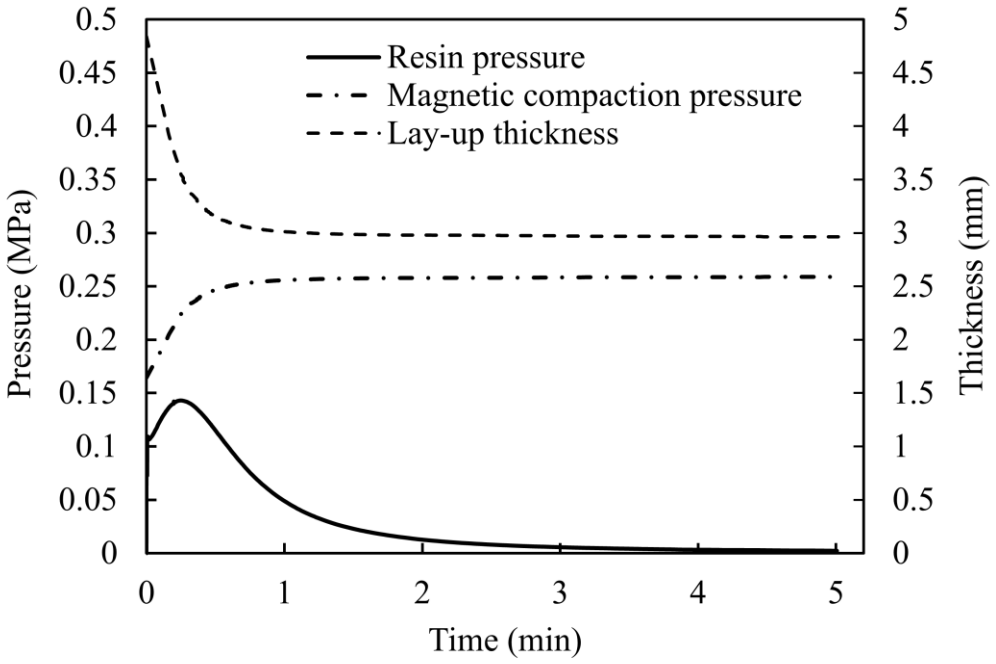

Figure 8. Variation of resin pressure during the application of magnets. The gage pressure is measured by a transducer installed at the bottom tool plate.

2.3.2. Fiber and Void Volume Fractions

The fiber volume fraction, void volume fraction, and an average thickness of the composite laminates produced under four fabrication scenarios: (a) M-T0; (b) M-T180; (c) M-T15S; and (d) M-T15E are presented in Table 2. Results show that in M-T0, the worst case scenario, fiber volume fraction is 17.34%, and void volume fraction is the highest at 5.81%. These values establish the baseline which can be improved by applying magnetic pressure. It can be seen that the moment and the duration of applying magnetic consolidation pressure had substantial effects on the fiber volume fraction and void content of the laminates. Scenario M-T180 shows the highest fiber volume fraction (26.88%) compared to the other scenarios and low void volume fraction (<3%) most likely because of the longer (180 min) application of the consolidation. Fiber volume

fraction of 27.5% was reported in the composites fabricated using 16 layers of the same random mat E-glass fiber in resin transfer molding process (RTM) [135]. Thus, applying magnetic compressive pressure in WLVB led to an increase in fiber volume fraction to levels observed in closed molding processes such as RTM, coupled with the substantial reduction of void content. It is also observed that in scenario M-T15S when magnets were applied at the start of the vacuum for only 15 min, the lowest void volume fraction (≈1.74%) with a considerable increase in fiber volume fraction to above 21% is achieved. This confirms the effectiveness of applying magnets for a finite time when the viscosity of the resin is relatively low.

Table 2. The fiber volume fraction, void content, and average thickness for composite laminates manufactured by four fabrication scenarios (n=6 samples, 95% confidence intervals).

Fabrication scenario		Fiber volume fraction (%)	Void volume fraction (%)	Average thickness (mm)
1	M-T0	17.34 ± 0.84	5.81 ± 1.24	3.18 ± 0.02
2	M-T180	26.88 ± 1.99	2.71 ± 0.36	1.99 ± 0.04
3	M-T15S	21.12 ± 0.79	1.74 ± 0.19	2.74 ± 0.06
4	M-T15E	19.99 ± 0.74	3.09 ± 0.09	2.74 ± 0.02

In scenario M-T15E, the fiber volume fraction is 20%, and void volume fraction is 3.09%. As expected, most of the resin flow have already taken place without the consolidation pressure before the gel point, so the application of magnets in this scenario was not as effective as scenario M-T15S in decreasing void content and increasing the fiber content. Also, Table 2 demonstrates that increasing the fiber volume fraction corresponds to a decrease in laminate thickness. Thus, the laminates

fabricated in scenario M-T180 has the lowest laminate thickness of 1.99 mm representing a 37% reduction in thickness and the highest fiber volume fraction of 26.88% due to magnetic compaction.

Fig. 9 presents percentage increase in fiber volume fraction and percentage decrease in void volume fraction of laminates manufactured using MACM/WLVB in scenarios M-T180, M-T15S, and M-T15E compared to using conventional WLVB in scenario M-T0. As evident in Fig. 9, the fiber volume fraction in scenario M-T180 increased by 55% compared to scenario M-T0 which indicates a very significant increase. It is also observed that the percentage increase in fiber volume fraction for scenario M-T15S is higher than scenario M-T15E since magnetic pressure were applied at 225 min, which is after the expected gel time of 115 min. Even though the resin system was gelled and reached a much higher viscosity at that point, applying magnetic pressure still had an effect on achieving better consolidation and reducing void content as depicted in Fig. 9.

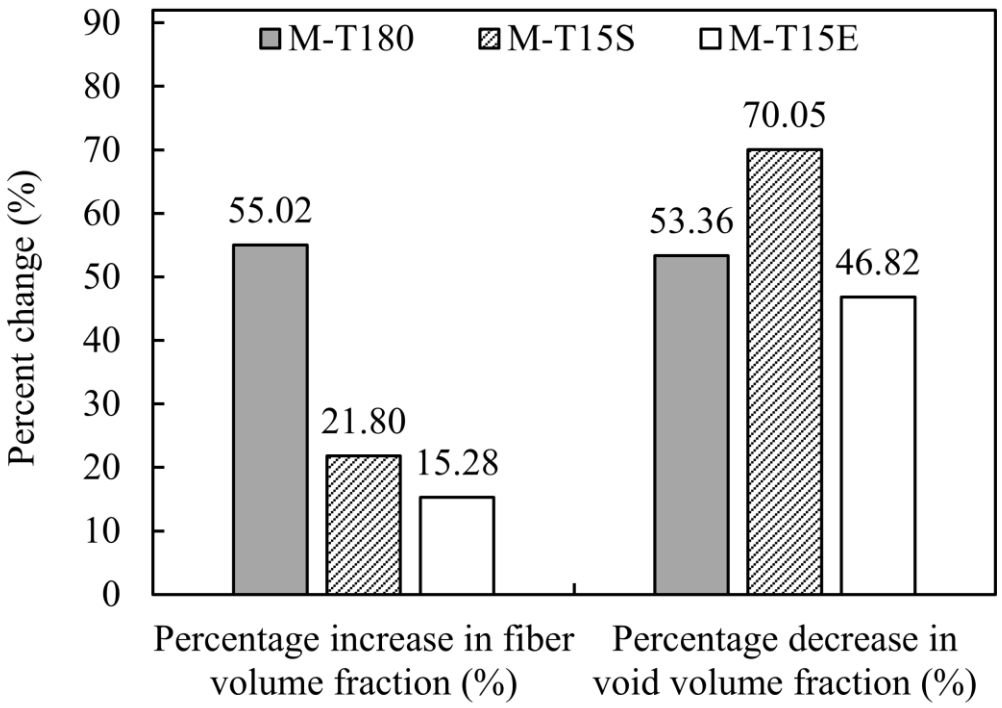

Figure 9. Percentage increase in fiber volume fraction and decrease in void volume fraction for laminates fabricated in scenarios M-T180, M-T15S, and M-T15E compared to scenario M-T0.

It is important to emphasize that the highest decrease of approximately 70% in void volume fraction, from 5.81% to 1.74%, occurred in scenario M-T15S. This is even lower than the 2.71% reported for the M-T180 scenario, where the magnets were kept throughout the cure. Although this finding seems to be counter intuitive at first, the likely reason is the fact that applying pressure throughout the cure yields thinner laminates and higher fiber volume fraction, which creates a lower permeability fiber bed during cure. Hence, removal of voids from a denser fiber bed with lower permeability becomes more difficult. In other words, applying consolidation pressure throughout the cure helped remove more resin and increase the fiber volume fraction, but some of the voids, which would have been removed if the pressure were to be removed after 15

minutes, became trapped by the increased compaction and became immobile. The presence of these immobile voids led to a slightly higher void content in M-T180 laminates.

2.3.3. Image Analysis

Figs. 10 (a-d) are representative SEM images at 35X magnification for scenarios (a) M-T0; (b) M-T180; (c) M-T15S; and (d) M-T15E. Fig. 10 provides a clear visual comparison of the laminate thickness as well as the shape morphology and size distribution of the voids. Fig. 10 shows that most of the voids are located in the matrix rich and inter-ply regions. These voids surrounded by the resin were either present in the resin before the lay-up or formed by the expelled volatiles during cure. Fig. 10 (a) shows that in the absence of external pressure, the majority of voids are circular or slightly elliptical. Comparing Fig. 10 (b) with Fig. 10 (a), it can be clearly seen that the thickness of the laminate, the number of voids, and void content significantly reduced which indicates the improved consolidation of the laminates by applying magnets throughout the vacuum for 180 min. It seems that the reduction in void content is primarily due to squeezing out the excess resin containing voids. In Fig. 10 (b), the majority of the voids are still circular or elliptical, but noticeably smaller than those in the laminates fabricated without consolidation pressure. Fig. 10 (c) demonstrates applying magnets for 15 min at the start of the vacuum (M-T15S) is not as effective as M-T180 in reducing the thickness of the laminates, although it is still successful in increasing the fiber content and reducing the voids compared to the baseline scenario (M-T0). Fig. 10 (d) presents that applying magnets for 15 min at the end of vacuum (M-T15E) when the resin was already gelled could still reduce or eliminate the macro voids.

The thickness of the laminate in scenario M-T15E is the same as M-T15S while the number of voids is markedly greater, indicating the difficulty of removing voids after the resin viscosity is increased to a much higher level.

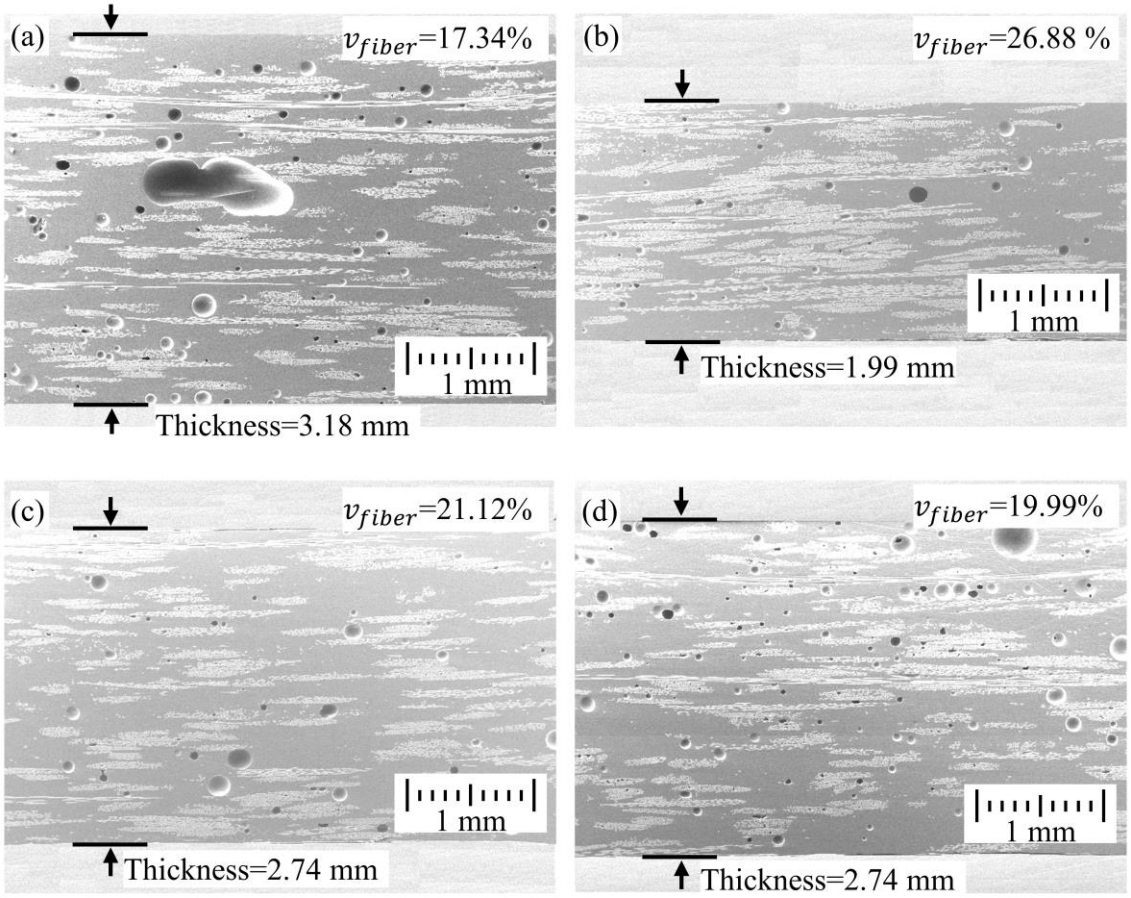

Figure 10. SEM images at 35X magnification for different fabrication scenarios: (a) M-T0; (b) M-T180; (c) M-T15S; and (d) M-T15E.

SEM images at 150X magnification for two fabrication scenarios: (a) M-T0 and (b) M-T180 are presented in Fig. 11. In scenario M-T180, higher compaction of fiber tows and plies under magnetic compressive pressure is observed compared to scenario M-T0. Comparing Figs. 11 (a) and (b), the number of voids in resin rich regions was also considerably lower in scenario M-T180.

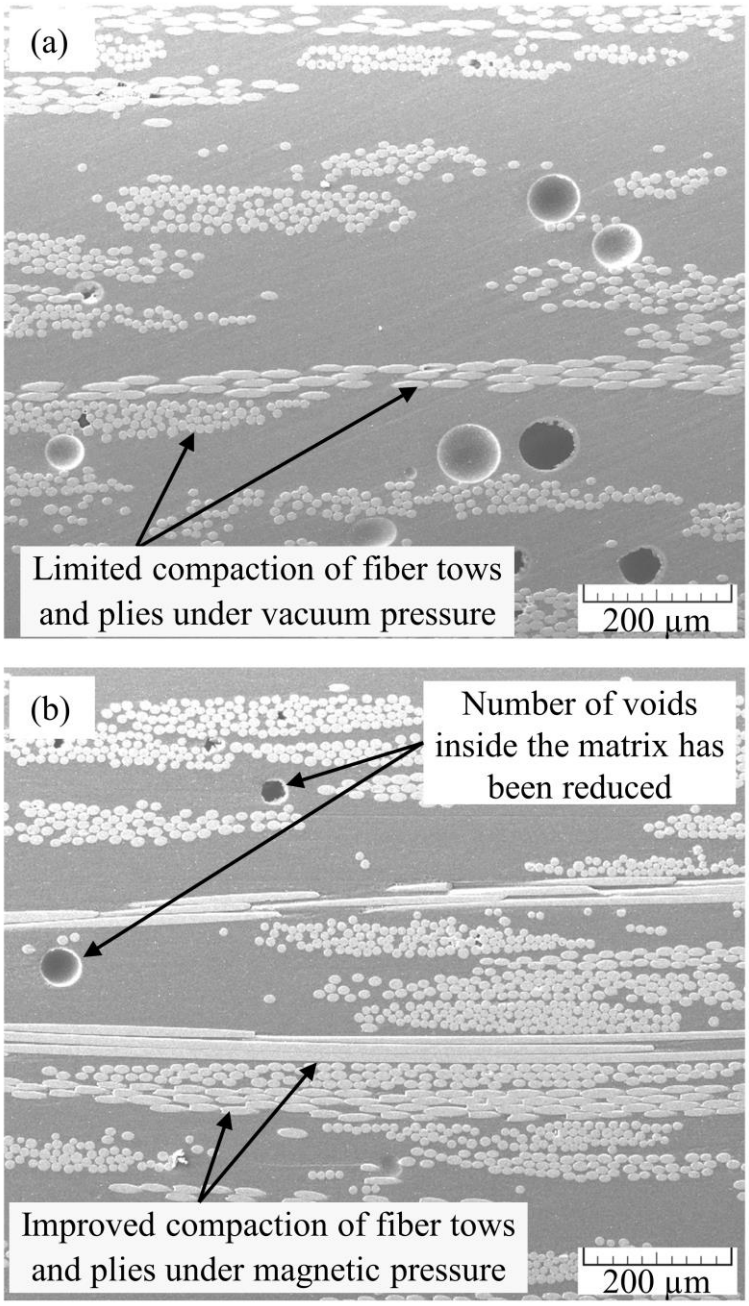

Figure 11. SEM images at 150X magnification for two fabrication scenarios: (a) M-T0 and (b) M-T180.

2.3.3.1. Size Distribution of Voids

Fig. 12 shows the void size distribution based on equivalent diameter, D_{eq}, for different fabrication scenarios. By averaging D_{eq} for each scenario, the void sizes of

52.9, 41.0, 46.6, and 39.5 μm for scenarios M-T0, M-T180, M-T15S, and M-T15E are achieved, respectively. As expected, the maximum average void size occurs in the first scenario (M-T0) with the void content of 5.81%, where the laminates have been consolidated only under a vacuum pressure of 95 kPa. However, applying an additional consolidation pressure via MACM decreased the average void size in all other scenarios, M-T180, M-T15S, and M-T15E. The average void size in scenario M-T180 (D_{eq}-Ave=41.0 μm) is less than scenario M-T15S (D_{eq}-Ave=46.6 μm), where in both cases magnets were applied immediately after starting the vacuum. This can be explained by the fact that keeping the magnets throughout the vacuum (180 min) is likely to reduce both the void mobility and overall size while removing the magnets after 15 min seems to help the removal of the mobile voids. As evident in Fig. 12, voids with $D_{eq} \leq 60$ μm are dominant for all scenarios. Also, in scenario M-T15E, the proportion of voids with an equivalent diameter less than 20 μm is the greatest (i.e. ≈41%) which indicates that applying magnetic pressure after resin gel point could reduce the voids size.

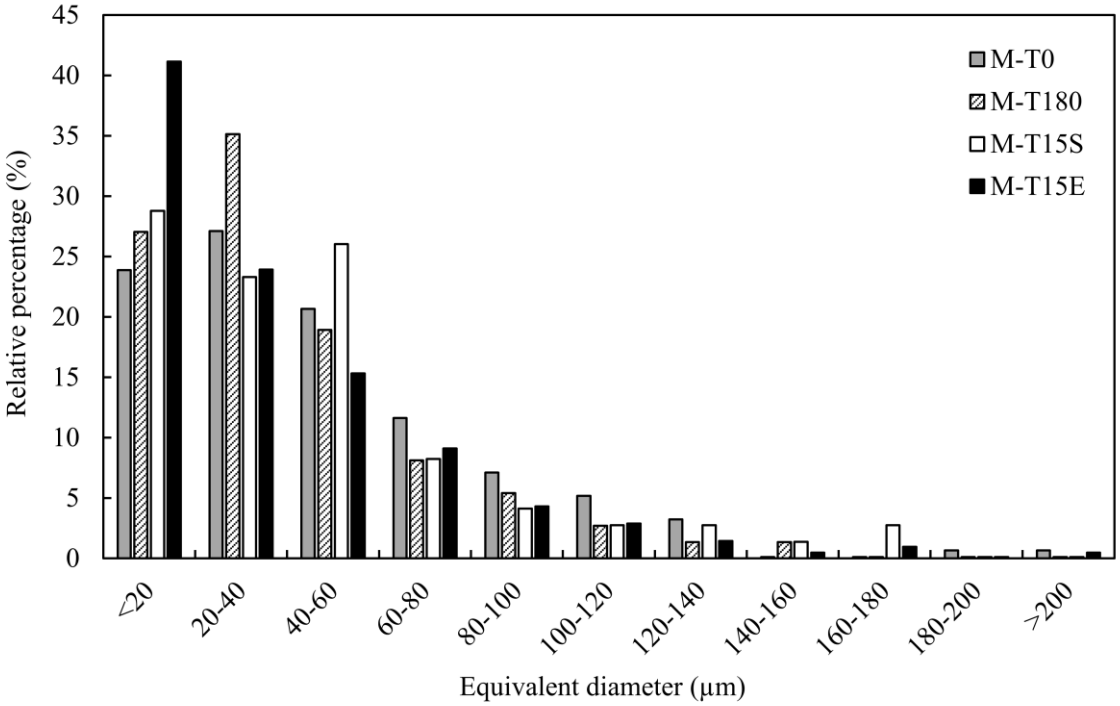

Figure 12. Void size distribution based on equivalent diameter for different fabrication scenarios.

Fig. 13 depicts the relative percentage of small ($D_{eq} \leqslant 50$ μm), medium (50 μm $\leqslant D_{eq} < 100$ μm), and large ($D_{eq} \geqslant 100$ μm) voids for laminates manufactured under four different scenarios. The relative percentage of small voids in scenario M-T0, is the minimum, 59%, compared to other scenarios. Interestingly, it is observed that the moment and duration of applying magnetic pressure critically affect the average void size as well as the relative percentage of small, medium, and large voids such that the relative percentage of small voids in scenario M-T180 is higher than scenario M-T15S. Also, the minimum average void size (D_{eq}-Ave=39.5 μm) and maximum relative percentage of small voids (73.7%) are seen in scenario M-T15E where magnetic pressure was applied for 15 min at the end of the vacuum. Accordingly, the trapped voids could not be removed after the gel point was reached, but the application of

magnetic pressure after the gelation led to an increase in resin pressure which results in a modest reduction in void size throughout the composite laminates.

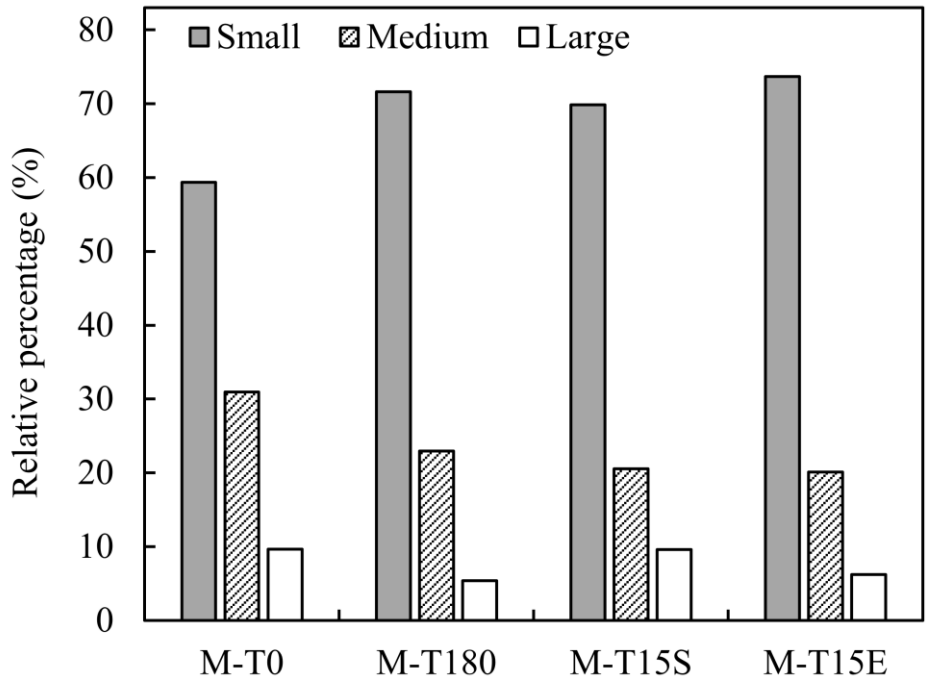

Figure 13. Relative percentage of small ($D_{eq} \leqslant$ 50 µm), medium (50 µm $\leqslant D_{eq} <$ 100 µm), and large ($D_{eq} \geqslant$ 100 µm) voids for different fabrication scenarios.

2.3.3.2. Variation in Void Shape

The geometrical features and the shape of voids are known to have an important effect on the failure of composite laminates [136-139]. For instance, high-aspect-ratio elliptical voids may cause premature failure of the laminate and lead to a reduction in the strength [140]. In addition, the presence of highly elongated voids might promote coalescences of microcracks and lead to interfacial debonding at higher stress levels [141]. Thus, characterizing the void shape, particularly the roundness, *R*, of the voids will be helpful in assessing the laminate propensity of a developing premature failure.

Fig. 14 presents the void shape morphology using the roundness value, *R*, defined in section 2.2.7. This figure corroborates that the vast majority of the voids are circular or elliptical since the elongated voids (i.e., $R \leqslant 0.25$) in all four scenarios are less than 5%. This observation can be explained by the fact that most voids are totally surrounded by the resin, and thus any application of pressure before the gel point primarily reduces the void size or remove the voids with the resin outflow. The voids that were trapped between the plies or located at the fiber-matrix interface would possibly be more elongated by the application of consolidation pressure. As expected, application of pressure after the gel point slightly increases the percentage of elongated voids as the higher resin viscosity enables attainment of higher resin pressure upon application of the magnets which in turn slows down the recovery of the circular void shape during the latter stages of cure.

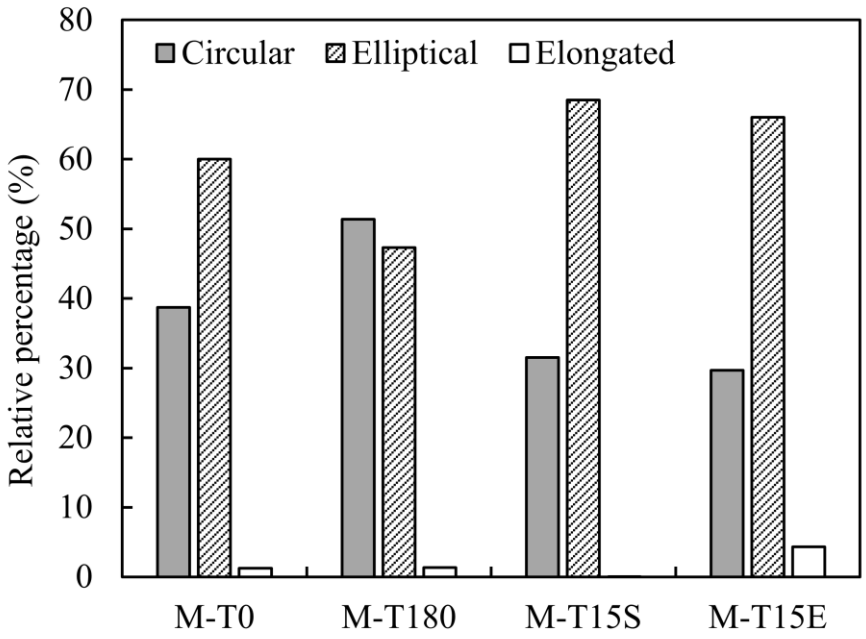

Figure 14. Voids shape morphology given by roundness, *R*, under different fabrication scenarios (i.e. Circular: $0.9 < R \leqslant 1$, Elliptical: $0.25 < R \leqslant 0.9$, and Elongated: $R \leqslant 0.25$).

2.3.4. Flexural Properties

The flexural strength and stiffness of composite samples from different fabrication scenarios are plotted in Figs. 15 and 16, respectively. The fiber and void volume fractions are also shown to illustrate the strong correlation between them and flexural properties. Flexural strength and stiffness in scenarios M-T180, M-T15S, and M-T15E are significantly higher than scenario M-T0 because of the increased fiber volume fraction and decreased void content. Specimens from scenario M-T180 with the maximum fiber volume fraction of 26.88% showed the highest flexural strength, above 250 MPa, because they were fabricated under compaction pressure throughout the cure cycle. As expected, increasing the fiber volume fraction and reducing the void content has a direct and most prominent influence on enhancing fiber dominated properties. In addition to the overall void volume fraction, however, a secondary but possibly an important effect may be the void size distribution. Figs. 15 and 16 show that the composites with the largest voids (i.e., greater than 200 μm in M-T0 and M-T15E shown in Fig. 12) had the lowest flexural properties. The sample with the lowest strength and stiffness (i.e., M-T0) also has the largest percentage of medium and large voids as shown in Fig. 13. The lower properties of the M-T15E compared to M-T180 and M-T15S could have been influenced by its highest percentage of elongated voids which could have acted as failure sites.

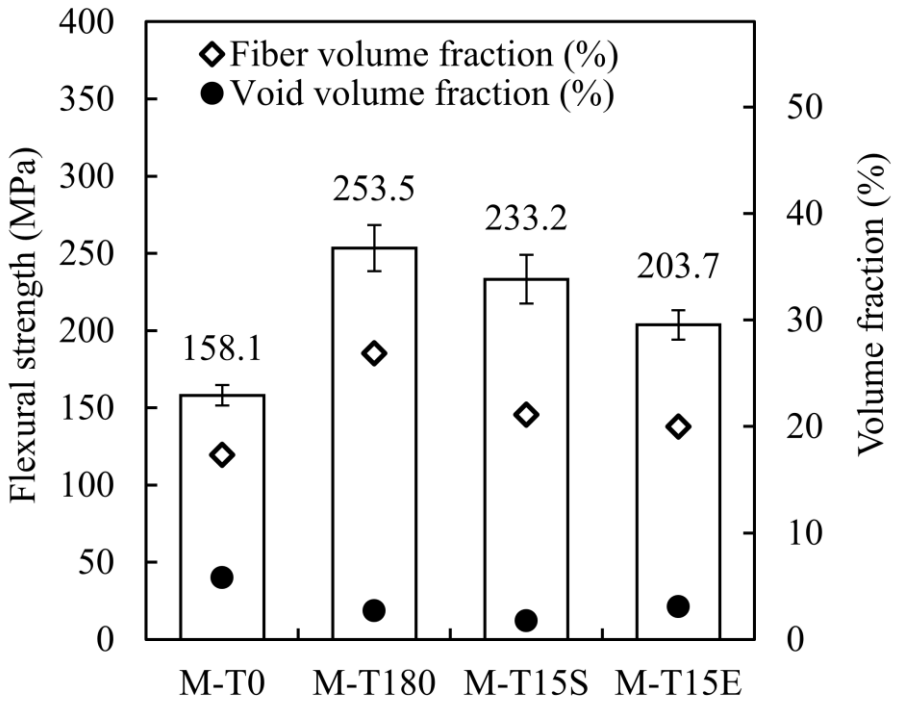

Figure 15. Flexural strength in different fabrication scenarios: (a) M-T0; (b) M-T180; (c) M-T15S; and (d) M-T15E as a function of void and fiber volume fraction. Note: Error bars show the 95% confidence interval (n=7 samples).

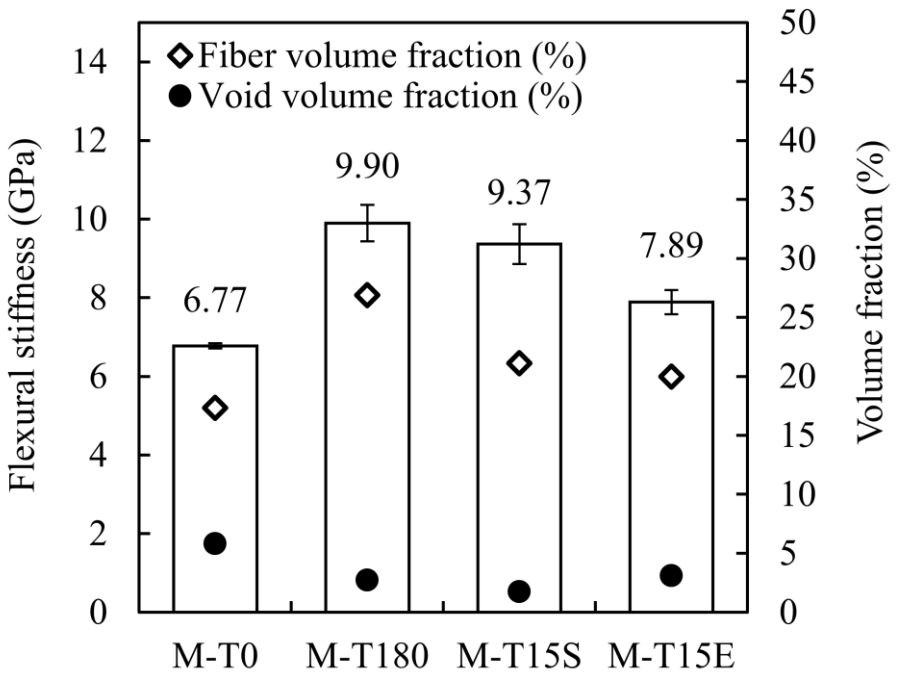

Figure 16. Flexural stiffness in different fabrication scenarios as a function of void and fiber volume fraction. Note: Error bars show the 95% confidence interval (n=7 samples).

In order to compare the relative effects of the processing methods on the mechanical properties more clearly, the percentage increase in flexural properties in scenarios M-T180, M-T15S, and M-T15E are compared to scenario M-T0 as shown in Fig. 17. The percentage increase in flexural strength and stiffness for laminates in scenario M-T180 are 60% and 46% higher than the traditional WLVB process (scenario M-T0). It is also interesting to note that using magnets for only 15 min early in the cure (scenario M-T15S), provides approximately 48% and 38% improvements in flexural strength and stiffness compared to WLVB process. Using magnets for 15 minutes at the latter stages of cure (scenario M-T15E) still provides 29% and 16% enhancements in flexural strength and modulus. These results indicate that employing magnetic pressure for only 15 min anytime during cure, even after the gel point, improves the flexural

properties, although the time of pressure application plays a significant role in defining the level of increase.

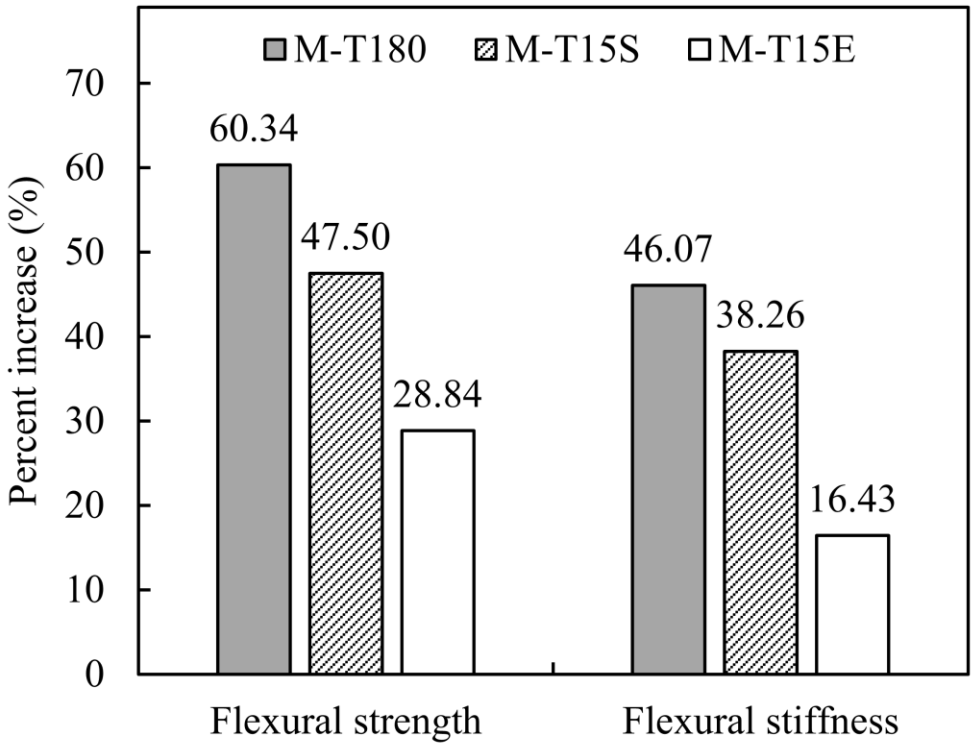

Figure 17. Percentage increase in flexural properties of scenarios M-T180, M-T15S, and M-T15E compared to scenario M-T0.

The mechanical properties are significantly influenced by both the fiber volume fraction and the void content. To ascertain the relative effects of these two important parameters independently, the flexural strength and stiffness of the fabricated composites were scaled with respect to those of the resin properties and plotted as a function of fiber volume fraction as shown in Figs. 18 and 19. Each fabrication scenario was labeled along with their void volume fraction to visually identify any discernable effect of the voids, despite the changes in fiber volume fraction. In both strength and stiffness results, the composite samples with the highest voids content (i.e., M-T0 @

5.81%) falls under the linear trend line, while the sample with the lowest voids (i.e., M-T15S, @ 1.74%) is clearly above the linear trend line shown in Figs. 18 and 19.

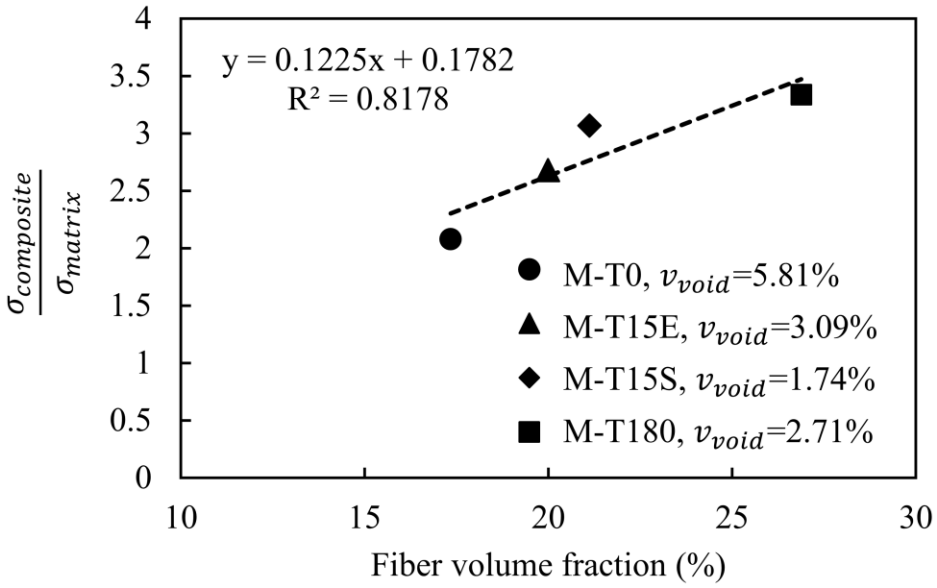

Figure 18. Variation of flexural strength ratio (composite/matrix) with fiber volume fraction obtained at different fabrication scenarios. Void volume fractions, v_{void}, of different scenarios are also given.

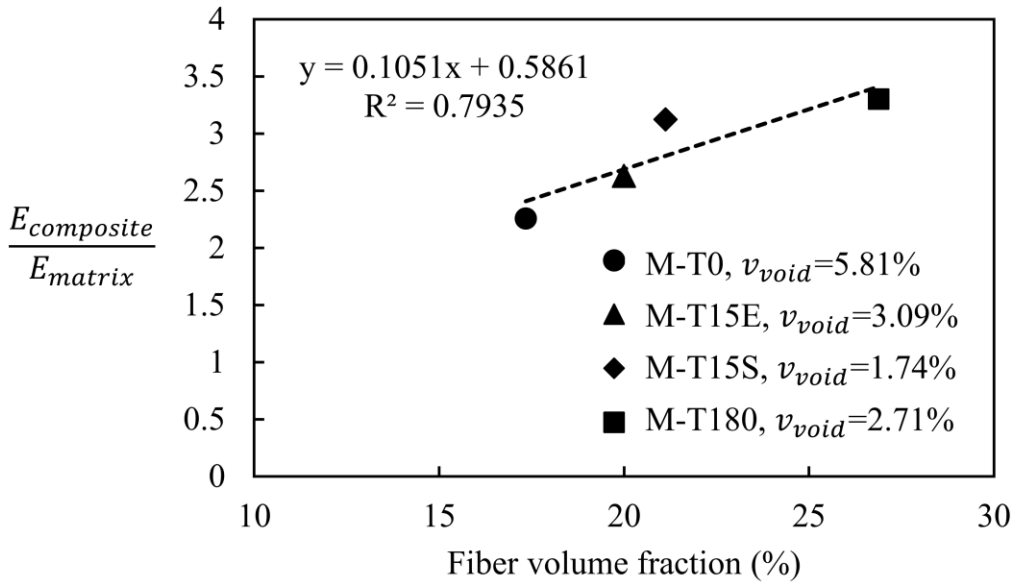

Figure 19. Variation of flexural stiffness ratio (composite/matrix) with fiber volume fraction obtained at different fabrication scenarios. Void volume fractions, v_{void}, of different scenarios are also given.

2.4. Concluding Remarks

An innovative composite manufacturing technique, magnet assisted composite manufacturing (MACM), was introduced to apply sufficiently high magnetic compressive pressure to composite laminates in the wet lay-up/vacuum bag (WLVB) process. The effectiveness of this manufacturing technique to increase the mechanical properties and improve laminate quality was investigated experimentally by comparing the performance of laminates fabricated by MACM/WLVB with the laminates made by the conventional WLVB process. It was shown that by MACM, more than 0.2 MPa additional consolidation pressure could be applied on top of the vacuum bag, which led to: (a) 70% reduction in void volume fraction to under 2%, (b) increase in fiber volume fraction by 55% to almost 27%, and (c) enhancement in flexural strength and stiffness

by 60% and 46%, to 253.5 MPa and 9.9 GPa, respectively compared to the WLVB process.

It was also observed that the time and duration of applying the magnets were extremely critical. Most of the voids were removed by utilizing magnets for only 15 min where the resin viscosity was at its minimum during cure, which resulted in a 70% decrease in void volume fraction to 1.74%. Interestingly, applying magnets for just 15 min even after gelation was shown to be effective enough to enhance the fiber volume fraction to 20%, and reduce the void volume fraction to 3.1%.

CHAPTER 3. Fabricating High-Quality VARTM Laminates by Magnetic Consolidation: Experiments and Process Model

In recently developed magnet assisted composite manufacturing (MACM) processes, a magnetic consolidation pressure is applied on composite laminates by a set of permanent magnets during fabrication. This magnetic pressure was shown to provide considerable benefits such as increased fiber volume fraction, improved mechanical properties, and reduced void content in wet lay-up/vacuum bag processes. In this chapter, the effectiveness of MACM to fabricate high-quality vacuum assisted resin transfer molding (VARTM) laminates is investigated and a new, transient process model for MACM is introduced. Towards this goal, 6-, 12-, and 18-ply, random mat E-glass/epoxy composite laminates were fabricated by placing Neodymium Iron Boron (NdFeB) permanent magnets on the vacuum bag either after or before the resin infusion. In both scenarios, the magnetic pressure was shown to considerably improve surface quality, reduce laminate thickness, and increase fiber volume fraction to above 50%. The flexural strength of the 6-, 12-, and 18-ply laminates was improved by more than 28%, 23%, and 11%, respectively. The flexural modulus was also enhanced substantially, at least by 41%, 34%, and 23%, for the same set of laminates. Applying the magnets before infusion increased the filling time due to decreased fabric permeability, and consequently reduced the process-induced voids to under 1%, while the baseline laminates made by conventional VARTM contained up to 6% void content. The transient magnetic consolidation model developed for this process is shown to accurately predict the fiber volume fraction and final laminate thickness for all the fabricated laminates.

3.1. Introduction

Vacuum assisted resin transfer molding (VARTM) is a commonly-used cost-effective, open-mold fabrication method for composite laminates in which the resin is infused into a fiber preform under vacuum [105]. This vacuum pressure facilitates the impregnation of the fabric, compacts the preform, and minimizes the formation and size of voids [142, 143]. The VARTM is especially suitable for fabricating large and complex parts, primarily due to the ease of fabrication and lower tooling cost [21]. This method, despite being extensively used in the energy, marine, and infrastructure industries, has two major drawbacks. First, the fiber volume fraction in VARTM is lower compared to that obtained from autoclave cure and resin transfer molding (RTM) [18, 23], which often leads to lower mechanical properties. Also, the thickness of the parts made by VARTM may vary along the resin flow direction, which is likely to yield variations of properties and fiber volume fraction within the laminate [144]. Apart from these disadvantages, resin flow during impregnation may cause flow-induced defects such as voids. It is well-known that the resin flow depends on the geometrical features of the fiber preform, whether it is single-scale such as a random mat or dual-scale such as woven or stitched fabrics [145]. The random mats, in general, have higher permeability and offer lower resistance to the flow because the fibers inside the tows are loosely arranged and randomly organized [146]. Thus, the inter-tow and intra-tow regions are impregnated simultaneously and the resin flow is governed by Darcy's law, in which flow rate is proportional to the local pressure gradient and the preform permeability [147, 148]. During the impregnation of fibrous reinforcement, since resin easily passes through high permeability zones, air entrapment may occur in local, low

permeability zones, thus forming voids within the final part [98, 99, 149, 150]. Moreover, random mats have often significant permeability variations due to inherent variations in their planar fiber density [151]. As a result, formation of voids at vastly different size scales has been observed in the laminates [87, 152]. For example, the results presented by Barraza et al. [90] revealed that random mat glass/epoxy parts manufactured by RTM at high flow rates contained as high as 7% voids. At the low flow rates, however, the void content was around 0.7% because the possibility of void entrapment became much lower.

Voids, even in small quantities, can lead to a considerable decrease of mechanical properties of composite laminates [153]. The presence of voids as low as 3% may cause early failure and reduce transverse and longitudinal tensile strength about 10-15% [154]. Moreover, at 5% void content, inter-laminar shear strength can be reduced about 20% compared to the void-free laminate [119]. In addition to the overall void fraction, the shape, size, and location of voids may considerably influence the level of degradation of mechanical properties [155]. Chambers et al. [143] found that the effect of void size distributions on mechanical properties is more significant than the bulk void content and shape. Chambers et al. also observed that large voids (area > 0.03 mm2) in the inter-ply region contribute to the propagation of the cracks and possibly influence final failure.

Fabricating high-quality VARTM composite laminates with enhanced mechanical properties is clearly of interest for a wide variety of industrial applications. To achieve this goal, an external pressure can be applied on the vacuum bag which facilitates removal of excess resin, resulting in a higher fiber volume fraction and lower

void content. Recently, a few variants of VARTM which apply additional pressure on the vacuum bag by either using autoclave or complex tooling were investigated. For example, vacuum enhanced resin infusion technology (VERITy), has been developed in which a 100 kPa autoclave pressure is applied after finishing the resin infusion in VARTM [35, 156, 157]. A uniform fiber volume fraction of 57-59% and void volume fraction of 0.4-0.6% were achieved in the unidirectional laminates made by VERITy [35]. Specialized elastomeric tooling for resin infusion (SETRI) [36] is similar to VERITy, except a uniform pressure is applied by a press instead of the autoclave after the resin infusion. In order to provide uniform consolidation pressure on the composite part, a reusable silicone vacuum bag is used [158, 159]. The fiber volume fraction of the laminates made by the SETRI process increased from 59 to 69%, and void volume fraction decreased from 3.33 to 0.45% when the consolidation pressure was increased from 103 to 689 kPa [36].

So far, all the aforementioned techniques to improve the quality of VARTM laminates are likely to require a significant capital investment with a high operating cost. The MACM method for improving laminate quality in wet lay-up/vacuum bag processes is recently introduced [160-162]. In this new fabrication method, the composite lay-up is placed between a magnetic tool plate/mold and a set of magnets which generate sufficiently high consolidation pressure. The MACM can be used for a number of industrial applications as it does not require complicated tooling or significant investment such as an autoclave or a press.

The current study extends the work on wet lay-up laminates presented in chapter 2 [160] and investigates the effectiveness of using magnetic consolidation in VARTM,

where, unlike the wet lay-up, the impregnation of the fibers takes place under vacuum. Flexural properties, fiber volume fraction, void content, and void morphology of the 6-, 12-, and 18-ply, random mat E-glass/epoxy laminates manufactured by applying magnets before and after infusion are presented and compared with those obtained from the conventional VARTM. In addition, a transient consolidation model that can predict the time-dependent magnetic pressure applied on the laminate, as well as the changes in resin pressure, laminate thickness, and fiber volume fraction during fabrication is developed, and the values obtained are compared with the experimental results. The consolidation model is then used to demonstrate the effects of critical process parameters such as the magnet type, resin viscosity, and fabric type on evolution of laminate thickness.

3.2. Experimental

3.2.1. Materials

E-glass chopped fiber mat with 0.228 kg/m^2 planar density (Fiberglast part #248) was chosen as the reinforcement. A PRO-SET epoxy resin system (resin: INF-114, hardener: INF-211; mixed at 100/27.4 wt.%) was used for all laminates. The INF-114 has a viscosity of 1433 mPa s and INF-211 has a viscosity of 14 mPa s at 22 °C. This is a low viscosity resin system (296 mPa s) developed for use in resin infusion processes with approximately 117-145 min pot-life (for 150 g mixture) at room temperature (22 °C).

3.2.2. Neodymium Iron Boron Permanent Magnets

The method reported here utilizes Neodymium Iron Boron (NdFeB) permanent magnets to apply a consolidation pressure transverse to the composite laminate. Table 3

shows the properties typically reported for the N52 grade, 2.54 × 2.54 × 1.27 cm^3 (length × width × thickness; magnetized through the thickness) NdFeB magnets (K&J Magnetics, Inc.) chosen for this work. N52 grade generates the highest magnetic field among the NdFeB magnets with a maximum energy product of 393.6 kJ/m^3, and can be used to generate the high pressure needed for effective consolidation. It is well-known that a higher temperature reduces the energy product of N52 NdFeB magnets such that the energy product will be lost reversibly by 20% at the maximum operating temperature of 80 ºC. The temperature rise above 80 ºC leads to a dramatic, irreversible reduction in energy product. Accordingly, 60 ºC was chosen for the cure temperature of laminate which is lower than the maximum operating temperature of the magnets. At this temperature, only a reversible 6% reduction in the energy product of the magnet is expected.

Table 3. Properties of NdFeB permanent magnets chosen in this work.

Magnetic characteristic	Values
Grade	N52
Dimensions (length × width × thickness)	2.54 × 2.54 × 1.27 cm^3
Weight	61.5 g
Surface magnetic field	0.49 T
Maximum operating temperature	80 ºC
Maximum energy product (BH_{max})	393.6 kJ/m^3
Maximum magnetic pressure	0.64 MPa

Another important factor that affects the magnetic pressure is the gap between the magnet and the bottom tool plate (i.e., lay-up thickness). The maximum magnetic

pressure of 0.64 MPa can be achieved when two magnetic plates are located on both sides of the N52-2.54 × 2.54 × 1.27 cm^3 magnet without any gap. Fig. 20 shows the change in magnetic compressive pressure with lay-up thickness. The dashed line shows experimental data measured by a mechanical testing system and the solid line represents the data from the N52 NdFeB magnet product specifications. The magnetic compressive pressure depends on the lay-up thickness and hence on the number of plies. It is seen that with increasing the lay-up thickness, the magnetic compressive pressure drops off almost exponentially. It should be noted that as the laminate consolidates from the initial to the final thickness during cure, the magnetic compressive pressure increases. For example, as the 6-ply lay-up thickness was reduced from 1.8 to 1.5 mm, the magnetic pressure increased from 0.35 to 0.38 MPa as shown in Fig. 20. Similarly, the thickness of the 12-ply lay-up reduced from 3.1 to 2.6 mm, indicating a pressure increase from 0.25 to 0.28 MPa. For the 18-ply laminate, the lay-up thickness decreased from 4.3 to 3.7 mm, indicating a pressure increase from 0.19 to 0.22 MPa.

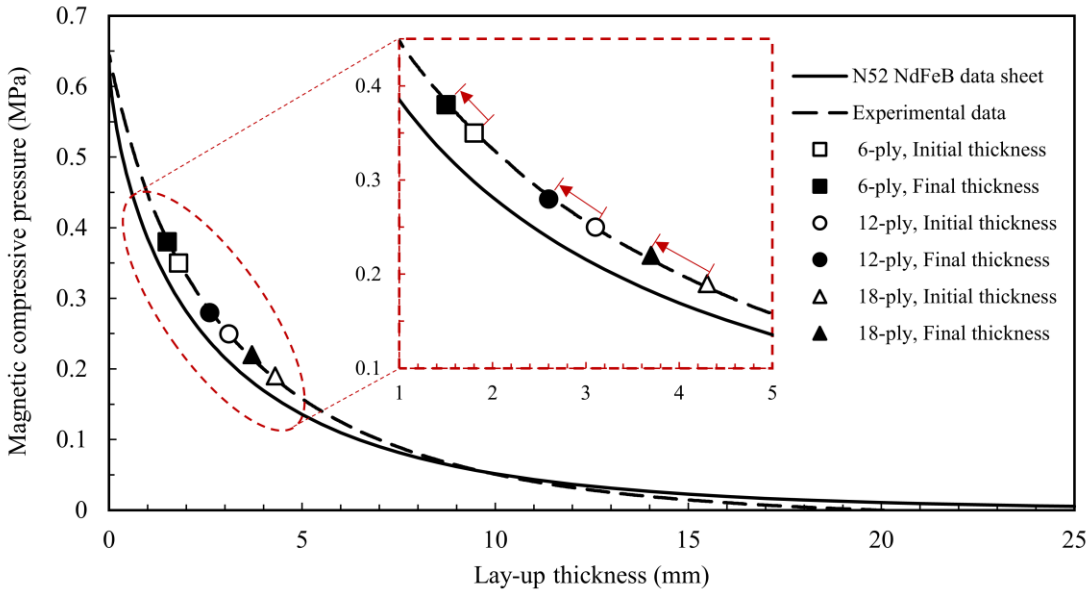

Figure 20. Variation of the magnetic compressive pressure generated by NdFeB N52-2.54 × 2.54 × 1.27 cm^3 magnets during the cure for different lay-up thicknesses. The inset displays the magnetic pressure variation during cure for 6-, 12-, and 18-ply laminates.

3.2.3. Fabrication of Composite Laminates

The implementation of magnet assisted composite manufacturing (MACM) in VARTM is schematically depicted in Fig. 21. The 16.5 × 12.7 cm^2 laminate in VARTM was compacted by the compressive force of twenty-five, N52-2.54 × 2.54 × 1.27 cm^3 permanent magnets arranged to cover a 12.7 × 12.7 cm^2 area. The magnets were first placed on a 4.76 mm-thick top steel plate in the five-by-five square configuration as shown in Fig. 22. Then, the typical VARTM lay-up was prepared on a 6.35 mm-thick, 400 series stainless steel bottom tool plate. The vacuum system consisting of the vacuum chamber, pressure regulator, and the vacuum pump was used to draw a sustained 93 kPa of vacuum pressure. A release film was placed over the multiple plies of E-glass mat, the mold was sealed with a vacuum bag, and then the resin was infused

at 20 °C under vacuum pressure. After the filling was complete, the inlet line was clamped while the exit vacuum line was kept open to remove excess resin.

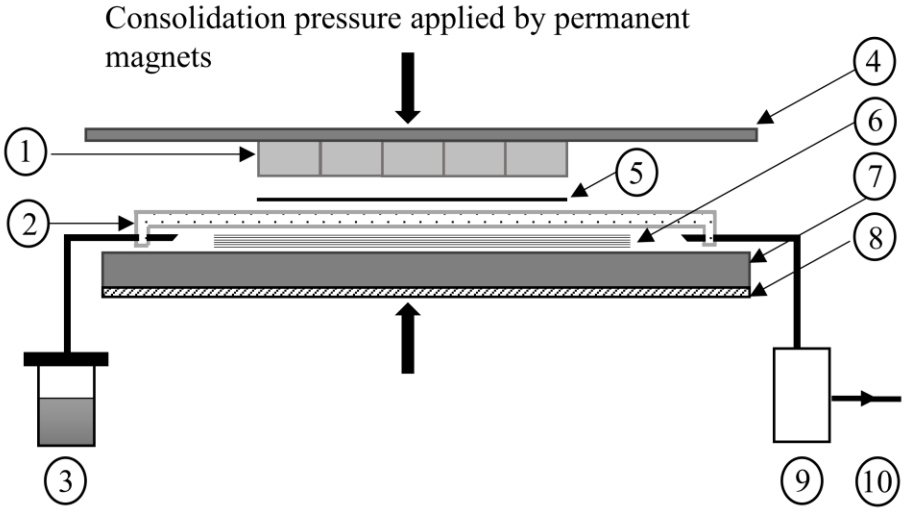

1-Magnets
2-Vacuum bag
3-Resin source
4-Magnetic steel plate
5-Aluminum caul plate
6-Lay-up
7-Magnetic bottom tool plate
8-Heating sheet
9-Resin trap
10-Vacuum line

Figure 21. Application of magnetic consolidation pressure on the composite lay-up in VARTM process.

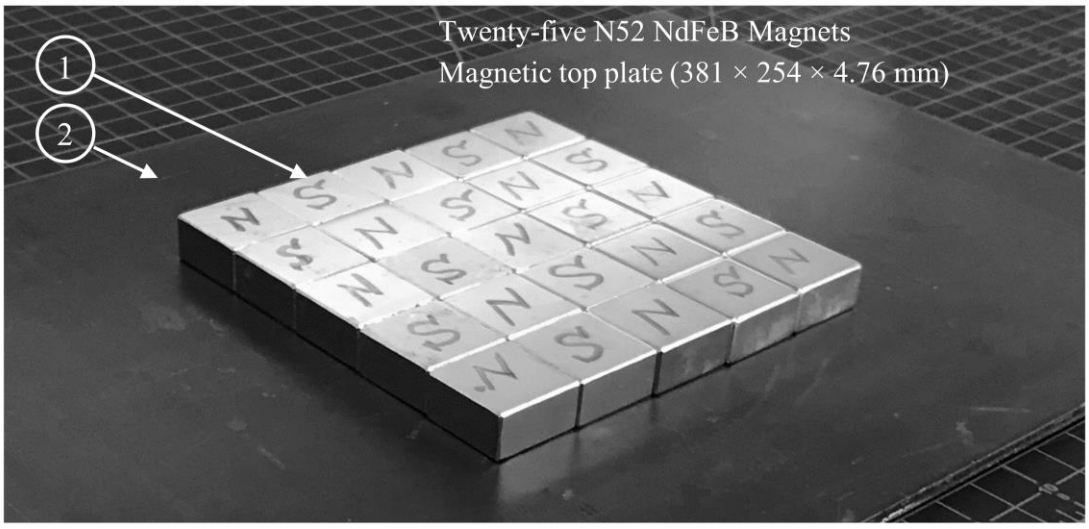

Figure 22. The square five-by-five configuration of NdFeB N52-2.54 × 2.54 × 1.27 cm^3 magnets used to apply the magnetic consolidation pressure on the lay-up.

As mentioned earlier, an important problem encountered in manufacturing random mat laminates has been the short filling time which raises the risk of trapping voids [90]. Meanwhile, the reinforcement permeability which primarily depends on the fibrous structure of the mat/preform would have a decisive influence on the filling time [163]. As a result, compacting multiple layers of fiber mats would reduce the pore volume and permeability, thus leading to a reduction in resin flow rates and an increase in filling time. Therefore, whether the pressure is applied on the lay-up after or before the infusion may have a direct effect on the formation and growth of voids in the part. From this viewpoint, the effects of applying magnetic compaction after or before infusion on the filling time and the overall quality of final parts are investigated. In the first case, the magnetic pressure was applied right after the resin infusion was completed. In the latter case, the magnetic pressure was applied on the dry fiber bed by placing the magnets on the lay-up before infusion, thus infusing the resin into the compacted fibers.

In addition, given that the applied magnetic pressure will be lower for the increased lay-up thickness, it is important to investigate the effectiveness of magnetic consolidation for thicker laminates. Consequently, a variety of fabrication scenarios is used to evaluate the performance of MACM for thin (6 plies) as well as moderately thick (12 and 18 plies) VARTM laminates.

Table 4 describes the nine different scenarios used to fabricate the composite laminates. The laminates were cured under the same thermal cycle in all scenarios. Forty-five minutes after the start of resin infusion, the mold was heated to 60 °C using a silicone-rubber heating sheet placed on the bottom surface of the tool plate. The mold

was kept at 60 °C for 8 h to complete the curing. To determine the repeatability of the fabrication process and uniformity of laminate properties, two laminates were manufactured under each scenario.

Table 4. Nine fabrication scenarios used in the manufacturing of random mat E-glass/INF 114-INF 211 epoxy laminates.

Fabrication scenario		Manufacturing process
1	V6	6-ply, VARTM, without external pressure
2	V6-M-AIN	6-ply, VARTM, magnets applied after infusion
3	V6-M-BIN	6-ply, VARTM, magnets applied before infusion
4	V12	12-ply, VARTM, without external pressure
5	V12-M-AIN	12-ply, VARTM, magnets applied after infusion
6	V12-M-BIN	12-ply, VARTM, magnets applied before infusion
7	V18	18-ply, VARTM, without external pressure
8	V18-M-AIN	18-ply, VARTM, magnets applied after infusion
9	V18-M-BIN	18-ply, VARTM, magnets applied before infusion

The first scenario, V6, is the conventional VARTM of 6-ply laminates without applying any external pressure. Scenario 1 was used as a reference to compare scenarios 2 (V6-M-AIN) and 3 (V6-M-BIN), where magnets were applied after and before the infusion. More specifically, in scenario 2, the magnets were placed on the 0.3-mm thick aluminum caul plate and vacuum bag/lay-up 45 min after the resin infusion. This is exactly when the mold temperature is increased to 60 °C which leads to a considerable drop in resin viscosity. It has been previously observed that applying consolidation pressure when the resin viscosity is minimum further enhances resin flow and facilitates void migration [79, 164]. In scenario 3, however, magnets were placed on the caul plate

and 6-ply lay-up before the resin infusion and kept on the lay-up during the whole cure cycle. In this case, the fiber mat was compacted before the infusion, which significantly decreased fabric permeability, increased the filling time, and thus affected the void content as well as the fiber volume fraction.

Following the same procedure utilized for the first three scenarios, 12-ply and 18-ply laminates were fabricated in the fourth, fifth, and sixth scenarios (V12, V12-M-AIN, and V12-M-BIN) and in the seventh, eighth, and ninth scenarios (V18, V18-M-AIN, and V18-M-BIN), respectively.

To determine the effects of magnetic consolidation pressure more accurately and avoid possible edge effects, all the composite specimens used in the void and fiber volume fraction characterization and mechanical properties measurements were removed only from an area under the magnets.

3.2.4. Void and Fiber Volume Fraction Measurement

The weight fraction of fiber and resin for each specimen were obtained using resin burn-off technique as per ASTM D2584-11. This is the most commonly used method for glass fiber reinforced polymer composites since the matrix burns at 450-600 °C while the glass fibers remain mostly unaffected [165, 166]. As per the standard, three samples from each laminate were used in resin burn-off inside a furnace at 600 °C for 4 h. Burn-off temperature and duration were chosen according to the thermogravimetric analysis (TGA) of composite samples, which indicated that approximately a 5.34% fiber mass loss occurs at 600 °C, probably due to the burning off the fiber sizing. This mass loss from fibers was accounted for in void and fiber

volume fraction calculations. The reinforcement and void volume fractions were obtained from the following equations according to ASTM D3171-15:

$$V_m = \frac{\rho_c}{\rho_m}\left(\frac{w_c - w_f}{w_c}\right) \quad (8)$$

$$V_f = \frac{\rho_c}{\rho_f}\left(\frac{w_f}{w_c}\right) \quad (9)$$

$$V_v = 1 - (V_m + V_f) \quad (10)$$

where V_m is the resin volume fraction, V_f is the fiber volume fraction, V_v is the void volume fraction, ρ_c is the density of composite, ρ_m is the density of resin, ρ_f is the density of fiber, w_c is the sample weight, and w_f is the fiber weight.

This technique relies on the knowledge of the composite, resin, and fiber density. The actual density of the composites was measured by suspending the specimens in a solution of Cargill Labs heavy liquids (2.49 g/cm^3) diluted with water. In the same way, the density of void-free resin cured under identical conditions was measured to be 1.152 ± 0.003 g/cm^3. The density of glass fibers was determined using a nitrogen pycnometer to be 2.470 ± 0.004 g/cm^3.

3.2.5. Image Analysis

Microscopic image analysis, one of the most accurate methods for characterizing the void morphology [79, 167-171], was used in this work to probe the salient features of the microstructure. Two 2.54 cm-long specimens were cut from each laminate, mounted in an acrylic resin, and polished. Then, the specimens were sputter coated with gold/palladium to avoid charge build-up. Scanning electron microscopy (SEM) with image analysis was carried out to characterize the location, size, and shape of voids

through-the-thickness of the laminates. SEM images at both the 20X and 150X magnifications were obtained using a Zeiss Neon 40 EsB model.

In order to evaluate the variation in void sizes at different specimens, equivalent diameter, D_{eq}, was used,

$$D_{eq} = \sqrt{\frac{4A}{\pi}} \tag{11}$$

where A represents the void area. Three different size-classes are then identified: small, medium, and large. The small voids have an equivalent diameter smaller than 100 μm, medium voids have equivalent diameters ranging from 100 μm to 200 μm, and the large voids have equivalent diameters larger than 200 μm.

The shape morphology of the voids can be characterized by a dimensionless roundness parameter, R, given by,

$$R = \frac{4A}{\pi d_{max}^2} \tag{12}$$

where d_{max} is the maximum diameter of void [167]. Higher values of roundness, $0.9 < R \leqslant 1$, correspond to more circular voids with regular shapes. A roundness value of $0.25 < R \leqslant 0.9$ represents elliptical voids. The lower roundness, $R \leqslant 0.25$, is related to the elongated voids.

3.2.6. Flexure Test

Three-point bending flexural tests were conducted according to ASTM D790 to evaluate flexural strength and modulus of each specimen. The fabricated laminates were cut into the 11.4 cm-long and 1.3 cm-wide flexural specimens. All measurements were conducted at a cross-head speed of 2 mm/min using a Com-Ten (Model #705TN) testing system. The span-to-depth ratio was maintained at 24:1. Since the support span-

to-depth ratio was large (>16) and the deflections occurred in excess of 10% of the support span, the following equations were used for calculating the flexural properties.

$$\sigma = \left(\frac{3PL}{2bd^2}\right)\left[1 + 6\left(\frac{D}{L}\right)^2 - 4\left(\frac{d}{L}\right)\left(\frac{D}{L}\right)\right] \quad (13)$$

$$E = \frac{L^3 m}{4bd^3} \quad (14)$$

In Eqs. (13-14), σ is the stress in the outer fibers at the midpoint, P is the load at a given point on the load-deflection curve, L is the support span, b is the sample width (≈ 1.3 cm), d is the sample thickness, and D is the deflection of the centerline of the sample at the middle of the support span. Also, E is the flexural modulus and m is the slope of the tangent to the initial straight-line portion of the load-deflection curve. Seven specimens from each laminate leading to total 14 test specimens for each fabrication scenario were tested to determine the average values with a confidence interval of 95% for flexural strength and modulus.

3.3. Modeling of Consolidation of VARTM Laminates under Magnetic Pressure

Predicting the final laminate thickness and fiber volume fraction is of particular importance in assessing the effectiveness of applying magnetic pressure in VARTM. Considering that the pressure would be dependent on the lay-up thickness and its change during the process, utilizing an appropriate set of magnets to generate the desired level of compaction is necessary. For this purpose, a time-dependent, one-dimensional consolidation model is developed by extending the consolidation model initially proposed by Gutowski et al. [50, 172]. In this extended model, the magnetic force acts normal to the saturated preform and is dependent on the lay-up thickness. The

resulting resin flow is parallel to the laminate and a uniform, through-the-thickness compaction takes place as schematically illustrated in Fig. 23.

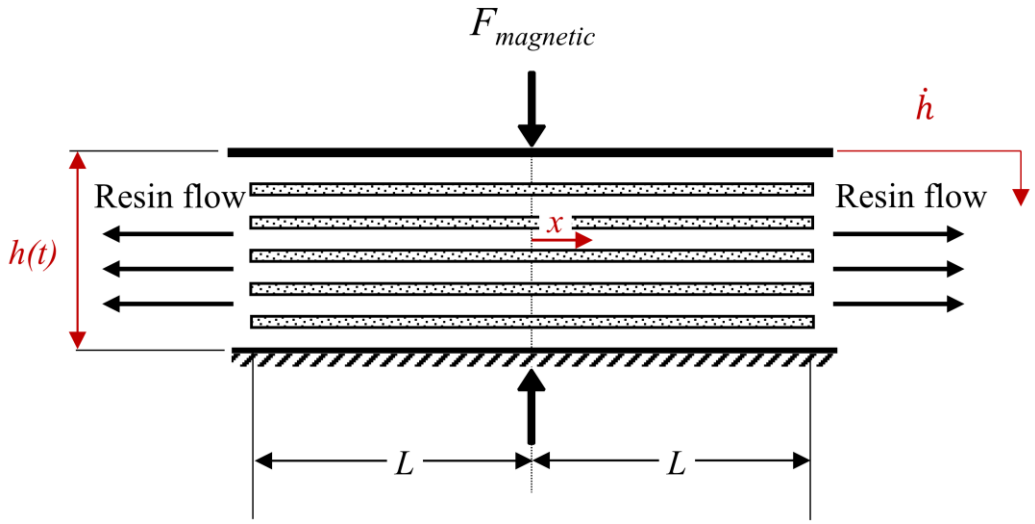

Figure 23. Schematic illustration of the resin flow parallel to the laminate plate due to magnetic force.

During consolidation, the applied pressure is supported by both the resin and the fiber. Thus, the change in resin pressure equation can be expressed by combining Darcy's law and the conservation of mass [173, 174],

$$\frac{\partial^2 P_r}{\partial x^2} = \frac{\mu \dot{h}}{K_{xx} h} \tag{15}$$

where P_r is the resin pressure, μ is the resin viscosity, h is the thickness of the saturated preform ($\dot{h}$ is the temporal thickness change), and K_{xx} is the planar fabric permeability in x direction (parallel to the laminate). The corresponding boundary conditions in the x direction can be expressed in terms of the resin pressure as (see Fig. 23),

$$x = 0, \quad \frac{\partial P_r}{\partial x} = 0 \quad \text{(symmetric boundary conditions)} \tag{16}$$

$$x = L, \quad P_r = 0 \tag{17}$$

where $2L$ is the length of the laminate ($2L$=12.7 cm). Integration of Eq. (8) from x=0 to x=L yields the resin pressure, as,

$$P_r(x) = \frac{\mu \dot{h}}{2K_{xx}h}(x^2 - L^2) \tag{18}$$

Thus, the total force generated by the resin pressure can be determined by an integral over the area of the laminate,

$$F_r = \int_{x=-L}^{x=L} P_r(x)dA = -\frac{2\mu \dot{h}}{3K_{xx}h}(WL^3) \tag{19}$$

where W is the width of the laminate (W=12.7 cm). The permeability is estimated by the commonly-used Carman-Kozeny equation as,

$$K_{xx} = \frac{\left(1 - V_f\right)^{n+1}}{C\left(V_f\right)^n} \tag{20}$$

where C=7.4×10^8 (m^{-2}) and n=0.9 are constants and V_f is the fiber volume fraction [163]. Considering these empirical constants, the permeability of the random mat used in this work would be in the order of 10^{-10} m^2. As the thickness of laminate is uniform at a given time, the fiber stress does not vary across the laminate, so the force carried by the fiber (F_f) can be calculated by:

$$F_f = \sigma_f S = \sigma_f(2LW) \tag{21}$$

where σ_f is the fiber stress and S is the surface area of the laminate. The non-linear fiber stress is estimated as a function of fiber volume fraction using [50]:

$$\sigma_f = A_s \frac{\sqrt{\frac{V_f}{V_o}} - 1}{\left(\sqrt{\frac{V_a}{V_f}} - 1\right)^4} \tag{22}$$

where A_s is the spring constant, V_a is the maximum possible fiber volume fraction, and V_o is the initial fiber volume fraction. To determine these fabric parameters, the wet compaction tests were performed for the random mat fibers used in the laminates at an Instron testing equipment. Then, from the compaction tests, the parameters in Eq. (22) are estimated to be A_s=0.48 kPa, V_a=0.65, and V_o =0.45. Also, the fiber volume fraction is related to the thickness using [175]:

$$V_f = \frac{M_s N_f}{h\rho_f} \tag{23}$$

where M_s is the areal density of fiber mat, N_f is the number of fabric plies, h is the thickness of fabric stack, and ρ_f is the fiber density. In order to maintain the force balance, the applied magnetic force should be equal to the sum of the forces taken by resin and fiber. Thus, the total magnetic force ($F_{magnetic}$) can be determined by the following equation:

$$F_{magnetic} = F_r + F_f = \sigma_f S + \int P_r dS \tag{24}$$

From the magnetic pressure versus lay-up thickness curve given in Fig. 20, the magnetic force generated by one NdFeB N52-2.54 × 2.54 × 1.27 cm^3 magnet can be expressed as an exponential function of thickness.

$$F_{magnetic} = N(Ae^{-Bh}) \tag{25}$$

where N is the number of permanent magnets placed on the lay-up (in this work N=25), and A and B are empirical constants, which are found to be 374.4 N and 260.2 m^{-1}, respectively from the data shown in Fig. 20. Substitution of Eq. (25) into Eq. (24) gives

the governing equation for the evolution of laminate thickness under a thickness-dependent magnetic compaction pressure.

$$\dot{h} = \left(\frac{-3K_{xx}h}{2\mu WL^3}\right)\left[N(Ae^{Bh}) - A_s \frac{\sqrt{\frac{M_s N_f}{h\rho_f V_o}} - 1}{\left(\sqrt{\frac{h\rho_f V_a}{M_s N_f}} - 1\right)^4}(2LW)\right] \tag{26}$$

Equation (26) is a first order nonlinear homogeneous differential equation which can be accurately solved by using an explicit finite difference scheme. First, the temporal change of laminate thickness in Eq. (26) is determined in each time step (Δt); then, the laminate thickness is updated as, $h^{n+1} = h^n + (\dot{h})^n \Delta t$, for the next time step (n+1). In this method, the truncation error is $O[\Delta t]$, thus a sufficiently small Δt needs to be used for accurate solution.

By using this model, the final thicknesses of the cured laminates are predicted and compared with the experimental results presented later in the results section. The effects of critical process parameters such as the selection of the magnet type, resin viscosity, and the preform permeability are also investigated and presented later.

3.4. Results and Discussion

3.4.1. Experimental Results

3.4.1.1. Laminate Thickness, Fiber Content and Void Volume Fraction

Laminate thickness, fiber volume fraction, void volume fraction, and the filling times of the 6-, 12-, and 18-ply laminates manufactured under nine different scenarios are presented in Table 5. In the baseline V6, V12, and V18 scenarios, the laminates were manufactured by conventional VARTM using 6-, 12-, and 18-ply random mat E-

glass fibers, respectively. The average thickness of these laminates was measured to be about 1.45 mm for 6-ply, 2.83 mm for 12-ply, and 3.99 mm for 18-ply laminates. The other six scenarios were used to investigate the effect of applying magnetic pressure after resin infusion (V6-M-AIN, V12-M-AIN, and V18-M-AIN) and before resin infusion (V6-M-BIN, V12-M-BIN, and V18-M-BIN) on the quality of VARTM laminates. Utilizing the magnetic pressure, either after or before the resin infusion, substantially reduced the average thickness of the laminates, ranging from more than 18% for the 6-ply to 13% for the 18-ply laminates. Interestingly, applying magnets after or before the infusion yielded similar thickness reduction levels, as compacting the dry or resin filled fibers did not seem to make a discernable difference in the level of compaction achieved. As expected, these reductions in the laminate thicknesses are highly correlated with the increase in the fiber volume fraction of the laminates where the fiber volume fraction of the 6-, 12-, and 18-ply laminates improved notably from 43-47% to 51-53% due to magnetic pressure, representing a fairly significant 10 to 22% increase.

In the 6-ply and 12-ply VARTM laminates (V6 and V12), 1.9 and 1.2% void volume fraction were obtained, respectively; whereas in 18-ply laminates (V18), void volume fraction was high at approximately 5.7%. When the magnets were applied after infusion (V6-M-AIN and V12-M-AIN), the void content was around 2%, which is slightly higher than those in the conventional VARTM laminates. In fact, applying external pressure on the 6- and 12-ply laminates by placing the magnets after infusion reduced the permeability of the fiber bed, and very likely, restricted the removal of mobile voids, which could have otherwise been removed by the vacuum. A similar

phenomenon has been recently reported for the laminates fabricated by wet lay-up/vacuum bag method [160]. Interestingly, in 18-ply laminates (V18-M-AIN), the high void content of 5.7% was considerably reduced to 2.3%, which suggests that, despite a reduction of void mobility, magnetic pressure can suppress the growth of voids, reduce their sizes, or break them into smaller ones, even after the infusion is complete and most of the voids are formed.

In contrast, placing magnets on the vacuum bag before the infusion had a strikingly different and much favorable effect on the void content. For all three laminates (i.e., V6-M-BIN, V12-M-BIN, and V18-M-BIN), a very low void content of 0.1 to 0.8% was recorded as listed in Table 5. Clearly, placement of the magnets before infusion increased the filling time from approximately 3 min for all cases to 23, 16, and 12 min for 6-, 12-, and 18-ply laminates, respectively. The increased filling times led to much lower infusion velocities and, thus, could decrease the risk of void entrapment as well as prevent the growth of voids due to the compacted fiber bed. The substantial reduction of void content at a lower infusion speed has also been reported in earlier experimental investigations [90, 176].

Table 5. The average thickness, fiber volume fraction, void volume fraction, and filling time for composite laminates manufactured by nine different scenarios (n=6 for fiber and void volume fractions and n=42 for thicknesses measurements, results reported with 95% confidence intervals).

Fabrication scenario		Number of plies	Average thickness (mm)	Fiber volume fraction (%)	Void volume fraction (%)	Filling time (min)
1	V6	6	1.45 ± 0.02	45.71 ± 0.14	1.86 ± 0.72	3
2	V6-M-AIN	6	1.19 ± 0.01	51.95 ± 1.07	2.32 ± 1.08	3
3	V6-M-BIN	6	1.16 ± 0.01	51.76 ± 0.99	0.21 ± 0.09	23
4	V12	12	2.83 ± 0.03	43.23 ± 0.17	1.15 ± 0.14	3
5	V12-M-AIN	12	2.31 ± 0.02	52.58 ± 0.63	2.16 ± 0.51	3
6	V12-M-BIN	12	2.31 ± 0.01	52.81 ± 0.66	0.82 ± 0.45	16
7	V18	18	3.99 ± 0.04	46.61 ± 0.18	5.66 ± 0.65	3
8	V18-M-AIN	18	3.39 ± 0.01	52.72 ± 0.41	2.28 ± 1.45	3
9	V18-M-BIN	18	3.49 ± 0.02	51.28 ± 0.36	0.12 ± 0.11	12

It should be noted that decreasing the filling rate may cause premature gelation during fabrication of large parts. To alleviate this concern, MACM can be used in different ways. One is placing the magnets before infusion only at a desired location, without covering the entire surface of the part, leading to the local improvement of part quality. Thus, without having a considerable effect on the total filling rate, it would be possible to fabricate a large VARTM part that has a region of higher fiber volume fraction and lower void content. Second is placing magnets after the filling is complete, where covering the entire laminate surface would only be practical for small to medium sized parts. Another possibility is to move the magnets with a small footprint over a

larger lay-up surface after the infusion, thus making fabrication of much larger laminates with MACM feasible.

It is also interesting to note that the average thickness per ply of the V6, V12, and V18 laminates were 0.242, 0.236, and 0.222 mm/ply, respectively which shows a slight descending trend. This could be because of the increased nesting effect with the number of plies which would lead to an improved compaction behavior of the fabric stack and reduction of the average thickness per ply as reported by Chen and Lin [177]. Moreover, the average thickness per ply of the V6-M-BIN, V12-M-BIN, and V18-M-BIN laminates was reduced to approximately 0.193 mm/ply for all three cases, which was primarily due to the magnetic pressure, and to a lesser extent, due to nesting.

3.4.1.2. Qualitative Analysis of Magnetic Pressure on the Laminates

In order to obtain the imprints of the magnetic pressure distribution on the lay-up, very thin (<0.2 mm) pressure films (Fujifilm Prescale) were used in separate experiments. These imprints would be helpful in the visual inspection of the level and spatial uniformity of the pressure applied by the magnets. The pressure films were wrapped, sealed under the release film and placed on the bottom tool plate, which ensures the films remained isolated from the resin. Using identical process parameters, several additional fabrication experiments were performed with pressure films to evaluate the magnetic pressure patterns on 6-, 12-, and 18-ply lay-up. However, considering the maximum allowed temperature of the films was 35 °C, the mold temperature was not increased to 60 °C as was done in fabricating laminates. Without the temperature increase, there would be less resin flow, which in turn would lead to a higher lay-up thickness and application of slightly lower magnetic pressures. Hence, the

primary goal in using the pressure films was not the quantitative measurement of pressure, but to validate the application of different pressure levels on three different laminate thicknesses as well as obtaining approximate values which can be cross-checked against the values given in Fig. 20.

Fig. 24 shows the scanned images of pressure films that were placed directly under the magnets for 6-, 12-, and 18-ply lay-ups. The three images clearly depict changing color intensities from dark to light pink as the lay-up thickness is increased. The pressure film used under the 6-ply lay-up shows a uniform, higher color intensity, indicating a uniform and higher magnetic pressure compared to both 12- and 18-ply laminates. As expected, the film under the 18-ply lay-up has the lowest color intensity, and thus shows the lowest pressure. Based on the analysis of color intensities, the average pressure for the 6-ply lay-up is estimated to be 0.37 MPa, whereas the images from 12-ply and 18-ply laminates indicate an average pressure of 0.26 MPa and 0.18 MPa, respectively. Although these pressure values are expected to contain a very high, more than 15% experimental uncertainty, they agree well with the pressure ranges presented earlier in Fig. 20.

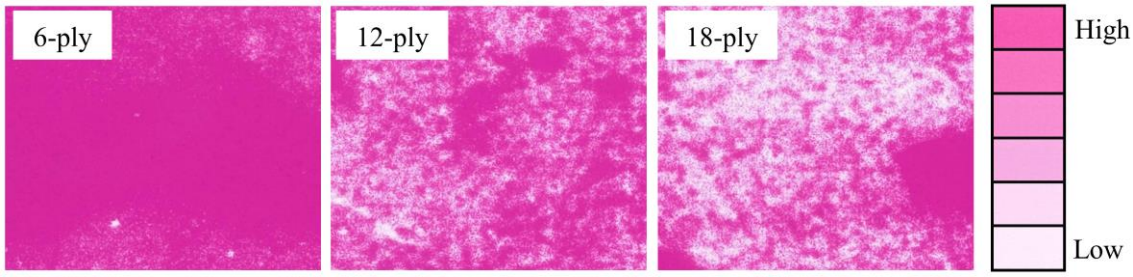

Figure 24. Samples of pressure films stained under magnetic pressure in 6-, 12-, and 18-ply lay-up. The pink coloration on the pressure film enhances with increasing pressure.

3.4.1.3. Changes in Lay-up Thickness due to Magnetic Compaction during VARTM

In order to elucidate the effect of magnetic pressure on the temporal changes of lay-up thickness and to provide further insight into the compaction behavior, the actual lay-up thickness of 6-ply laminates, fabricated by three different scenarios (V6, V6-M-AIN, and V6-M-BIN), was measured over time. For this purpose, a dial gage was placed at the center of the lay-up, 83 mm away from the inlet. Fig. 25 shows the change in thicknesses for these three cases during 120 min, including the labels for completion of the impregnation/clamping the inlet (C), placement of magnets (M), and heating of the mold (H) in each case.

Fig. 25 can best be analyzed by highlighting the distinct consolidation behavior in the following three different time zones: i) impregnation; ii) consolidation after the impregnation is complete and the inlet is clamped until the start of the mold heating (H); iii) consolidation behavior after the first 45 min (i.e., after magnets are placed for V6-M-AIN and the start of the heating for all cases).

During impregnation, the advancing resin front caused a rapid drop in the lay-up thickness due to the nesting of the fiber layers. The nesting of fibers can be explained by the lubrication effect which facilitates movement of tows or fibers [24]. This behavior is captured in Fig. 25 when the resin front reached the dial gage location within the first few minutes. If the fiber bed was not under magnetic pressure, the lay-up thickness was reduced from approximately 2.0 mm to 1.9 mm within seconds. If the fiber bed has been under magnetic pressure and already compacted, the nesting effect was slightly less, evidenced by the thickness change from 1.30 to 1.25 mm, and took place over a longer time period of a few minutes. The significant effect of the magnets on the fill

time is also shown in Fig. 25, where the fill time was increased to 23 min from 3 min without the magnets.

After the impregnation was complete and resin reached the exit, the inlet was clamped (refer to point (C) in Fig. 25), preventing further resin intake. However, the reduction in the lay-up thickness continued, albeit at a much lower rate in all scenarios because of the removal of additional resin as the exit remained open. It is worth noting that compaction evolution of scenarios V6 and V6-M-AIN follow very similar paths, revealing the repeatable nature of laminate consolidation, including the nesting effects in VARTM.

The consolidation behavior after the first 45 min was mostly determined by the increase in mold temperature from room temperature to 60 ºC in all three cases (see point (H) in Fig. 25). For the scenario V6-M-AIN, the magnets were placed right before the heating started, causing a substantial drop of almost 0.4 mm within a minute in the laminate thickness from 1.70 to 1.34 mm, shown as Δh in Fig. 25. Interestingly, after the placement of magnets, the lay-up thickness reduced to a level close to that in the laminates which have been under the magnetic pressure from the start of the resin infusion (i.e., V6-M-BIN).

With the start of the temperature rise at 45 min, the lay-up thickness slightly increased ranging from 0.07 to 0.15 mm in all three scenarios which may be due to the thermal expansion effects. Simultaneously, the resin viscosity started decreasing and facilitated the removal of additional resin which, as shown in Fig. 25, led to the continuation of the thickness reduction after the brief increase in all three scenarios. At

the later stages of cure, the slope of thickness reduction is gradually reduced, and the lay-up thickness becomes almost constant after 90 min.

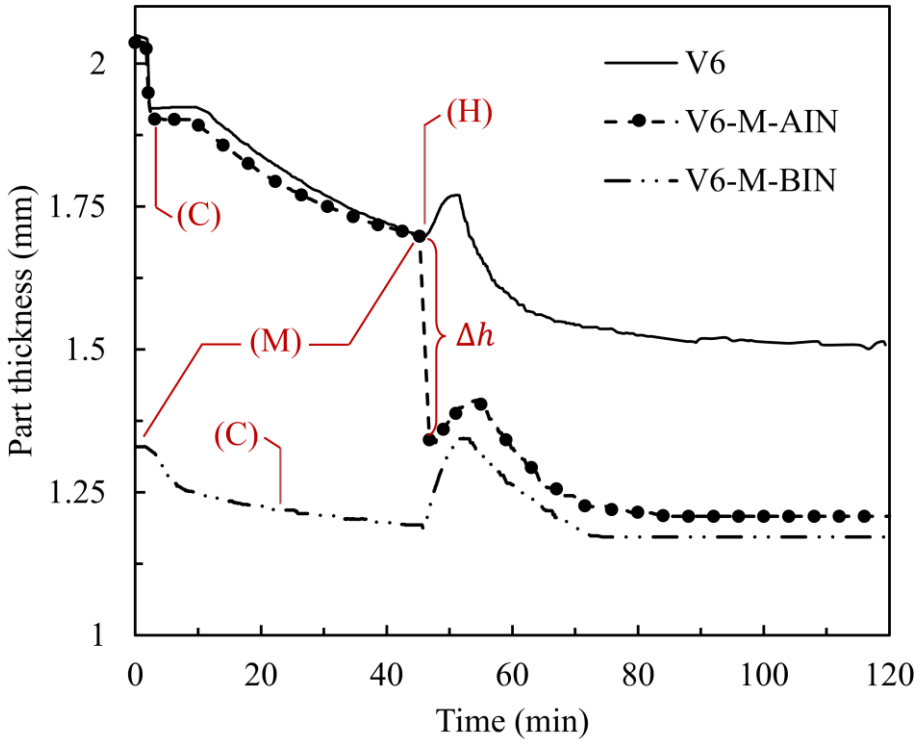

Figure 25. Temporal thickness change of the 6-ply lay-up during processing and consolidation of the laminates fabricated by conventional VARTM (V6), VARTM with applying magnetic pressure after infusion (V6-M-AIN), and VARTM with applying magnetic pressure before infusion (V6-M-BIN). Note: Impregnation is complete and inlet is clamped at point (C), magnets are placed at point (M), and the mold is heated to 60 ºC at point (H). For V6-M-AIN, the thickness reduction due to placement of magnets at 45 min is shown as Δ*h*.

3.4.1.4. Microstructural Analysis of Composite Laminates

In addition to the average void content of a laminate, the void microstructure such as shape, size, and location may have detrimental effects on mechanical properties [155]. Thus, the SEM images of the 6-, 12-, and 18-ply E-glass/epoxy laminates fabricated under different scenarios were taken at a low 20X magnification (Figs. 26-28) to inspect the cross sections of the laminates and also to characterize their

microstructure as well as void morphology. The images on the right side of the figures represent the 150X magnification of boxed area shown on the left and are helpful for the detailed analysis of the location, shape, and size of the voids and the quality of the impregnation of individual tows. The 20X magnification was chosen to cover the entire cross-section of the laminates so that the reduction of laminate thicknesses and the quality of overall laminate can be easily viewed and compared with each other. The images given in Figs. 26-28, clearly show the extent of thickness reduction and reduction of void content for all the laminates when the magnetic pressure is applied.

The representative images for the 6-ply laminates fabricated by three different scenarios (V6, V6-M-AIN, and V6-M-BIN) are given in Figs. 26 (a-c). Fig. 26 (a) shows the presence of rather large, resin rich areas between the plies, extending along the laminate length due to the lack of external pressure. These resin rich regions could possibly contribute to the spatial variation of fiber volume fraction in the laminate which would lead to nonuniform properties. Also, a low number of small- and medium-sized elliptical voids are trapped between the plies while no voids are found inside the tows. On the other hand, in Fig. 26 (b), where the magnetic pressure applied after infusion, a good consolidation of the plies can be observed, favoring the fabrication of thinner laminates with smaller resin rich regions compared to Fig. 26 (a). However, applying pressure after formation of voids restricted their mobility as removing voids from tightly compacted fiber zones would be more difficult [160]. When the magnets are placed on the part before the infusion, almost no voids and a highly-compacted fiber bed are observed, as shown in Fig. 26 (c).

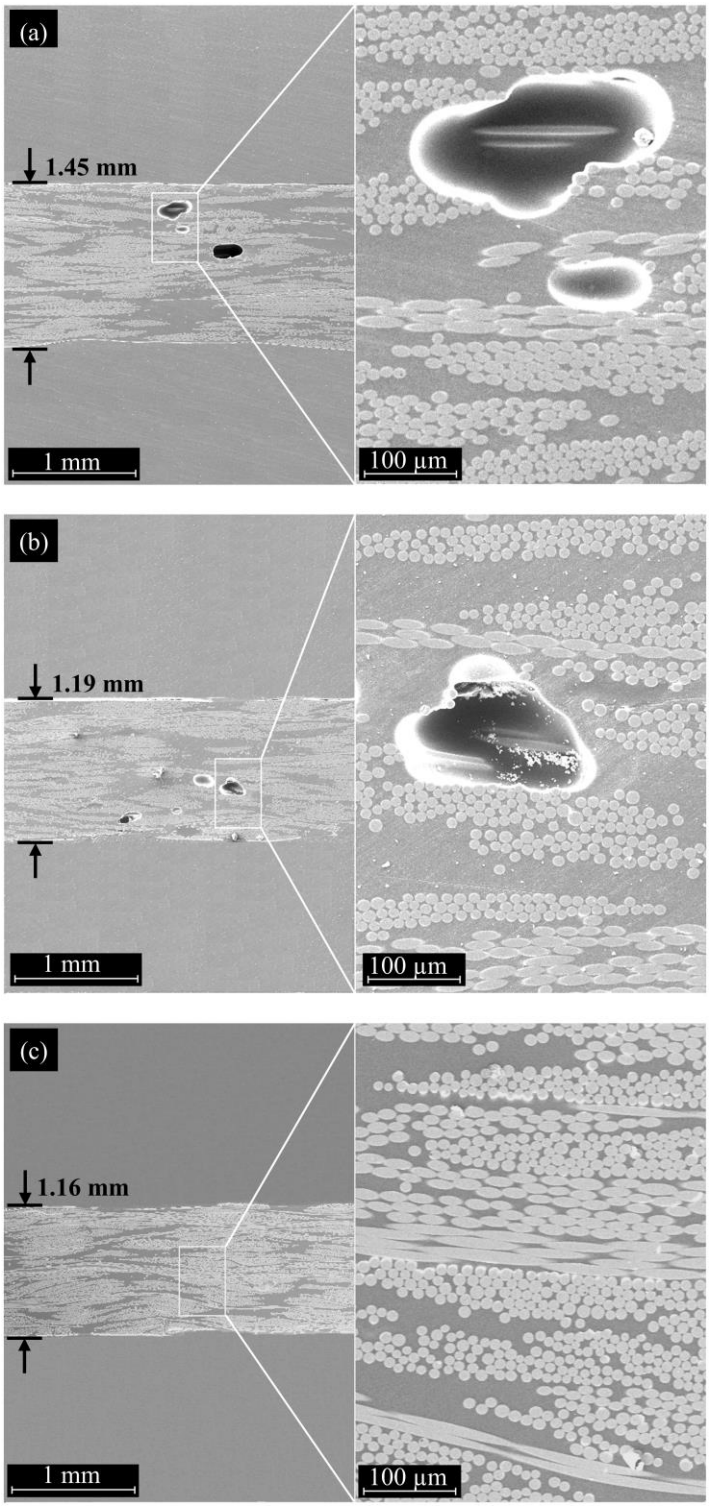

Figure 26. SEM images of the 6-ply random mat E-glass/epoxy composite laminates fabricated in different scenarios: (a) V (VARTM); (b) V-M-AIN (Magnets applied after infusion in VARTM); and (c) V-M-BIN (Magnets applied before infusion in VARTM process). Note: The left side shows 20X magnification, and the right side presents 150X magnification of the rectangular area.

Similar SEM images of 12-ply laminates are shown in Figs. 27 (a-c). In V12 laminates, voids are mostly circular or elliptical in shape, and they are mainly located between the plies. Also, no voids are noted inside the tows in these laminates (see Fig. 27 (a)). Applying magnetic pressure after infusion (V12-M-AIN) does not completely remove the trapped voids, however, the pressure seems to reduce the number and size of the voids, as well as making them more elongated as the laminate thickness is reduced (see Fig. 27 (b)). Fig. 27 (c) proves that applying magnetic pressure before infusion (V12-M-BIN) yields the best result and almost completely eliminates the void formation.

The salient features of the microstructure observed in Fig. 26 and Fig. 27 are also present in SEM images for the 18-ply laminates given in Fig. 28. The high void content (i.e. $\approx 5.7\%$) of the V18 laminate is very visible in Fig. 28 (a). Voids with different sizes and shapes are distributed nearly homogenous throughout the laminates as has been reported in Ref. [119]. When the magnets are applied after infusion (V18-M-AIN), the plies are compacted, fewer and more elongated voids appear (see Fig. 28 (b)). As in the case of 6- and 12-ply laminates, the void-free, high level of compaction is achieved for the V18-M-BIN laminate (see Fig. 28 (c)).

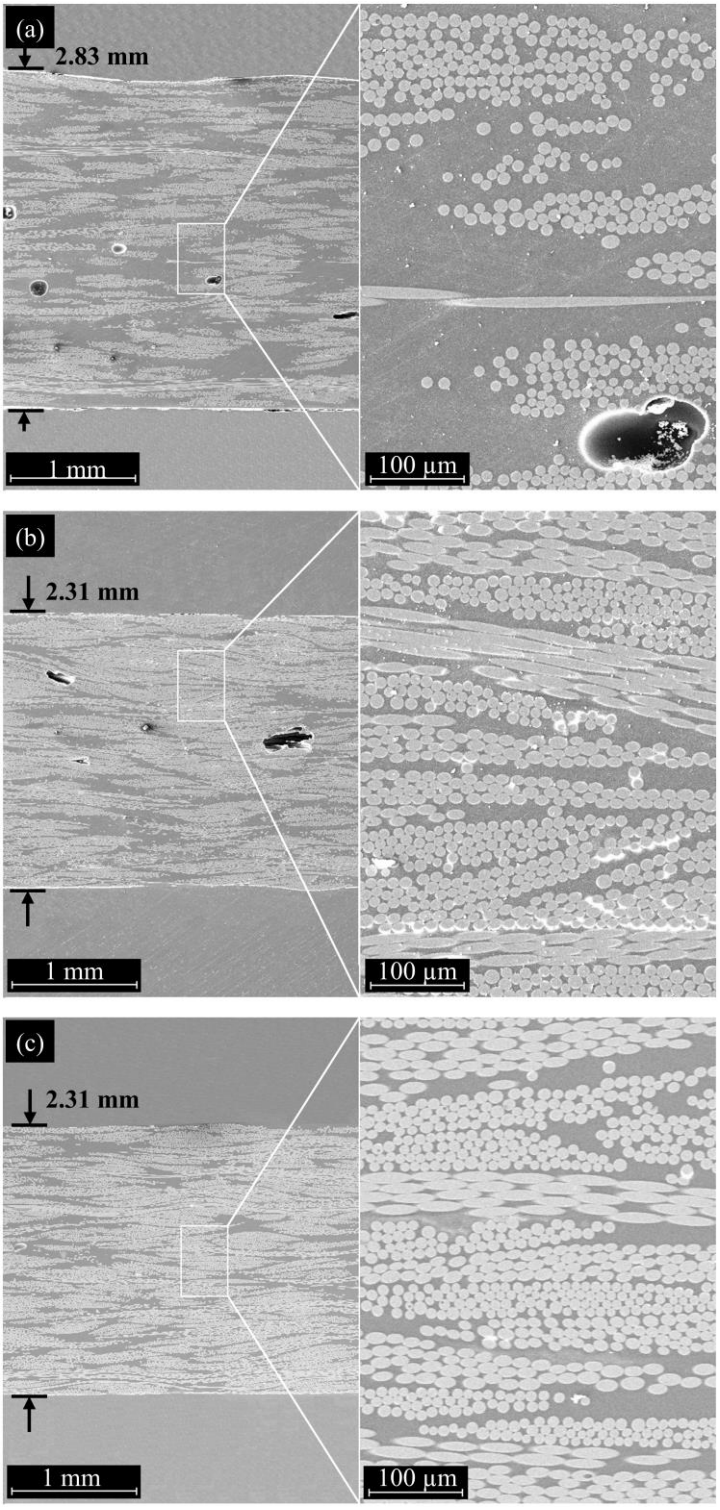

Figure 27. SEM images of the 12-ply random mat E-glass/epoxy composite laminates fabricated in different scenarios: (a) V (VARTM); (b) V-M-AIN (Magnets applied after infusion in VARTM); and (c) V-M-BIN (Magnets applied before infusion in VARTM process). Note: The left side shows 20X magnification, and the right side presents 150X magnification of the rectangular area.

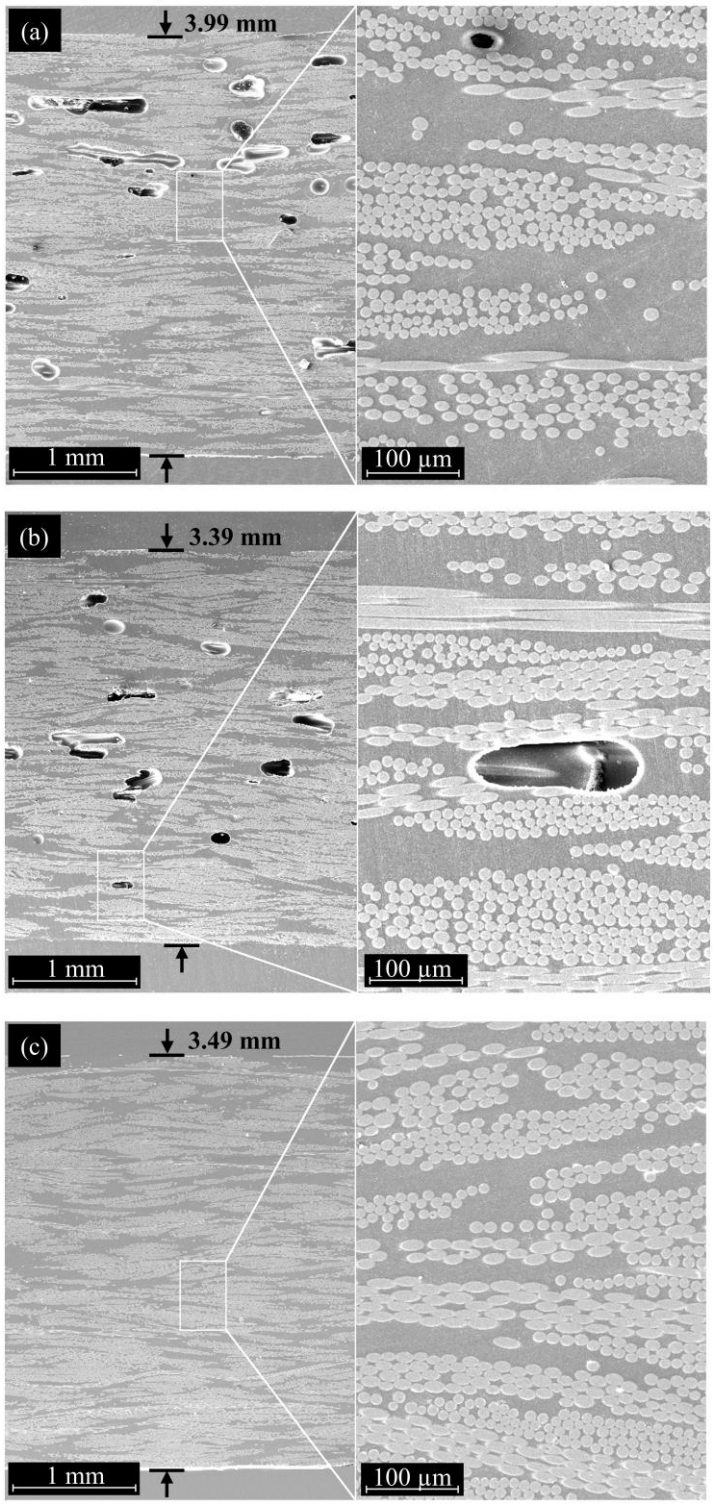

Figure 28. SEM images of the 18-ply random mat E-glass/epoxy composite laminates fabricated in different scenarios: (a) V (VARTM); (b) V-M-AIN (Magnets applied after infusion in VARTM); and (c) V-M-BIN (Magnets applied before infusion in VARTM process). Note: The left side shows 20X magnification, and the right side presents 150X magnification of the rectangular area.

3.4.1.5. Shape and Size of Voids

Detailed analyses of shape and size variations of void morphology are performed for 18-ply composite laminates. After processing all data on voids, the average void size in the conventional VARTM laminates is found to be 162.5 μm. However, after placement of magnets (V18-M-AIN), the average void size is slightly reduced to 151.4 μm. Interestingly, compaction of the lay-up before the infusion is even more effective in reducing the void size down to 115.3 μm. This could be due to the formation of smaller voids during infusion as the resin advances through a more compacted fiber bed.

Fig. 29 compares the relative percentage of small ($D_{eq} \leqslant 100$ μm), medium (100 μm < D_{eq} < 200 μm), and large ($D_{eq} \geqslant 200$ μm) voids in the 18-ply laminates. The inset in Fig. 29 depicts a sample SEM image containing different size voids. It can be seen that by applying consolidation pressure after infusion, the relative percentage of small voids increases from 27% to 33%, but in contrast, the relative percentage of large voids experiences a drop from 29% to 26%. Applying consolidation pressure seems to have prevented the expansion of the process-induced voids and also caused larger voids to break up into smaller ones, as the distance between plies became smaller. Moreover, larger voids would deform during consolidation and conform to the available space between fiber tows, creating a higher resistance to transport through the fiber bed. However, as the voids become smaller, the adhesion force reduces, and therefore they become more mobile [167, 178]. This confirms the observation in Fig. 28 that the voids in the laminates made under magnetic pressure not only become smaller, but their number is also reduced. Magnetic pressure on the lay-up has a more favorable effect

when applied before infusion such that the relative percentage of small voids remarkably increases to 43% while the relative percentage of large voids becomes almost negligible. This is because the already compressed fiber bed prevents the formation of large voids, which is highly significant as large voids can have a detrimental effect on mechanical properties and reduce the long-term durability of composites [143].

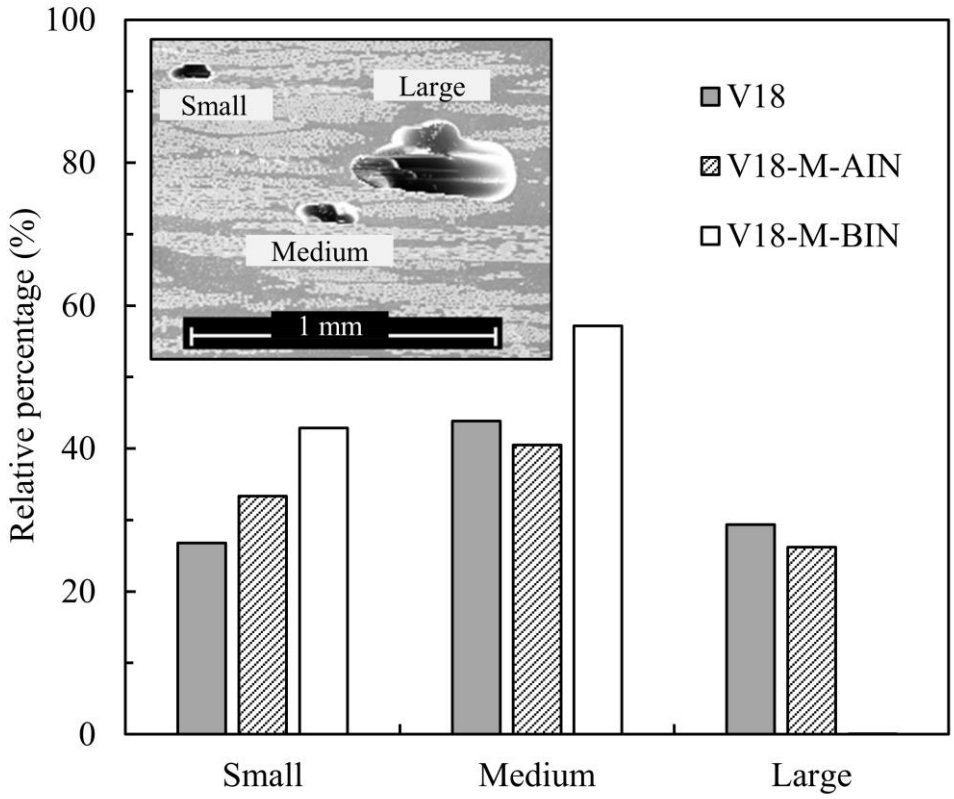

Figure 29. Relative percentage of small ($D_{eq} \leqslant 100$ µm), medium (100 µm < D_{eq} < 200 µm), and large ($D_{eq} \geqslant 200$ µm) voids for different fabrication scenarios of 18-ply random mat E-glass/epoxy composite laminates. The inset displays the SEM image of typical small, medium, and large voids.

Fig. 30 provides insight to the shape morphology of the voids, expressed in terms of relative percentage of circular ($0.9 < R \leqslant 1$), elliptical ($0.25 < R \leqslant 0.9$), and

elongated ($R \leqslant 0.25$) voids. A sample SEM image containing different void shapes are shown in the inset for visual reference. Fig. 30 shows that, unlike the conventional VARTM laminates, the laminates made using magnetic pressure contain almost no circular voids. Moreover, the relative percentage of elongated voids in these scenarios are higher than that in the laminates made without external pressure. Placement of magnets before infusion leads to even a much higher percentage of elongated voids as these voids can only form in a highly compacted fiber bed where the voids are much more likely to be extended along the laminate.

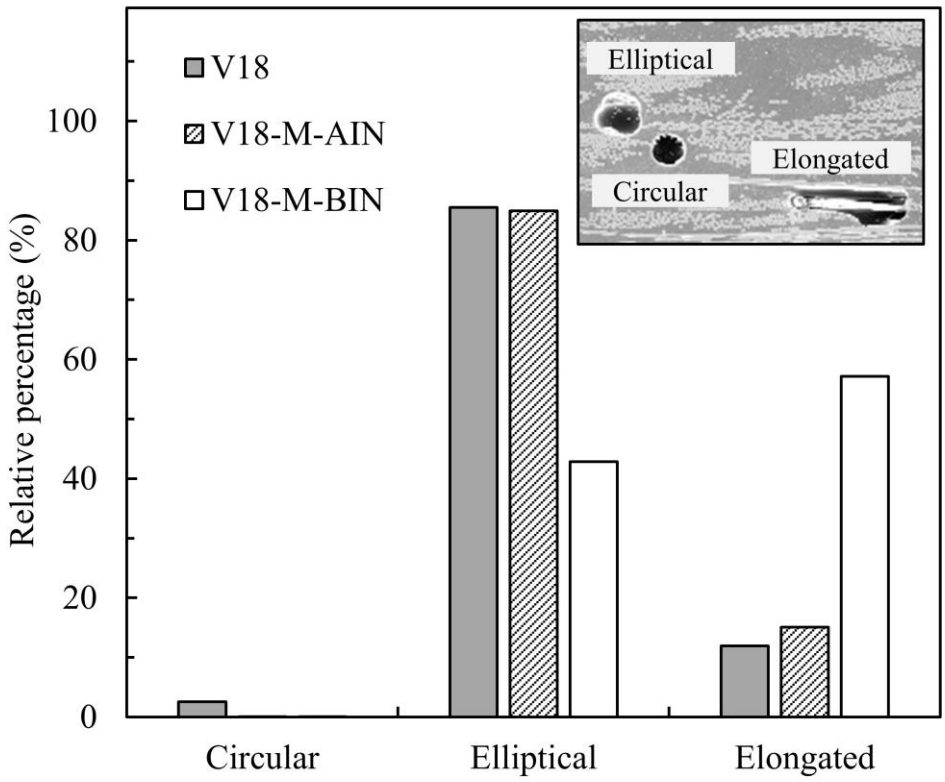

Figure 30. Relative percentage of Circular: $0.9 < R \leqslant 1$, Elliptical: $0.25 < R \leqslant 0.9$, and Elongated: $R \leqslant 0.25$ voids under different fabrication scenarios of 18-ply random mat E-glass/epoxy composite laminates. The inset displays the SEM image of typical circular, elliptical, and elongated voids.

3.4.1.6. Flexural Properties of Composite Laminates

The flexure strength and modulus of the laminates manufactured by all nine scenarios are shown in Figs. 31 and 32, respectively. The void volume fraction is also presented in the same figures to demonstrate the possible adverse effects of void content on the flexural properties. Regardless of the number of plies, the laminates manufactured by applying magnetic pressure either after or before the infusion are found to have significantly better flexural properties compared to conventional VARTM laminates.

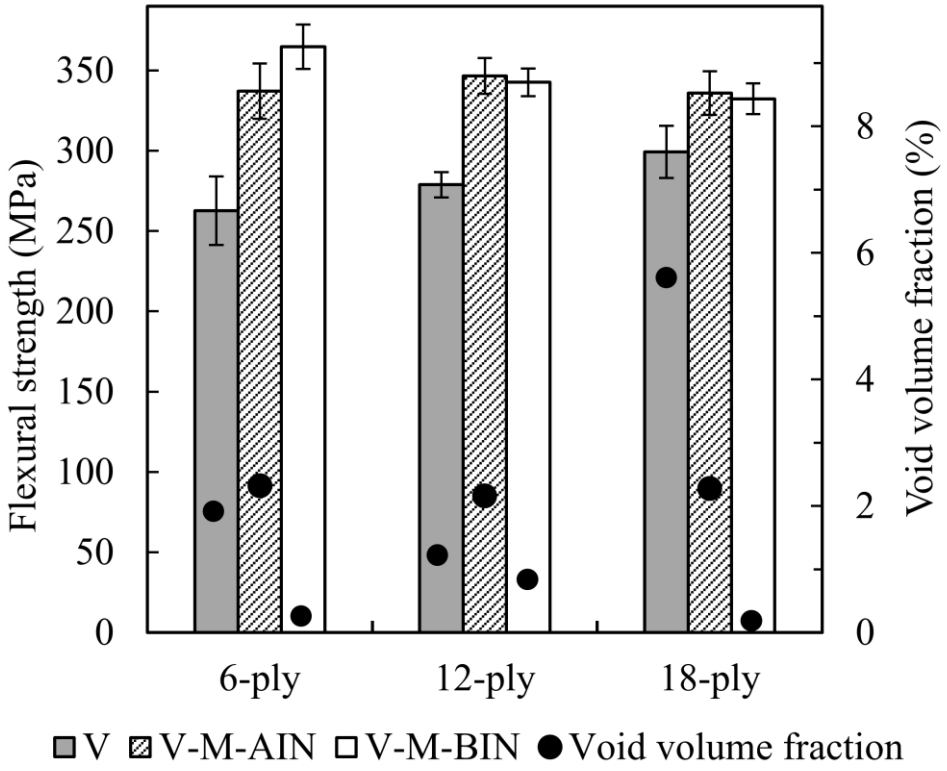

Figure 31. Flexural strength as a function of void volume fraction in different fabrication scenarios: (a) V (VARTM); (b) V-M-AIN (Magnets applied after infusion in VARTM); and (c) V-M-BIN (Magnets applied before infusion in VARTM process); with different number of plies. Note: Error bars show the 95% confidence interval (n=14 samples).

Placement of magnets on 6-ply laminates after infusion increased flexural strength by 28% to 337 MPa and flexural modulus by 41% to 14.8 GPa. Since the void content did not reduce for this case, the improvement in flexural properties seems to be entirely due to almost 14% increase in fiber volume fraction. Similarly, the 12-ply laminates fabricated under magnetic pressure exhibited 24% and 34% enhancement in the flexural strength and modulus compared to VARTM samples. The 18-ply laminates, on the other hand, displayed a slightly lower improvement of 12% and 24% for the flexural strength and modulus, respectively.

The properties reported above can further be improved if the magnets are placed on the lay-up before the infusion. A higher percentage increase in the flexural properties is expected since void contents below 1% were reached for all laminates (Table 5). Corroborating the positive effect of low void content, flexural strength increased by 39% to 365 MPa and flexural modulus increased by 46% to 15.5 GPa for the 6-ply laminates. For the 12- and 18-ply laminates, the percentage improvements were also substantial, but slightly lower than the 6-ply results. For example, strength increased by 23% and 11% and modulus increased by 37% and 24% for the 12-ply and 18-ply laminates, respectively. It is also important to note that the percentage increase in properties is reduced for thicker laminates, which can be explained by the application of lower pressure due to the increased lay-up thickness.

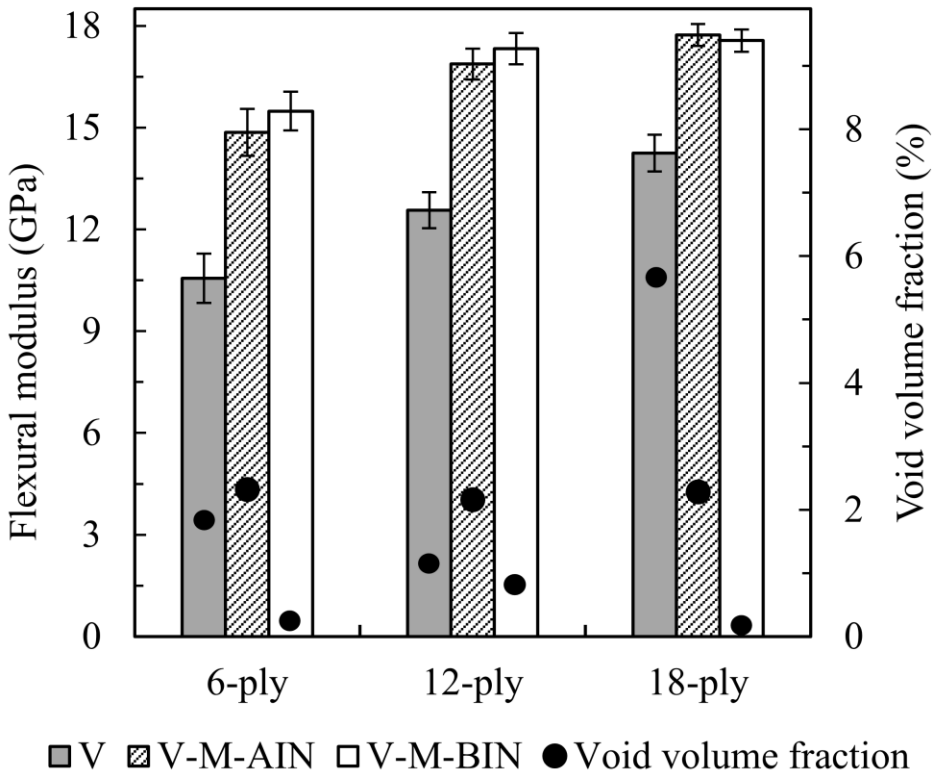

Figure 32. Flexural modulus as a function of void volume fraction in different fabrication scenarios: (a) V (VARTM); (b) V-M-AIN (Magnets applied after infusion in VARTM); and (c) V-M-BIN (Magnets applied before infusion in VARTM process); with different number of plies. Note: Error bars show the 95% confidence interval (n=14 samples).

The flexural properties were found to be dependent on both the fiber volume fraction and void content of the laminates. In order to identify the adverse effects of voids, flexural properties of the laminates were plotted as a function of their fiber volume fraction as illustrated in Figs. 33 and 34. The linear lines shown were fitted through two data points: one point is the properties of neat resin which has the strength and modulus of 121 MPa and 3.41 GPa and the other point is the properties of the laminate that has the lowest void content (i.e., V6-M-BIN, V12-M-BIN, and V18-M-BIN). As expected, both in Figs. 33 and 34, the samples with higher void content

remained below the trendlines, thus revealing the extent of possible adverse effect of increased void content. However, to predict the rate of decline in flexural properties, the void content, as well as the void morphology such as shape, size, and location, may need to be considered. For instance, applying magnetic pressure after the infusion prevented the void growth, thus leading to smaller sized voids as shown earlier. The adverse effects of small voids seem to be less pronounced such that the samples with smaller voids (i.e. V6-M-AIN, V12-M-AIN) did not show considerable property reduction even at a slightly higher void content and remained below but closer to the trendlines.

The importance of using magnetic consolidation on VARTM laminates can be better ascertained when the change in fiber content is compared with that of the wet lay-up laminates reported in chapter 2 [160]. The fiber volume fraction of 6-ply wet lay-up laminates was increased from 17% to 27% by magnetic consolidation [160], whereas, in the current study, the fiber volume fraction of the 6-ply VARTM laminates was increased from 46% to 52%. These results demonstrate that, despite starting from a much higher fiber volume fraction (i.e., a more compacted fiber bed), VARTM laminates can still be substantially compacted by the magnetic pressure.

In addition, the flexural strength and modulus of the wet lay-up laminates were increased by 60% to 253 MPa and by 46% to 9.9 GPa, respectively [160]. Hence, magnetic consolidation elevates the properties of wet lay-up laminates closer to the properties of conventional VARTM parts (i.e., flexural strength = 263 MPa; flexural stiffness = 10.6 GPa obtained in the current study). Similarly, utilizing magnetic

consolidation on VARTM resulted in even higher flexural properties, which could possibly reach levels typically obtained in closed-mold processes.

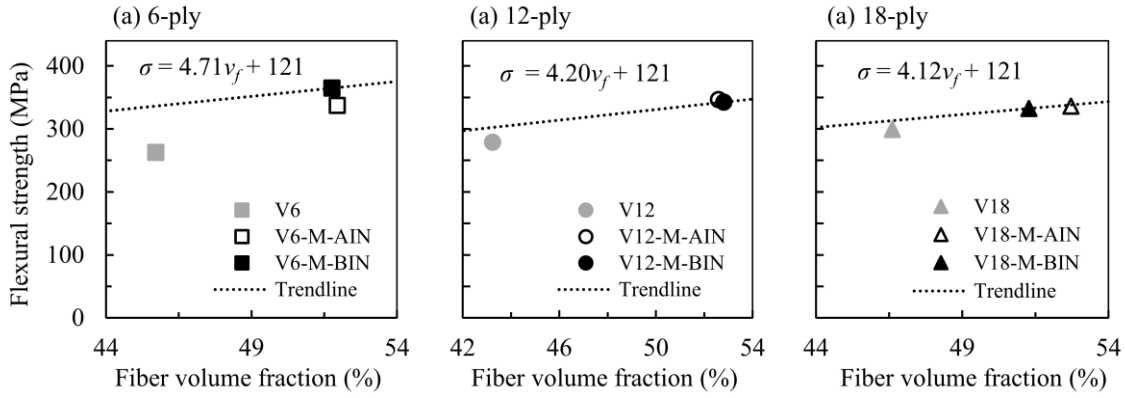

Figure 33. Changes in flexural strength of the 6-, 12-, 18-ply laminates fabricated under different scenarios with respect to the fiber volume fraction. Trendlines are drawn using the properties of the neat resin and the properties of the laminate with the lowest void content, illustrating the adverse effect of increased void content.

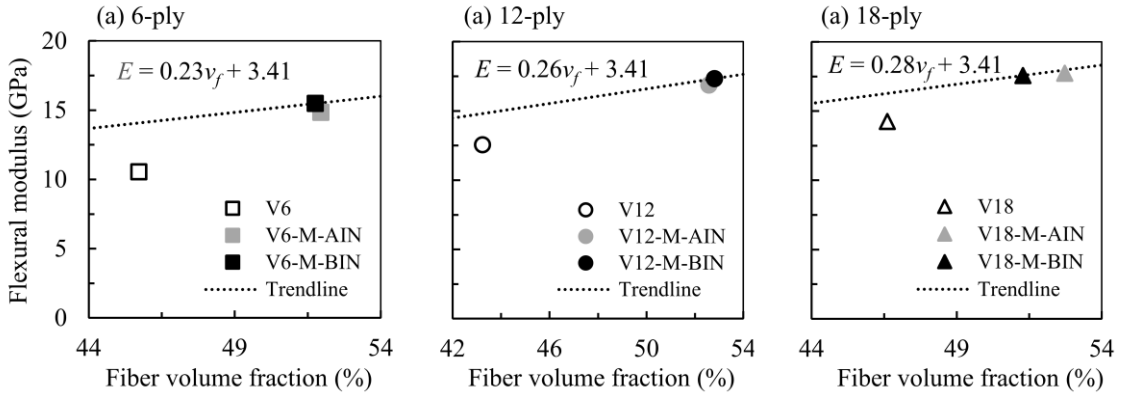

Figure 34. Changes in flexural modulus of the 6-, 12-, 18-ply laminates fabricated under different scenarios with respect to the fiber volume fraction. Trendlines are drawn using the properties of the neat resin and the properties of the laminate with the lowest void content, illustrating the adverse effect of increased void content.

3.4.2. Validation of the Consolidation Model: Prediction of Laminate Compaction, Fiber Volume Fraction, and Thickness

The temporal change of magnetic pressure and part thickness predicated by the consolidation model developed earlier in Section 3.3 are shown in Fig. 35 for the 6-, 12-, and 18-ply laminates. In the model, the initial thickness and fiber volume fraction of the laminates are chosen based on the data of the conventional VARTM laminates. The thicknesses of the fabricated laminates and the model predictions are in excellent agreement as illustrated in Fig. 35. Fig. 35 further depicts that, for the particular set of process parameters used in this work, both the magnetic pressure and the part thickness reach their final values within less than a second. This rapid compaction of the fiber bed could contribute to the trapping of some voids, which would otherwise be removed by a slower compaction, achieved by the proper selection of the process parameters. For example, for fabrics with much lower permeability (i.e., unidirectional preforms, $K_{xx} \approx 10^{-12}$ m^2 at V_f=40-80% [172]) and for resin systems with higher viscosity (i.e., much higher than the 296 mPa s viscosity of INF 114-INF 211), the compaction may take several minutes as explained later in next section. It should also be noted that for solving the consolidation model given in Eq. (26), the resin viscosity is assumed to be constant since the compaction takes place within less than a second and the change in resin viscosity is negligible.

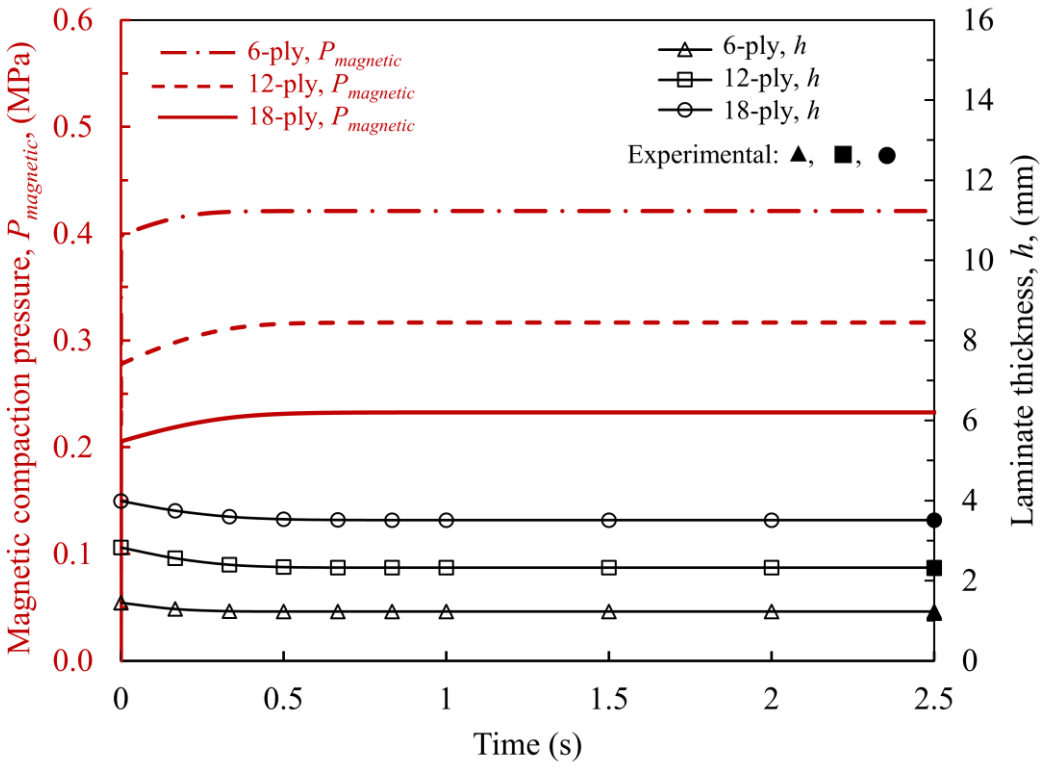

Figure 35. Model predictions of the temporal change of magnetic pressure and laminate thickness for 6-, 12-, and 18-ply laminates.

The fiber volume fraction and final laminate thicknesses obtained from experiments are compared with model predictions in Table 6. The model predictions for the fiber volume fraction are also in excellent agreement with experimental data for all laminates.

Table 6. Fiber volume fraction and final laminate thickness obtained from experiments and model predictions.

Fabrication scenario		Number of plies	Fiber volume fraction (%)		Final thickness (mm)	
			Experimental	Model	Experimental	Model
1	V6-M-AIN	6	51.95 ± 1.07	53.79	1.19 ± 0.01	1.23
2	V12-M-AIN	12	52.58 ± 0.63	52.58	2.31 ± 0.02	2.33
3	V18-M-AIN	18	52.72 ± 0.41	52.94	3.39 ± 0.01	3.51

3.4.3. Effect of Process Parameters on Consolidation Behavior of Laminates during Fabrication

In the consolidation model developed earlier in this chapter, permanent magnet type, resin viscosity, and fabric type are considered as critical parameters, which are responsible for the compaction dynamics, as well as final thickness and fiber volume fraction of the laminates. In addition, the number of plies is another critical parameter since the magnetic pressure varies considerably with the laminate thickness. Thus, the effect of these parameters on the evolution of laminate thickness is investigated by using the consolidation model.

3.4.3.1. Effect of Magnet Type on Consolidation Behavior

The proper selection of the magnets is critical in achieving the desired consolidation as the level of magnetic pressure governs the final thickness of a composite laminate. Thus, one can use the developed model to determine the magnet type and size which could generate the necessary pressure to achieve the desired consolidation behavior and the laminate thickness. The magnetic force is an exponential function of separation gap (i.e., lay-up thickness) and can be estimated by two empirical

constants as expressed in Eq. (25). These empirical constants, A and B, can be calculated using the magnetic force versus gap data which is usually available from the supplier (K&J Magnetics). In order to illustrate the effect of different magnet types on the final thickness of the 18-ply random mat laminate, six different permanent magnets with different thicknesses ranging from 1.59 to 76.2 mm (i.e. 1/16" to 3") are considered. The empirical constants, A and B, for each magnet are calculated based on data sheet provided by K&J Magnetics and given in Table 7. Then, using the consolidation model given in Eq. (26), the final laminate thicknesses compacted by these six different magnets are determined.

Table 7. The empirical constants, A and B, for six different permanent magnets used for the prediction of the magnetic force as a function of lay-up thickness.

Magnet thickness (mm) (in)	1.59 1/16	6.35 1/4	12.7 1/2	25.4 1	50.8 2	76.2 3
A (N)	329.8	350.0	357.4	369.4	441.0	463.5
B (m^{-1})	260.2	391.2	292.4	230.1	187.1	167.6

Fig. 36 shows the final thicknesses of the six laminates normalized with respect to the initial, uncompacted thickness of 3.99 mm. The maximum pressure level applied by these magnets are also determined and depicted in Fig. 36. The results show that by increasing the thickness of permanent magnet from 1.59 to 76.2 mm, the magnetic pressure on 18-ply laminates increases from 40 to 360 kPa. As expected, higher magnetic compaction pressure results in substantially thinner laminates such that the normalized final thickness decreases from 0.96 to 0.86 when the magnet thickness is increased from 1.59 to 76.2 mm. Thus, if the desired final thickness of the laminate is known, it is possible to estimate the required magnetic pressure. Then, the appropriate

magnet that can produce this compaction pressure can be selected among the available magnet types and sizes.

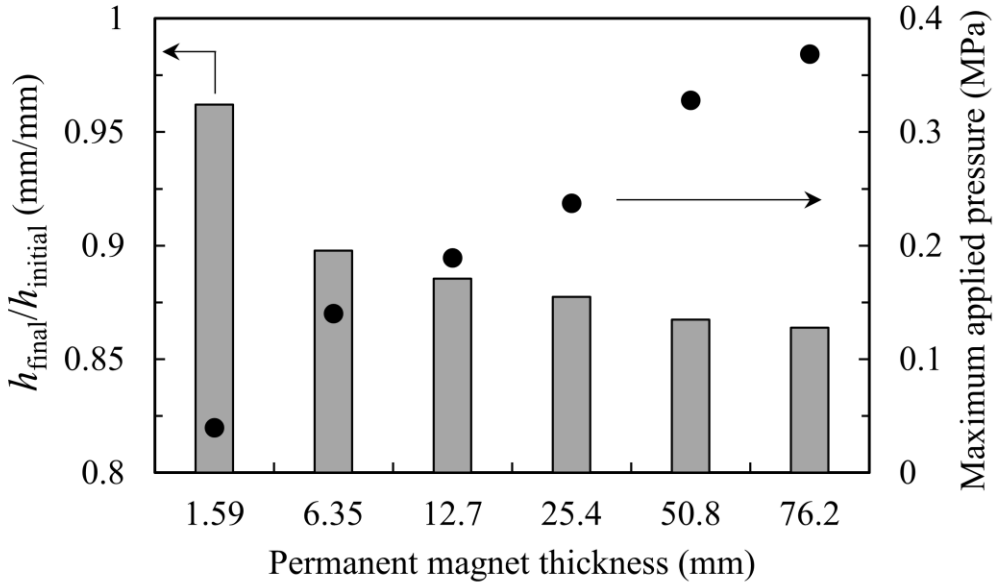

Figure 36. Normalized final thickness of the 18-ply laminates made under six different permanent magnets and the maximum pressure applied by these magnets. ($h_{initial}$ = 3.99 mm).

3.4.3.2. Effect of Resin Viscosity

Resin viscosity is another process parameter which affects the consolidation behavior of a composite laminate. To investigate the effects of resin viscosity on consolidation time and final laminate thickness, three different resin systems with different viscosities (μ=1, 10, 100 Pa s) are considered. The other process or design parameters such as fabric type, number of plies, permanent magnet type, etc. used in the magnetic consolidation model are the same as the fabrication experiments presented earlier.

Fig. 37 shows the evolution of laminate thickness under magnetic consolidation with different resin viscosities (μ=1, 10, 100 Pa s) and for different number of plies (6,

12, and 18). The results show that the change in resin viscosity does not change the final laminate thickness. However, laminates made by resin system with higher viscosity require substantially more time to fully consolidate. For example, 18-ply laminates made of three different resin systems with viscosities of 1, 10, and 100 Pa s consolidate in 5, 25, and 200 s, respectively. Therefore, for resin systems with low viscosity (i.e. less than 1 Pa s), the consolidation is expected to take place in few seconds. This rapid consolidation confirms that moving magnets with a small footprint over a much larger lay-up surface could be a feasible and effective approach for fabrication of large laminates. Fig. 37 also shows that by increasing the number of plies, the consolidation time increases. This difference between the consolidation times is more pronounced when a resin system with higher viscosity (μ=10 and 100 Pa s) is used. For example, for the resin with a viscosity of 100 Pa s, the 6-, 12-, and 18-ply laminates consolidate in 130, 185, and 193 s.

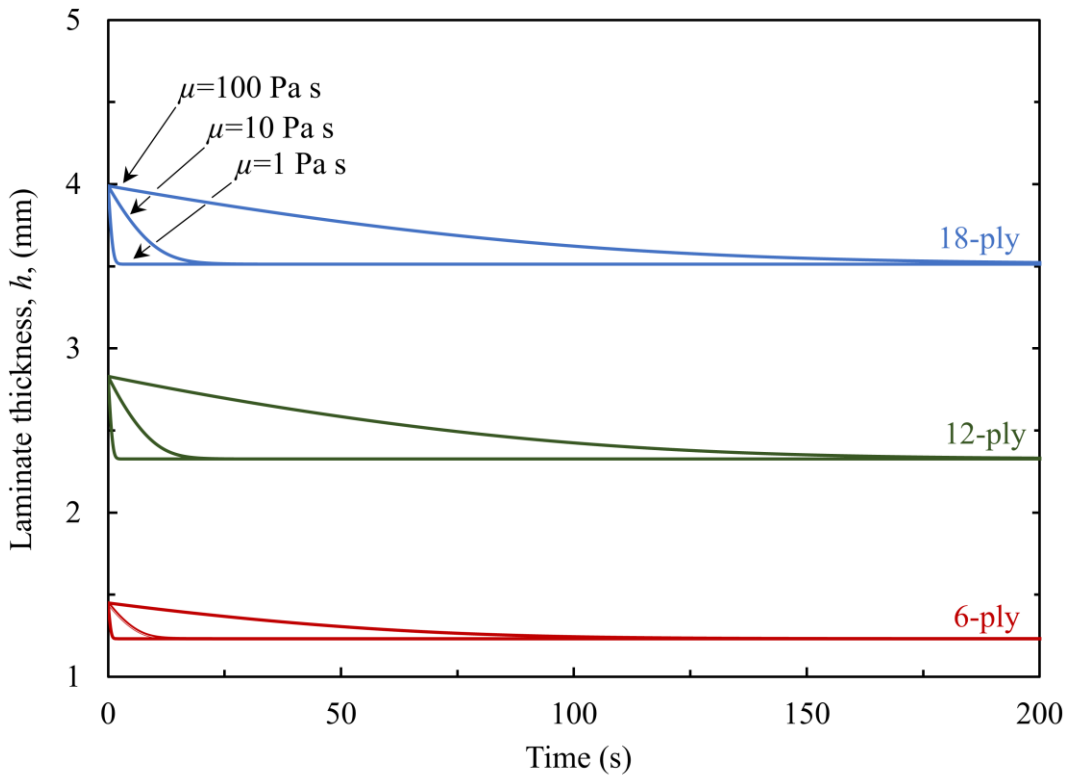

Figure 37. Evolution of thickness for 6-, 12-, and 18-ply laminates made under magnetic consolidation using different resin viscosities (μ=1, 10, 100 Pa s).

3.4.3.3. Effect of Fabric Type

In addition to permanent magnet type and resin viscosity, the fabric type plays an important role in the consolidation dynamics of a composite laminate. The reason is that the tow size and the fabric architecture strongly affect the compaction behavior and permeability of a fabric. In this section, the consolidation analysis is carried out for a unidirectional graphite fiber (AS-4) with a planar density of 0.172 kg/m^2 as an example reinforcement. The planar permeability for this fabric is modeled by Eq. (20) where, C=1.75×10^{11} (m^{-2}) and n=2, and the fiber stress is modeled by Eq. (22) where, A_s=0.41 kPa, V_a=0.80, and V_o =0.50, as presented in Ref. [172]. In addition, different number of

plies (10, 20, 30, and 40), as well as a resin system with a viscosity of 10 Pa s, are chosen as the inputs of the consolidation model.

Fig. 38 presents the evolution of thickness and final fiber volume fraction for all the laminates made under consolidation pressure of twenty-five NdFeB N52-2.54 × 2.54 × 1.27 cm^3 magnets. The results show that the consolidation of 10- to 40-ply unidirectional laminates takes places in 3-11 hours which is much longer than the consolidation of random mat laminates (i.e. 25 s for 18-ply with resin viscosity of 10 Pa s). It should be noted that the results presented here are for constant resin viscosity. However, in several resin systems, the viscosity may change significantly during the laminate consolidation, particularly if the consolidation spans over multiple hours as in this case of unidirectional fibers. Thus, for such cases, one needs to incorporate a model for cure kinetics that gives the viscosity as a function of time into the consolidation model to more accurately predict the evolution of laminate thickness. Fig. 38 also presents that the final fiber volume fraction of the laminates increases from 61 to 65% by decreasing the number of plies from 40 to 10 which is due to higher magnetic pressure applied on thinner laminates. Generally, the higher the applied magnetic pressure, the higher is the final fiber volume fraction and the shorter is the time required for consolidation.

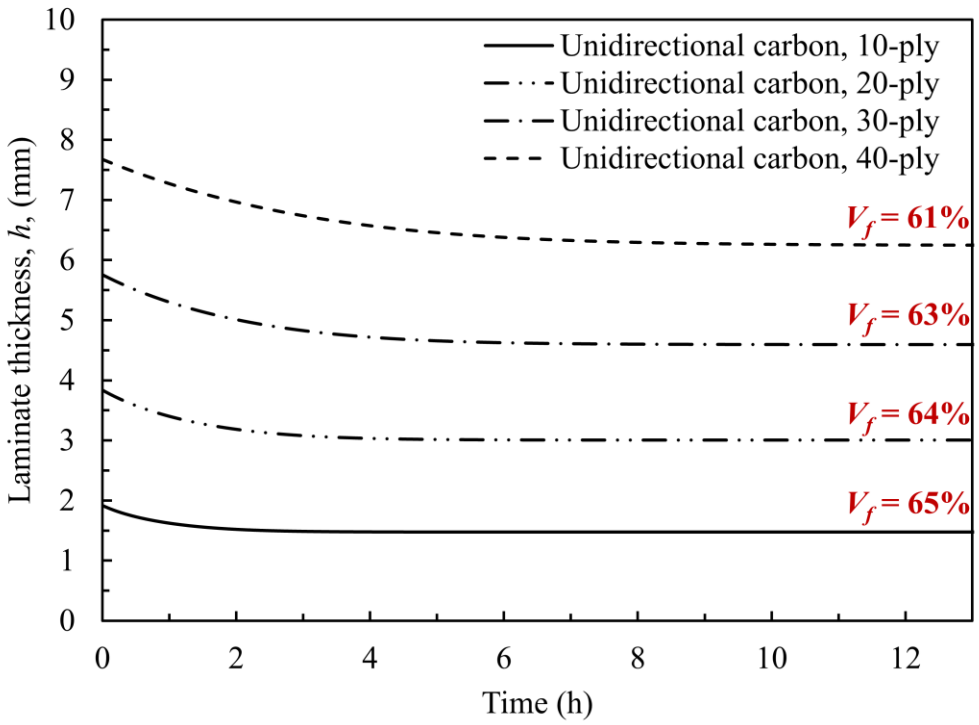

Figure 38. Evolution of thickness and final fiber volume fraction of 10-, 20-, 30-, and 40-ply unidirectional graphite laminates made under magnetic consolidation.

3.5. Concluding Remarks

The focus of this chapter is to: (i) demonstrate the effectiveness of utilizing magnet assisted composite manufacturing (MACM) in VARTM processes, and (ii) develop a transient process model that can be used to characterize the laminate consolidation as well as predict the final laminate thickness and fiber volume fraction. Towards this goal, significant property improvements for the 6-, 12- and 18-ply laminates are observed when the MACM is utilized with the conventional VARTM process. Placing a set of Neodymium Iron Boron (NdFeB) magnets on the lay-up either after or before the infusion yielded similar levels of enhancement in fiber volume fraction (from 43-47% to 51-53%), flexural strength (11-28% improvement) and

flexural modulus (23-41% improvement). In addition, placing the magnets before infusion led to substantially low void content, below 1%, for all three laminates, while the baseline laminates fabricated by conventional VARTM contained up to 6% void content. A transient magnetic consolidation model was developed in this chapter and shown to accurately predict the final fiber volume fraction and thickness of all the laminates studied. In addition, the effect of permanent magnet type, resin viscosity, and fabric type on the consolidation behavior of the laminates is presented. It is concluded that the proposed consolidation model can provide valuable information on the selection of process or design parameters to achieve the desired laminate thickness and fiber content.

CHAPTER 4. Void Reduction in VARTM Composites by Compaction of Dry Fiber Preforms with Stationary and Moving Magnets

Voids are the most common process-induced defects in composite laminates fabricated by vacuum assisted resin transfer molding (VARTM). Reduction or total elimination of these defects are essential for the improved performance and long-term durability of the structural composites. This chapter introduces a novel method that reduces the void content in VARTM laminates to below 1% by compacting the fibrous mat before infusion. The compaction is achieved by applying magnetic pressure on the vacuum bag by either stationary or moving magnets which are removed before the resin infusion. To assess the effectiveness of the proposed method, 6-, 12, and 18-ply random mat glass/epoxy laminates are fabricated by VARTM using compacted and uncompacted mats and their properties are compared. In addition, different sets of magnets are used to investigate the effect of compaction levels on the resin flow and the quality of the final part. The placement of stationary magnets on the entire vacuum bag surface is practical for fabrication of small parts. For medium to large parts, however, magnets with a smaller footprint can be moved to apply the compaction pressure over a larger vacuum bag surface. The results show that by applying compaction pressure of 0.2 MPa or higher either by stationary or moving magnets on the dry preforms, the void volume fraction was decreased by 65-95% to 0.1-0.8% in all laminates.

4.1. Introduction

Fiber-reinforced polymer composites have been used in a wide range of applications including sporting goods, civil infrastructure, aerospace, marine, and automotive industries due to their high specific mechanical properties and durability.

However, the occurrence of manufacturing defects such as resin-rich areas, distorted fibers, and voids may dramatically degrade the mechanical performance of composite laminates. Among these defects, the commonly-observed voids are formed due to mechanical entrapment of air, absorbed moisture, and volatiles expelled during cure [179]. Fabrication problems such as vacuum leakage or poor vacuum can also contribute to their formation [106]. In liquid composite molding (LCM) processes such as resin transfer molding (RTM) and vacuum assisted resin transfer molding (VARTM), however, the main source of void formation is the rate of impregnation of fibrous reinforcement [58, 180-182]. At the micro level, the formation of voids is generally due to the difference in the resin flow rate inside and between the fiber tows [183]. At the macro level, however, voids are formed due to the non-uniform, rapid progression of resin front [27]. Accordingly, Patel et al. optimized the resin flow rate during mold filling to reduce the overall void content and improve fiber wetting in the RTM laminates [94, 95]. For selecting an optimized impregnation rate, the geometrical features of the preform needs to be considered. Based on the formation of voids, the fabrics are classified into two types, a single-scale such as random mats where the fibers are loosely arranged inside the tows and dual-scale directional mats like woven, braided, or stitched fabrics [145, 146]. In single-scale reinforcements, unlike dual-scale ones, the resin flow rate inside and between the fiber tows are almost the same, so the possibility of entrapment of micro-voids may become low. However, the spatial variation of planar density of random fiber mats causes high- and low-permeability zones within the fabrics, leading to a non-uniform resin flow and as a result, entrapping voids in the local low permeability zones [98, 99, 151]. Barraza et al. reported that by

reducing the injection velocity in random mat RTM laminates, the probability of void entrapment became lower, and thus the void content reduced from an unacceptable high level of 7% to less than 1% [90].

A number of different methods have been proposed to control the flow rate and consequently reduce the void content. For example, Johnson et al. [98, 99] proposed an induction heating method to reduce the resin viscosity, and thus increase the flow rate at low permeability regions. Using this method, they could guide the flow along a desired path during the filling stage and, as a result, eliminated the void and dry spot formation. However, this method would be limited to the resin systems with long gelation times. Kedari et al. [106] used a dual pressure controlled and heated VARTM setup to control the inlet pressure, outlet pressure, and mold temperature. They found that to prevent void entrapment during the filling at an elevated temperature, the impregnation speed needs to be reduced, which was achieved by decreasing the pressure difference between the inlet and outlet. Bender et al. [105] used a fuzzy logic controller to adjust the pressure difference between the resin supply and exit and controlled the flow rate during filling to prevent dry spots.

The adverse effects of voids on the compressive strength [48, 184], flexural strength [185], flexural modulus [154], interlaminar shear strength [118, 186, 187], and fatigue life [58, 143, 185] can be significant, even at low void levels. For example, increasing void volume fraction from 1.3% to 5.9% in carbon/epoxy prepreg laminates caused approximately 15% reduction in flexural strength [185]. Additionally, the presence of voids was shown to increase the rate and maximum level of moisture absorption [188], which led to poorer long-term performance of the epoxy-based

composites [83, 189]. For instance, Thomson [82] reported that a 1% void content may even double the water uptake of glass fiber reinforced epoxy composites. Aktas et al. [189] found that the random mat E-glass/epoxy composite laminates with fiber volume fraction of 24.5% after 1.9% moisture absorption showed approximately 17.4% and 16.8% reduction in interlaminar shear strength and flexure modulus, respectively. Thus, it is of critical importance to avoid the formation of voids and minimize the void content to produce reliable and high-quality laminates.

In this work, a new, more effective method to control the resin flow in VARTM to substantially reduce or eliminate the process-induced voids is presented. For this purpose, the VARTM lay-up is first prepared on a magnetic tool plate. Then, the magnetic attraction force generated between a set of magnets and magnetic tool plate is used to compact the dry preforms inside the vacuum bag. The magnets are removed after the compaction is achieved, and then the resin infusion is conducted under only vacuum. Covering the entire surface of the preform by stationary magnets, however, is not feasible for medium to large parts. In these cases, the approach of moving magnets with a smaller footprint over the larger vacuum bag surface is explored. Then, the properties of the laminates fabricated by the compacted preforms -either by stationary or moving magnets- are compared with the properties of the laminates fabricated by conventional VARTM. In addition, a set of more powerful magnets is used to investigate whether a higher level of compaction is more effective in preventing the formation of voids in thicker laminates. The quality of the cured laminates is assessed through their void content and morphology, fiber volume fraction, and flexural properties.

4.2. Materials and Experimental Details

4.2.1. Materials

Randomly oriented, chopped-strand, E-glass fiber mat with a planar density of 0.228 kg/m^2 was used as the reinforcement (Fiberglast). The resin system used in this work was INF-114/INF-211 (PRO-SET). The resin/hardener mix ratio is 100:27.4 by weight. The low viscosity (296 mPa s at 22 °C) and sufficiently long pot-life (117-145 min at 22 °C) make this resin system suitable for resin infusion processes.

4.2.2. Neodymium Permanent Magnet

In this work, the magnetic pressure is utilized to compact the fibrous mat inside the vacuum bag before resin infusion. The pressure is generated by Neodymium Iron Boron (NdFeB) permanent magnets (KJ Magnetics, N52 grade) with a maximum energy product, $(BH)_{max}$, of 413.8 kJ/m^3. Recently, NdFeB magnets were used to apply consolidation pressure during WLVB, VARTM, and out-of-autoclave prepreg curing to improve laminate properties [160, 164, 190]. In the present study, two sets of magnets, magnetized through the thickness, were used for inducing different levels of pressure. The first set (A), includes N52-2.54 × 2.54 × 1.27 cm^3 NdFeB magnets with a surface magnetic field of 0.49 T. The second set (B), contains N52-2.54 × 2.54 × 5.08 cm^3 NdFeB magnets, which are thicker and can generate a stronger surface magnetic field of 0.71 T. The pull force generated by one magnet placed on a top steel plate is measured as a function of the gap from a bottom steel plate using a mechanical testing machine. The magnetic compaction pressure was then determined as the measured force over the area (i.e., 2.54 × 2.54 cm^2) of the magnet.

Figure 39 shows the variation of compaction pressure of one 1.27-cm and one 5.08-cm thick N52 NdFeB magnet as a function of air-gap (i.e. VARTM lay-up thickness) measured from the bottom steel plate. It can be seen that the magnetic pressure reduces exponentially with increasing the VARTM lay-up thickness. Moreover, at the same lay-up thickness, the magnetic pressure generated by 1.27-cm magnet (set A) is lower than that generated by 5.08-cm magnet (set B). The initial thicknesses of the VARTM lay-up consisting of 6-, 12-, and 18-ply of random fiber mats covered by vacuum bag and 0.3-mm thick caul plate are in total about 2.4, 4.3, and 6.0 mm, respectively. According to Fig. 39, the compaction pressure of 0.33 MPa (48 psi), 0.20 MPa (29 psi), and 0.14 MPa (20 psi) are predicted to be applied by the first set of magnets (A: N52-2.54 × 2.54 × 1.27 cm^3 NdFeB) on 6-, 12-, and 18-ply VARTM lay-up, respectively. For achieving better compaction in 18-ply lay-up, a thicker set of magnets (set B) that apply higher magnetic pressure than set A can be utilized. Thus, using the second set of magnets (set B), N52-2.54 × 2.54 × 5.08 cm^3 NdFeB, a compaction pressures of 0.19 MPa (28 psi) is expected to be applied on 18-ply lay-up.

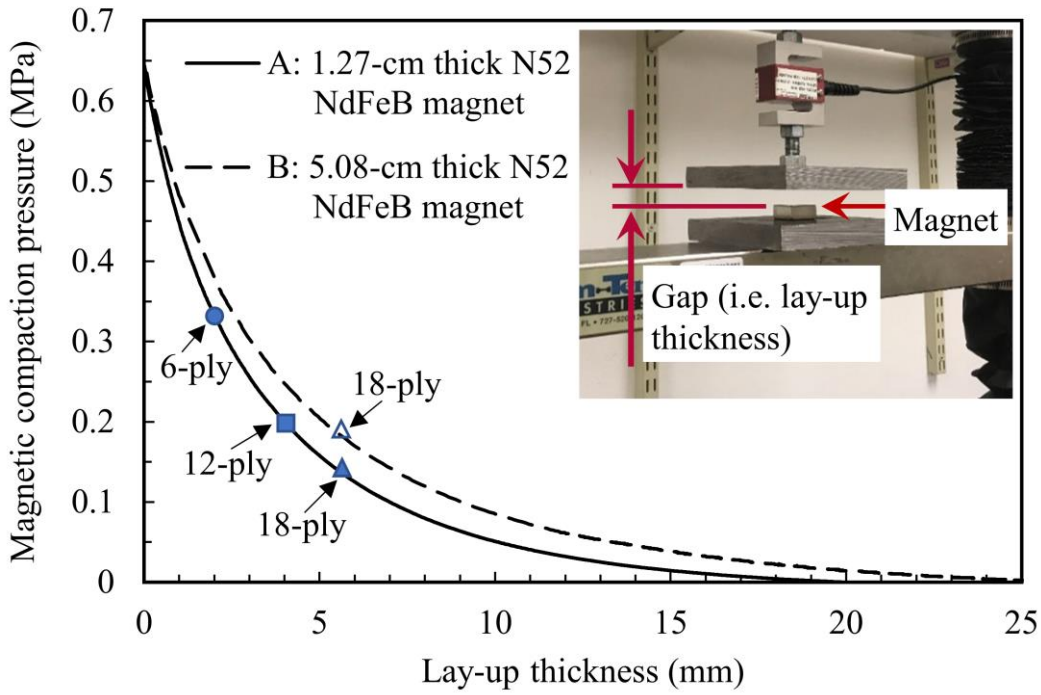

Figure 39. Variation of magnetic pressure on the lay-up thickness where a magnet is sandwiched between two steel plates. A refers to N52-2.54 × 2.54 × 1.27 cm^3 NdFeB magnet and B refers to N52-2.54 × 2.54 × 5.08 cm^3 NdFeB magnet.

4.2.3. Composite Laminate Fabrication

The variation of planar density and high impregnation speed of random fiber mats have been regarded as the two key factors that increase the risk of entrapping voids in the final part [90]. The new method utilized in the present work controls the resin flow and, as a result, reduces or eliminates the process-induced voids in the VARTM laminates. In this method, a set of permanent magnets is used to compact the fibrous mat inside the vacuum bag before resin infusion as shown in Fig. 40. The magnets are removed after the mats are fully compacted and the resin is infused similar to a conventional VARTM process. Compacting the fiber preforms would result in a reduction of the pore spaces, thus leading to a lower preform permeability. Therefore,

the reduction in the filling rate and the pore spaces are expected to avoid or minimize the formation of voids in random mat laminates.

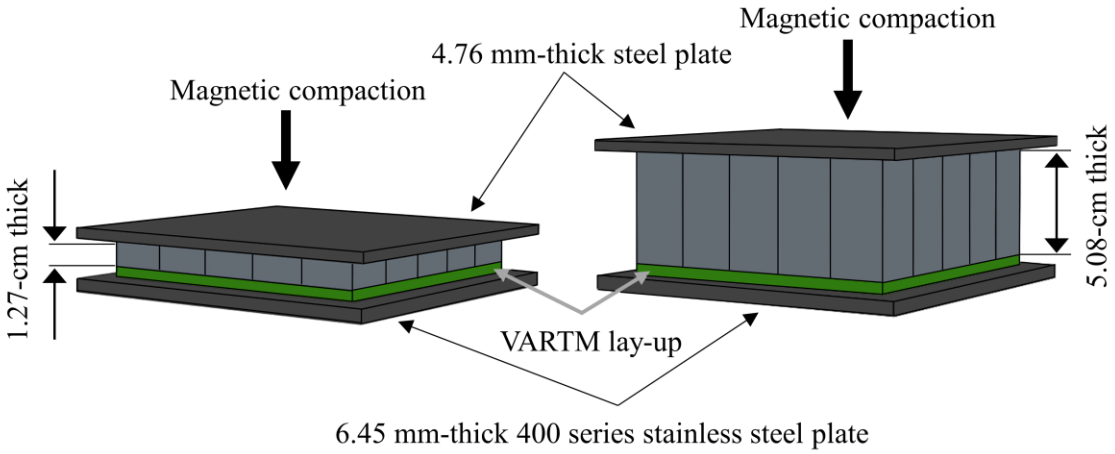

Figure 40. Compaction pressure applied by the two sets of twenty-five N52 NdFeB magnets, one set (A) comprising 2.54 × 2.54 × 1.27 cm^3 magnets and the other set (B) comprising 2.54 × 2.54 × 5.08 cm^3 magnets, to compact the VARTM lay-up before resin infusion.

In this work, the following series of experiments were performed to illustrate the effect of different levels of magnetic compaction on the resin flow and overall quality of the laminates using:

(i) different number of plies (i.e. 6, 12, and 18),

(ii) different sets of magnets (i.e. 1.27- and 5.08-cm thick N52),

(iii) moving magnets with a smaller footprint over a larger vacuum bag surface as a feasible method to apply compaction on medium to large parts

For all the experiments, a VARTM lay-up was prepared by placing a stack of 16.5 × 12.7 cm^2 fabrics on a 6.35-mm thick, 400-series stainless steel bottom tool plate. The resin inlet and outlet ports were also positioned at opposite ends of the mats on the tool plate. A distribution media was placed just on the inlet side to have a uniform flow

front. The release film and vacuum bag were applied over the entire lay-up assembly and the vacuum bag was sealed. The outlet tubing was connected to a resin trap, pressure regulator, and vacuum pump. The inlet tubing was clamped and a constant vacuum of 93 kPa was drawn. Then, the clamp was removed to allow the resin to flow into the preform. After completion of the filling, the inlet tubing was clamped. The mold was heated to 60 °C for 8 hours 45 minutes after the start of resin infusion to complete the curing of the laminate. Fig. 41 depicts the composite lay-up and the dial gages used to record the lay-up thickness at two locations during and after the resin infusion.

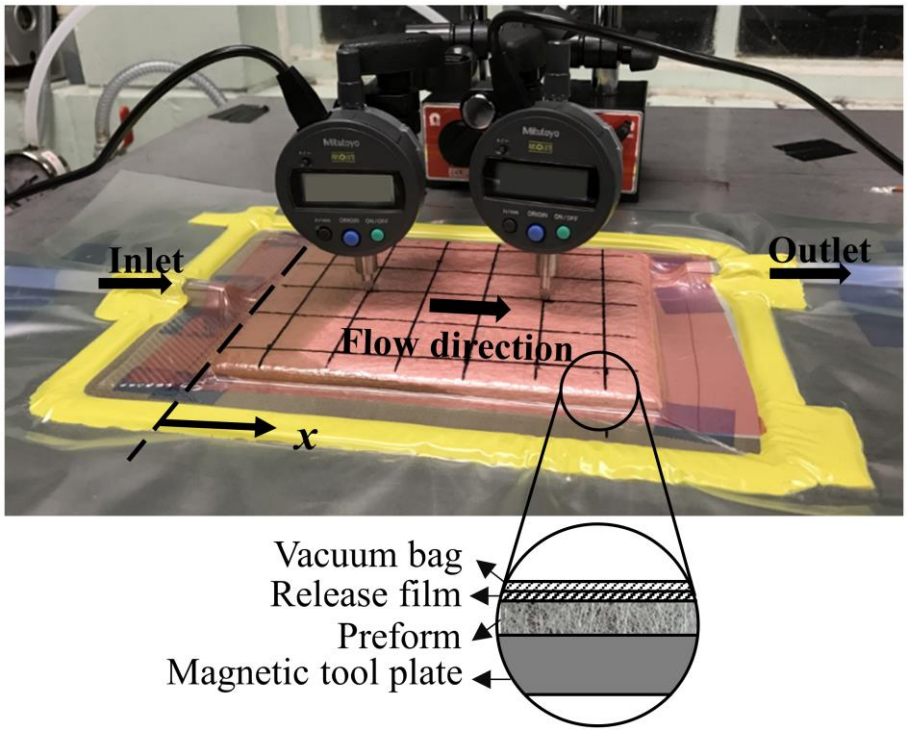

Figure 41. Composite lay-up during resin infusion in VARTM process. The two dial gages record the thickness at gage location (x=44.5 and x=120.7 mm) during and after the resin infusion.

Table 8 presents eight types of random mat E-glass/INF 114-INF 211 laminates that were fabricated in this work. For each laminate type, two laminates were

manufactured to ensure the repeatability of the results. The baseline laminates (V-6-U, V-12-U, and V-18-U) were made by conventional VARTM using 6-, 12-, and 18-ply of uncompacted fabrics, respectively.

Table 8. Summary of the experimental parameters varied in different fabrication scenarios.

Fiber Mats	Fabrication Scenario	No. of Plies	Type and Configuration of Permanent Magnets
Uncompacted	V-6-U	6	—
	V-12-U	12	—
	V-18-U	18	—
Compacted by **stationary magnets**	V-6-C-A	6	Twenty-five of type A 1.27-cm thick N52 NdFeB
	V-12-C-A	12	Twenty-five of type A 1.27-cm thick N52 NdFeB
	V-18-C-A	18	Twenty-five of type A 1.27-cm thick N52 NdFeB
	V-18-C-B	18	Twenty-five of type B 5.08-cm thick N52 NdFeB
Compacted by **moving magnets**	V-18-C-B-M	18	Three magnets of type B: 5.08-cm thick N52 NdFeB

4.2.3.1. Effect of Different Number of Plies

Considering that the applied magnetic pressure exponentially decreases as the lay-up thickness is increased, it is important to investigate the effectiveness of using magnetic compaction of thicker laminates. Therefore, different fabrication scenarios (V-6-C-A, V-12-C-A, and V-18-C-A) are used to evaluate the performance of the proposed method for thin (6 plies) as well as moderately thick (12 and 18 plies) lay-ups. In these

cases, twenty-five, type A, magnets were first positioned in a 5×5 arrangement on a 4.76-mm thick top steel plate. After the vacuum was drawn in the vacuum bag, the magnets attached to the top plate were placed on the vacuum bag before infusion. To avoid any surface impression defects and to better distribute the pressure, a 0.3-mm thick caul plate (16.5 × 12.7 mm^2) was placed between the magnets and the vacuum bag. After 90 minutes, the magnets were removed and the resin was infused. The rest of the process was similar to those of the baseline VARTM laminates.

4.2.3.2. Effect of Using Different Sets of Magnets

Given that the magnetic pressure decreases exponentially by increasing the lay-up thickness, to achieve a higher level of compaction in the thickest lay-up (18-ply), the thicker magnets (B: 2.54 × 2.54 × 5.08 cm^3) which are stronger than set A were utilized. The set of B magnets can apply 0.19 MPa compaction pressure which is considerably higher than 0.14 MPa pressure applied by the set of A magnets. Thus, the V-18-C-B laminates were made of 18-ply fabrics compacted by twenty-five magnets from set B, as illustrated in Fig. 42 (a). Then, the properties of V-18-C-A and V-18-C-B laminates were compared to investigate the effect of different level of compaction of dry preforms on the part quality.

4.2.3.3. Effect of Using Moving Magnets for Manufacturing of Medium to Large Parts

The proposed method of compaction of fabrics with stationary magnets, as described above, can be used for fabrication of small parts. However, covering the entire lay-up with magnets may not be practical for medium to large parts. Therefore, for much larger parts, sliding magnets with a smaller footprint over a larger vacuum bag surface may be more feasible and can be adopted by composite industry. However, the

use of proper lubricant to reduce the friction between magnet and vacuum bag is very critical. Also, the duration and how this sliding motion should be carried out on the vacuum bag should be investigated to ensure the preform is sufficiently compacted.

Hence, in the last fabrication scenario (V-18-C-B-M), the 16.5×12.7 cm^2 preforms were compacted by moving of only three, 5.08-mm high B magnets as shown in Fig. 42 (b). For this case, only a smaller area (2.54×7.62 cm^2) of the vacuum bag was covered by the magnets. First, the magnets were positioned in a 3×1 arrangement on a 4.76-mm thick top steel plate. The 18-ply lay-up was prepared as previous cases. Then, to prevent the tear of the bag due to contact with the edges of the magnet, the magnets were taped to a piece of breather cloth and then, covered by a bag. After coating the vacuum bag with a thin layer of grease ("Red-N-Tacky", Lucas Oil Products, Inc), the set of magnets were placed on the vacuum bag. The compaction was achieved by smoothly sliding the magnets back and forth on the vacuum bag for 30 min.

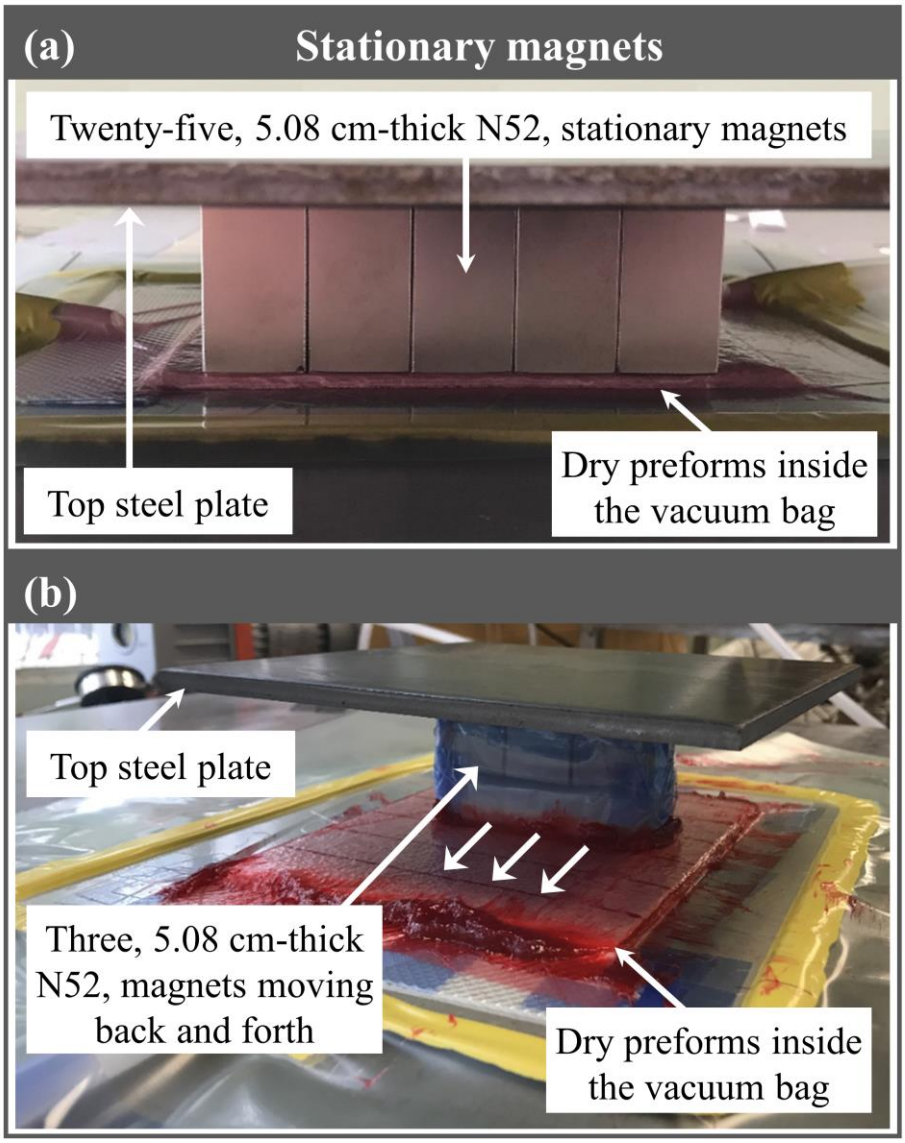

Figure 42. Compaction of 16.5 × 12.7 cm^2 dry fiber mats before infusion using (a) twenty-five N52-2.54 × 2.54 × 5.08 cm^3 stationary magnets (V-18-C-B), and (b) three N52-2.54 × 2.54 × 5.08 cm^3 moving magnets (V-18-C-B-M).

4.2.4. Fiber and Void Volume Fractions

The volume fractions of composite constituents were measured to determine if the compaction of dry preforms by permanent magnets would result in a decreased void content. For this purpose, three 38.1 × 19.1 mm^2 specimens were cut from each laminate and the density of each sample was measured using suspension method [133].

The fiber and matrix weight fractions of the composite specimens were obtained by removing the matrix using the matrix burn-off test according to the ASTM D2584-11. The specimens were placed in a 600 °C oven for four hours to burn off the resin. Burn-off temperature and time were chosen based on the thermogravimetric analysis (TGA) results. In addition, TGA test showed that at 600 °C, a 5.34% glass fiber mass loss occurred. The 5.34% fiber mass loss, probably due to the burning off the fiber sizing, was also considered in the calculation of the fiber volume fraction. The fiber and void volume fractions were then calculated using the weight fractions and density of the primary constituents as recommended by ASTM D3171-15.

$$v_m = \frac{\rho_c}{\rho_m}\left(\frac{w_c - w_f}{w_c}\right) \tag{27}$$

$$v_f = \frac{\rho_c}{\rho_f}\left(\frac{w_f}{w_c}\right) \tag{28}$$

$$v_v = 1 - (v_m + v_f) \tag{29}$$

where v_m is the matrix volume fraction, v_f is the fiber volume fraction, v_v is the void volume fraction, ρ_c is the density of composite, ρ_m is the density of matrix, ρ_f is the density of fiber, w_c is the composite sample weight, and w_f is the fiber weight.

The density of the fiber was obtained with a nitrogen pycnometer to be 2.470 ± 0.004 g/cm^3. Also, the density of cured neat resin is obtained by suspension method to be 1.152 ± 0.003 g/cm^3.

4.2.5. Scanning Electron Microscopy Imaging

The characterization of voids in terms of size, location, shape, and spatial distribution has been the subject of numerous studies [79, 167]. For instance, it has been observed the failure in composites may originate or accelerate due to the presence of

voids [191]. Also, crack initiation and growth can be caused by the voids greater than 400 μm [192]. In addition, it has been reported that the void size and location play significant roles in the transport of the voids and their mobility [193]. For instance, the mobility of the voids between the fiber tows is higher than the voids located within the tows [194]. Thus, the changes in void morphology such as size, shape, and location in different laminates were studied using scanning electron microscopy (SEM). In order to perform the observation two 25.4 mm × 6.4 mm specimens were removed from each laminate, mounted in an acrylic resin to expose the through-the-thickness cross-section of the laminates, and polished. Then, approximately 5 nm of gold/palladium coating was used to eliminate charging effects under SEM.

To quantify void size, an equivalent diameter, D_{eq}, is defined as,

$$D_{eq} = \sqrt{\frac{4A}{\pi}} \tag{30}$$

where A is the measured void area. The voids are divided into three categories according to their equivalent diameter: small (50 μm < D_{eq}), medium (50 μm ≤ D_{eq} < 150 μm), and large (D_{eq} ≥ 150 μm).

The shape of the voids is defined by roundness, R, described in equation (31),

$$R = \frac{4A}{\pi d_{max}^2} \tag{31}$$

where d_{max} is the maximum diameter of the void. The roundness represents the degree of shape irregularity of the voids. If the roundness value is 1, then the void has a perfect circular shape, and for more irregular and elongated voids, roundness becomes smaller. Thus, the voids are divided into circular ($0.9 < R \leq 1$), elliptical ($0.2 < R \leq 0.9$), and highly elongated ($R \leq 0.2$) categories.

4.2.6. Flexural Strength and Modulus of Elasticity

The mechanical properties of the 6-, 12-, and 18-ply laminates were characterized by the flexure test. All tests were performed on a Com-Ten® 705TN testing device. The flexural strength and modulus were determined by three-point bending test according to ASTM D790-17. A total of 14 specimens for each case (seven from each laminate) were cut to the approximate size of 114.3 × 12.7 mm^2. All tests were carried out with a span-to-depth ratio of 24:1 at a crosshead speed of 2 mm/min. Since the span-to-depth ratio is greater than 16 and deflections are large in comparison with the span (greater than 10% of the span), the flexural stress and modulus were determined by the following equations:

$$\sigma_f = \left(\frac{3PL}{2bh^2}\right)\left[1 + 6\left(\frac{D}{L}\right)^2 - 4\left(\frac{h}{L}\right)\left(\frac{D}{L}\right)\right] \tag{32}$$

$$E_f = \frac{L^3 m}{4bh^3} \tag{33}$$

where, σ_f is the stress in the outer layer of the specimen, P is the load at a given point on the load-deflection curve, L is the support span, D is the deflection of the centerline of the specimen at the middle of the support span, and b and h are the sample width and thickness, respectively. Moreover, E_f is the flexural modulus and m is the slope of tangent to the initial straight line portion of the load-deflection curve.

4.3. Results and Discussion

4.3.1. Thickness, Fiber and Void Volume Fraction, and Filling Time

Table 9 gives the thickness, fiber volume fraction, void volume fraction, and filling time of the 6-, 12-, and 18-ply random mat E-glass epoxy laminates fabricated by compacted and uncompacted preforms under eight scenarios. The resulting laminates

including those made with uncompacted and compacted 6-, 12-, and 18-ply random mats have nearly the same thickness of 1.5, 2.9, and 4.0 mm, respectively. Also, the fiber volume fractions of the 6-, 12-, and 18-ply laminates using uncompacted and compacted preforms did not differ considerably and are approximately 43-47%. These results prove that the compacted mat relaxed and expanded to its uncompacted thickness as the resin flow front progressed along the lay-up. However, despite having similar thickness and fiber volume fraction, the void content and filling time of the laminates that use uncompacted and compacted preforms completely differ.

Interestingly, the filling time of the laminates made with uncompacted mats (V-6-U, V-12-U, and V-18-U) is the same (i.e. 3 min) regardless of the number of plies. Clearly, the use of compacted preforms increased the filling time for all other five scenarios (V-6-C-A, V-12-C-A, V-18-C-A, V-18-C-B, and V-18-C-B-M) to more than 3 min depending on the level of compaction. This increase in filling time is due to the decrease in the permeability of the preforms. For instance, the filling time in the 6-, 12-, and 18-ply preforms compacted by set of A magnets are 13, 9, and 6 min. These different filling times with the same set of magnets indicate that by increasing the number of plies, level of compaction is reduced due to the higher lay-up thickness and thus lower magnetic pressure. As explained earlier, in order to have a higher level of compaction pressure, especially in 18-ply laminates, set of B magnets was utilized and, as a result, the filling time of the laminates increased to 8 min.

It is important to note that the three moving magnets compacted the preforms to an even higher level compared to the twenty-five stationary magnets from the same set (set B), and increased the filling time to 10 min. These results clearly demonstrate the

feasibility of moving magnets over the larger vacuum bag surface and effectively compacting the preforms of much larger parts.

The void volume fraction of the laminates made from 6- and 12-ply uncompacted preforms (V-6-U and V-12-U) was 1.9 and 1.2%, respectively; whereas, in the 18-ply laminates (V-18-U), the void volume fraction was quite high at approximately 5.7%. By compaction of dry 6- and 12-ply preforms by a set of A magnets, void volume fraction is remarkably reduced by 95% to 0.1% and by 65% to 0.4%. Using the same set of stationary magnets, in 18-ply laminates voids volume fraction decreased by 43% to 3.2%. To achieve higher compaction in 18-ply laminates, stronger stationary magnets (set B) were utilized which resulted in a more significant reduction of void volume fraction by 84% to 0.9% compared to that of uncompacted preforms.

More importantly, in the 18-ply laminates that were compacted by moving magnets over the vacuum bag, the void content was found to be reduced even more to less than 0.8%. These results prove that due to the significant reduction in the permeability of compacted preforms, the resin flow becomes more uniform and slower that prevents the entrapment of voids at the flow front. Hence, using this method, the voids formed by the high resin flow rate at the flow front [90, 176] can be minimized or eliminated. In addition, reduction in the pore spaces within the random mat as a result of compaction may have also contributed to the decreased void content. Thus, by applying magnetic compaction pressure of 0.19 MPa (or higher) whether by stationary or moving magnets, full compaction of dry preforms can be achieved, and as a result, the void content in VARTM laminates can be notably reduced.

It should be noted that with decreasing the filling rate, depending on the size of the part and the cure properties of the resin, premature gelation may occur during fabrication. To address this concern, compaction of preforms can be performed by either stationary or moving magnets only at the desired location, without covering the whole surface of the preform, leading to the local improvement of part quality. Thus, considering that the compacted regions relax as the flow front advances and recover the initial, uncompacted thickness, it would be possible to fabricate a larger laminate with uniform thickness while achieving a very low void content at critical locations within the part compacted by the magnets.

Table 9. Thickness, fiber volume fraction, void volume fraction, and filling time of the 6-, 12-, and 18-ply random mat E-glass epoxy laminates fabricated under eight scenarios (n=6 for fiber and void volume fraction; n=42 for average laminate thickness; 95% confidence interval for all data).

Processing scenario	No. of plies	Average thickness (mm)	Fiber volume fraction (%)	Void volume fraction (%)	Filling time (min)
V-6-U	6	1.45 ± 0.02	45.71 ± 0.14	1.86 ± 0.72	3
V-6-C-A	6	1.45 ± 0.03	43.41 ± 1.09	0.09 ± 0.05	13
V-12-U	12	2.84 ± 0.03	43.23 ± 0.17	1.15 ± 0.14	3
V-12-C-A	12	2.85 ± 0.03	44.15 ± 0.77	0.40 ± 0.23	9
V-18-U	18	3.99 ± 0.04	46.61 ± 0.18	5.66 ± 0.65	3
V-18-C-A	18	3.92 ± 0.03	47.35 ± 0.20	3.20 ± 0.97	6
V-18-C-B	18	4.07 ± 0.03	45.58 ± 0.92	0.90 ± 0.70	8
V-18-C-B-M	18	4.00 ± 0.04	45.50 ± 0.47	0.79 ± 0.14	10

4.3.2. Part Thickness Variation during VARTM for Compacted and Uncompacted Preforms

The thickness of the actual lay-up was measured over time using the dial gage (at x=44.5 mm) to demonstrate the influence of compaction of dry preforms on the evolution of lay-up thickness and to investigate the compaction behavior of preforms.

Fig. 43 presents the variation of 6, 12, and 18-ply lay-up thickness of uncompacted and compacted preforms during the 120 min of VARTM. As can be seen, the magnetic compaction pressure applied by a set of A magnets caused a reduction in the initial thickness (i.e., $t=0$) of the 6-, 12-, and 18-ply fabrics from 2.05 to 1.71 mm, from 3.96 to 3.74 mm, and from 5.68 to 5.19 mm, respectively. The fabrics became more compacted when the set of B magnets is used and, thus, the initial thickness of 18-ply fabrics declined from 5.68 to 5.05 mm. Interestingly, sliding the same set of magnets (set B) over the vacuum bag for 30 minutes resulted in a higher compaction level, evidenced by the considerably lower initial thickness of 4.3 mm shown in Fig. 43.

During impregnation of uncompacted preforms, it is found that once the resin flow wets the fiber mat, a sharp drop in the thickness occurs possibly due to the nesting effects. The nesting of fibers near the flow front can be explained by the lubrication effect, which will facilitate movement of fibers [24, 195]. In particular, the influence of nesting increases [177] with the higher number of plies, so the reduction in thickness becomes more significant. Furthermore, Fig. 43 reveals that, for the compacted preforms, the nesting effect becomes almost negligible as the lay-up thickness remains almost constant when the resin front reaches the dial gage within the first few minutes of the resin infusion.

After the flow front moves ahead, the thicknesses of both uncompacted and compacted preforms gradually increase due to the spring-back behavior of the fabrics. This behavior occurs due to the increase in the local resin pressure by the further advancement of the flow front [25, 196]. In compacted preforms, especially in 12- and 18-ply lay-ups, the thickness increase is higher compared to uncompacted ones, reflecting the larger spring-back potential of the compacted preform.

In all cases, when the impregnation of the preform is complete and the resin reaches the exit, the inlet is closed and the first local maximum in part thickness occurs (i.e. after the fill time). Filling time for each scenario is also labled by ● in Fig. 43. As can be seen in Fig. 43, all the curves have the rise to a local maximum and slow decline thereafter, but the maximum is shifted to the right for the parts with compacted fiber mats which demonstrates the significant effect of the compaction on the fill time. For example, the fill time of 18-ply fabrics compacted by stationary magnet sets A and B was increased from 3 min to 6 and 8 min, respectively. Also, the fill time of 18-ply fabrics compacted by moving the B magnets was increased from 3 min to 10 min. After closing the inlet, the vacuum assists the bleeding of the excess resin to increase the fiber volume fraction and, as expected, leading to a slight reduction in part thickness. All the curves for compacted and uncompacted fabrics follow very similar trends which are attributed to the repeatable nature of consolidation dynamics in VARTM. At about 45 min, the thicknesses of the compacted parts become very similar to those in uncompacted ones.

Forty-five minutes after the start of the process, the temperature is increased to 60 °C, thus, the entire lay-up slightly expands and a small increase of 0.02 to 0.12 mm

in lay-up thickness is observed in all cases. At the same time, the viscosity will drop with the increase in temperature, facilitating additional bleeding of the resin and further thickness reduction. Since the exit remains open, the uncured resin will be removed at a decreasing rate and all the parts slowly approach their final thicknesses at approximately 90 min.

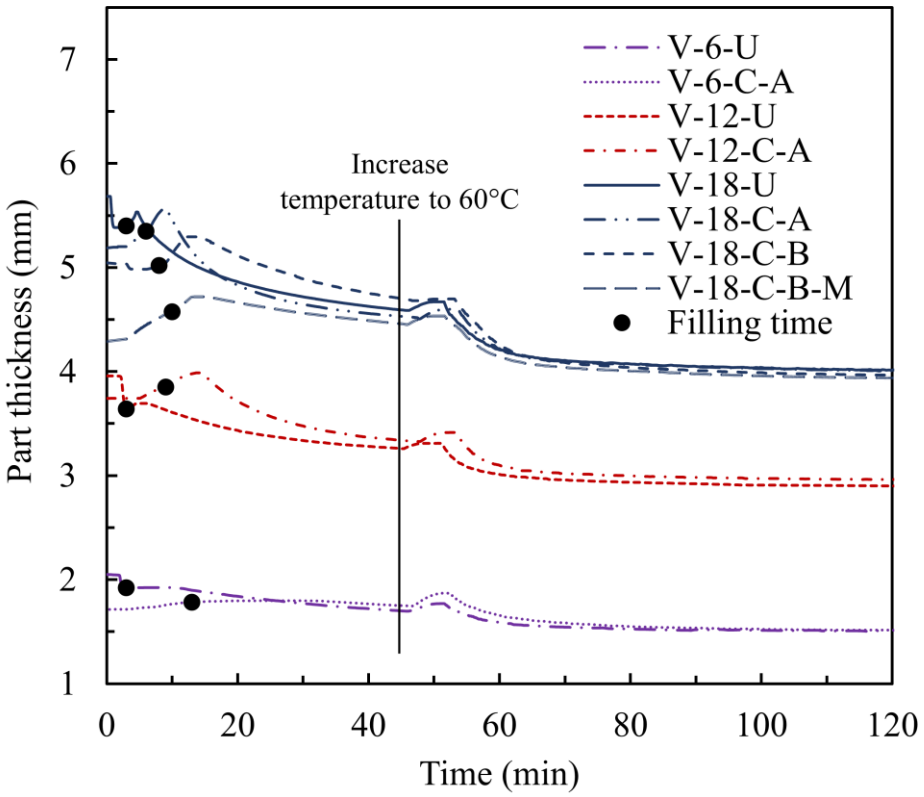

Figure 43. Part thickness variation during VARTM using 6, 12, and 18 plies of uncompacted and compacted random mat preforms. The laminate thickness was measured by a digital dial gage located 44.5 mm away from the inlet. Filling time for each scenario is also labled by ●.

4.3.3. Microstructural Analysis of Composite Laminates

SEM images of the through-the-thickness cross-section of 6-ply laminates made from compacted and uncompacted mats are displayed in Fig. 44 to better understand the differences in the process-induced microstructure. Figs. 44 (a) and (c) show the images

for the laminates with uncompacted preforms at 20× and 150×, respectively, while Figs. 44 (b) and (d) are with compacted preforms at the same magnifications. The range of equivalent diameter, average size, and roundness of the voids inside 6-ply laminates are also presented in Fig. 44 (e). It can be seen that there are some voids, ranging from 25 to 240 μm in size, inside the laminates made from uncompacted preforms. The presence of large voids causes higher stress concentration and thus considerably degrade the mechanical properties of composite laminates as reported by Chambers et al. [143]. Also, it is noted that the voids in Fig. 44 (a) are elliptical, with roundness in between 0.2-0.8, and their sharp edges increase the likelihood of crack initiation [197]. The voids seem to be preferentially located between the plies that make them detrimental to fiber/matrix interfacial behavior and adhesion [167]. Thus, it is critical to avoid the formation of such voids extending along the fiber/matrix interface. This goal is achieved by the compaction of the fiber mats before infusion such that no void is found between or inside the tows on the cross-section of samples made by compacted mats (see Fig. 44 (b)). This implies that the reduction in the pore spaces within the fiber mat along with controlling the resin flow have been successful to achieve a striking reduction in the formation of voids. Comparing Figs. 44 (a) and (b), the laminate thicknesses and the resin rich regions seem very similar for both laminates. From the higher magnification (150×) images shown in Figs. 44 (c) and (d), it is obvious that no micro-void is present inside the fiber tows which implies that the formed voids inside the random mat VARTM laminates are primarily macro-voids between the fiber tows.

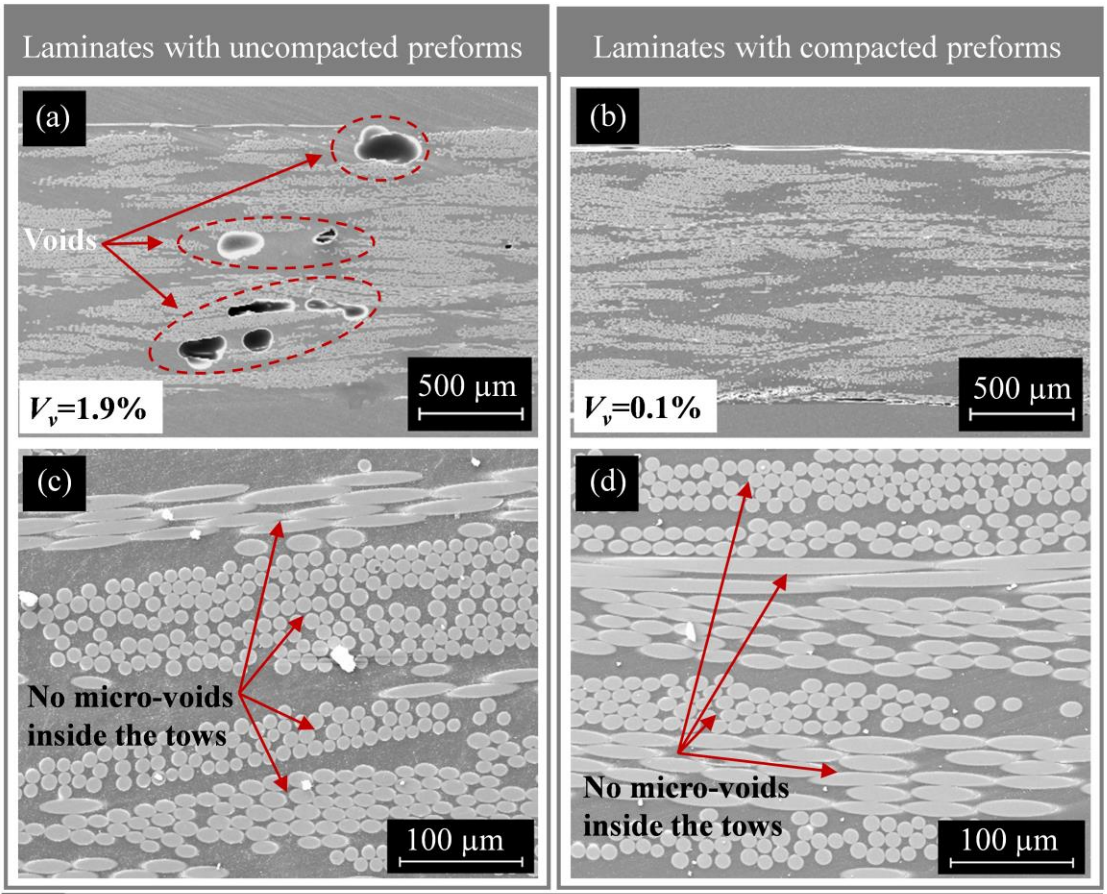

(e)

Specimen	Equivalent diameter (µm)	Average size (µm)	Roundness
V-6-U	25 – 240	195	0.2-0.8
V-6-C-A	–	–	–

Figure 44. SEM images of the cross-section of 6-ply laminates made from uncompacted (V-6-U) and uncompacted (V-6-C-A) preforms using set A of stationary magnets: (a) V-6-U at 20×, (b) V-6-C-A at 20×, (c) V-6-U at 150×, and (d) V-6-C-A at 150×. (e) Equivalent and roundness of voids in the V-6-U and V-6-C-A samples.

Similarly, Fig. 45 illustrates the SEM images of the 12-ply laminates made by uncompacted and compacted mats (20× and 150× magnification) as well as the range of equivalent diameter, average size, and roundness of the voids. As previously seen, voids are mostly located between the plies made by uncompacted preforms (see Fig. 45 (a)). Although the void content is lower in 12-ply laminates (i.e. 1.15%) compared to that in

6-ply laminates, large voids are still observed in the laminate (having average size of 150 µm). Thus, there is a need to eliminate such detrimental, large voids in 12-ply laminates which is achieved using compacted fabrics (V-12-C-A). As a result, the voids become significantly smaller with a lower average equivalent diameter of 82 µm (see Fig. 45 (b)). Similar to that in 6-ply laminates, no voids are observed inside the tows of 12-ply laminates which implies the complete wetting of the tows (see Figs. 45 (c) and (d)).

Fig. 46 shows the effects of different levels of compaction pressure (with magnet sets A and B) and moving versus stationary magnets on the microstructure of 18-ply laminates. The range of equivalent diameter, average size, and roundness of the process-induced voids are also presented. Fig. 46 (a) shows that the laminates with uncompacted preforms (V-18-U) contain numerous voids with different shapes (roundness of 0.2-0.9) which are mostly large with an equivalent diameter of 204 µm. It can be noted from Fig. 46 (b) that compaction of fabric by stationary magnets set A decreased the number as well as the size of the voids such that the average equivalent diameter of voids reduced to 164 µm. However, still, few large voids can be found within these laminate (V-18-C-A). Fig. 46 (c) demonstrates that the laminates made by stronger, stationary magnet set B contain smaller and fewer voids, where the average void size is declined even more, to about 92 µm. Interestingly, moving magnet set B is even more effective than their stationary placement in decreasing the void content and size such that the average void size is the lowest (i.e. 86 µm) in V-18-C-B-M laminates.

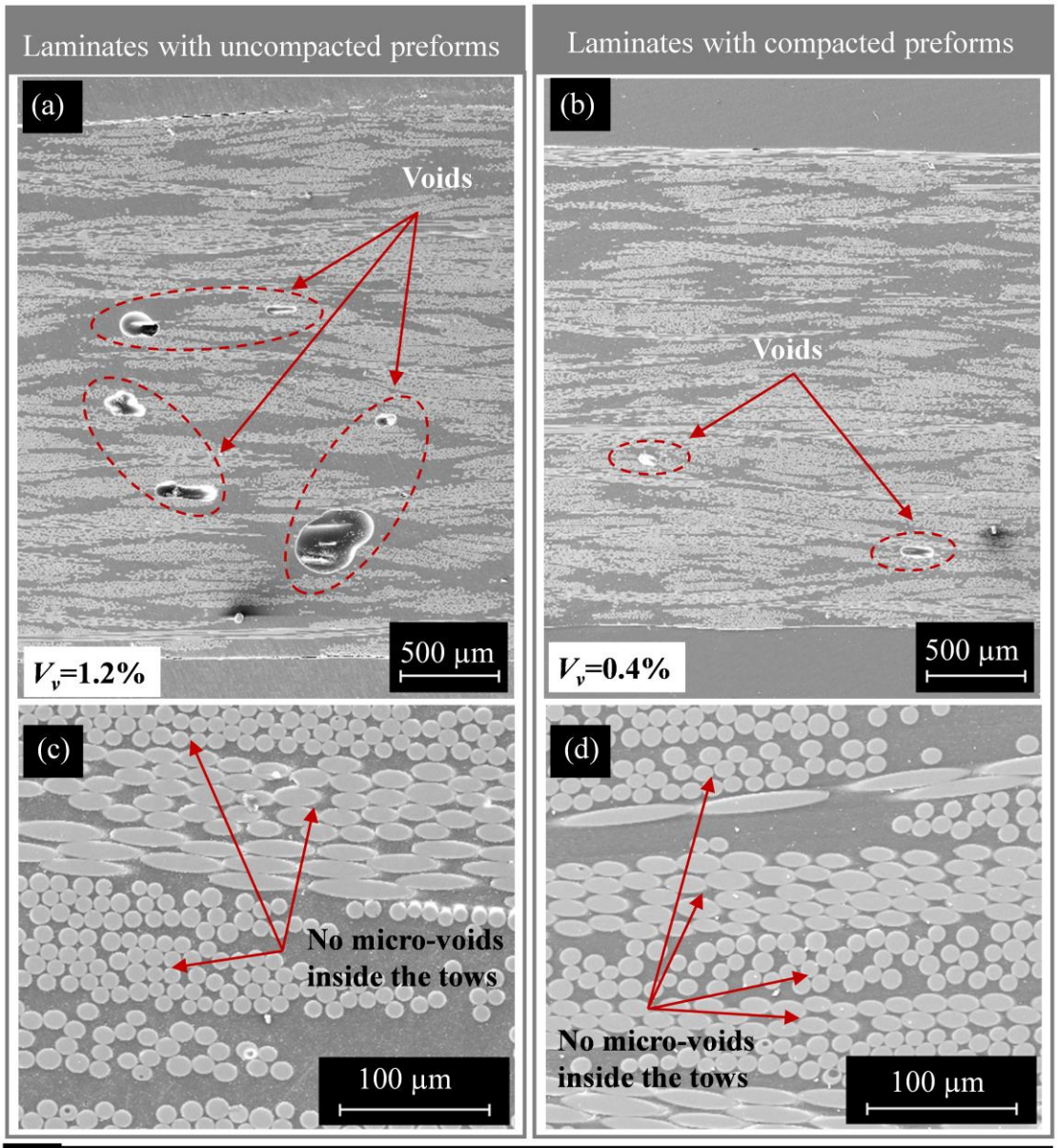

(e)

Specimen	Equivalent diameter (µm)	Average size (µm)	Roundness
V-12-U	31-347	150	03-0.7
V-12-C-A	20-140	82	0.3-0.9

Figure 45. SEM images of the of 12-ply laminates made from uncompacted (V-12-U) and compacted (V-12-C-A) preforms using set A of stationary magnets: (a) V-12-U at 20×, (b) V-12-C-A at 20×, (c) V-12-U at 150×, and (d) V-12-C-A at 150×. (e) Equivalent diameter, average size and roundness of voids in the V-12-U and V-12-C-A samples.

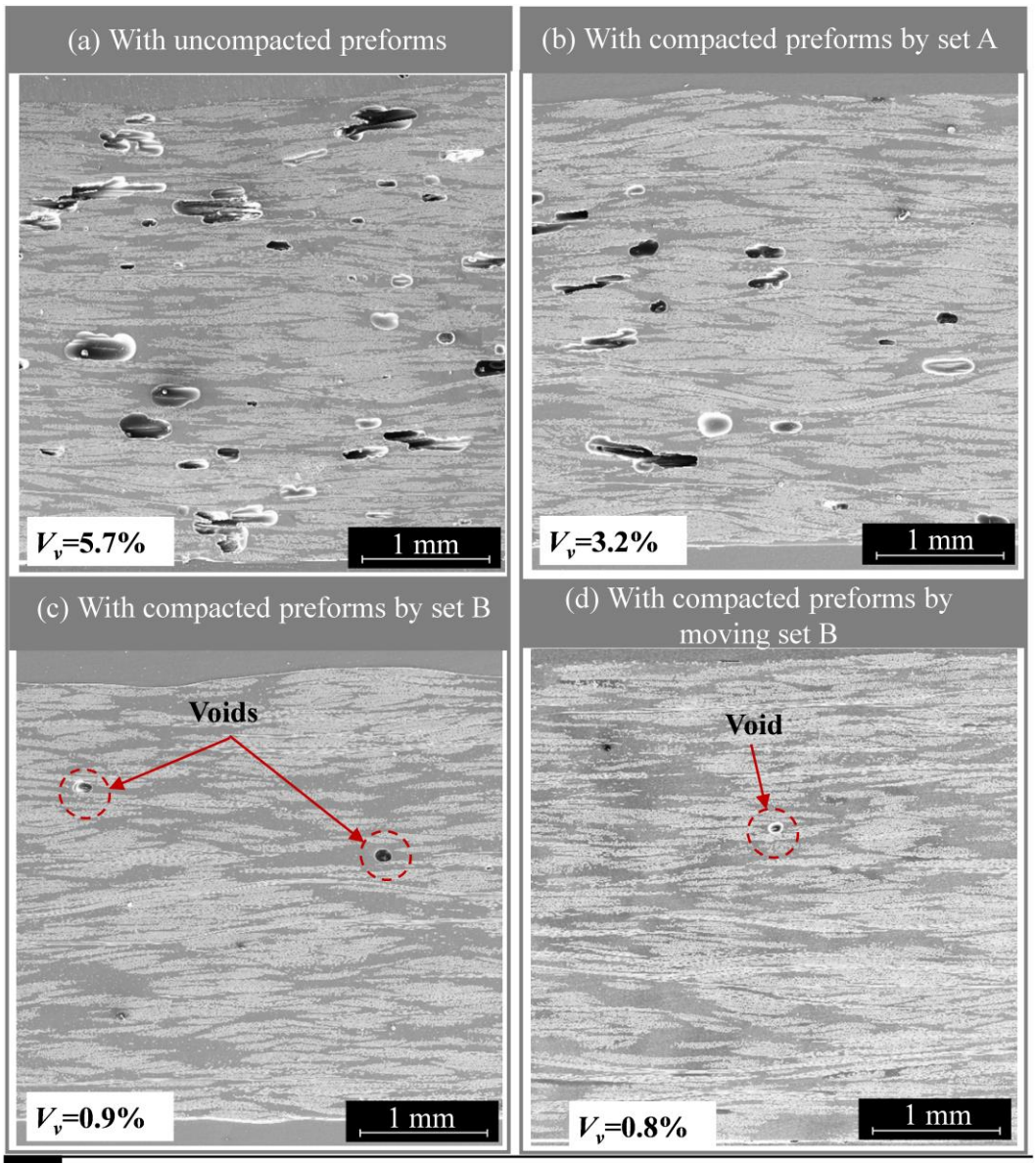

(e)

Specimen	Equivalent diameter (μm)	Average size (μm)	Roundness
V-18-U	40-440	204	0.2-0.9
V-18-C-A	85-229	164	0.2-0.6
V-18-C-B	29-148	92	0.4-0.8
V-18-C-B-M	16-206	86	0.2-0.9

Figure 46. SEM images of 18-ply laminates at 20× made by: (a) uncompacted preforms (V-18-U), (b) compacted preforms with set A of stationary magnets (V-18-C-A), (c) compacted preforms with set B of stationary magnets (V-18-C-B), and (d) compacted preforms with set B of moving magnets (V-18-C-B-M). (e) Equivalent diameter, average size, and roundness of voids in the V-18-U, V-18-C-A, V-18-C-B, and V-18-C-B-M laminates.

Thus, applying sufficiently high compaction pressure (i.e. 0.2 MPa or higher) either by stationary or moving magnets on the dry preforms greatly decreases the number and average size of voids which help reduce the void content.

4.3.4. Mechanical Properties of Laminates

The flexural strength and modulus of the 6-, 12-, and 18-ply laminates fabricated under eight manufacturing scenarios are shown in Figs. 47 and 48. To discern the adverse effect of voids on flexural properties, void volume fraction values are also presented on both figures.

Fig. 47 clearly shows that regardless of the number of plies, the flexural strength of the laminates made by compacted preforms is higher than those fabricated with uncompacted ones. Using permanent magnets to compact the lay-up improved the flexural strength of the 6-, 12-, and 18-ply laminates by 14% to 301 MPa, 9% to 304 MPa, and 6% to 319 MPa, respectively. Since the fiber volume fraction of the laminates made with and without compaction are almost the same, the increase in flexural strength most likely is due to the reduction in void content. Although not investigated in this work, reducing void content can also lead to other possible improvements in the part quality including increased fatigue life and enhanced resistance to crack initiation and growth [185, 198, 199]. In addition, several authors have reported that the presence of voids in the composite increases the moisture absorption and gas diffusion process which have an adverse effect on long-term durability and high-pressure storage applications of composites [81, 200, 201]. Thus, it is important to develop new processing strategies that can reduce or totally eliminate voids in composite laminates with relative ease. Magnetic compaction of dry preforms could be adopted in industrial

applications as the results presented in this work demonstrated the effectiveness of this method in achieving almost void-free VARTM laminates.

As shown in Fig. 48, the flexural modulus of all laminates made with compaction of preforms slightly increased (≈2%) while their void content is reduced. This increase is insignificant because the flexural modulus is mostly dependent on the fiber modulus [133] and the fiber volume fraction of the laminates, both of which are not changed noticeably.

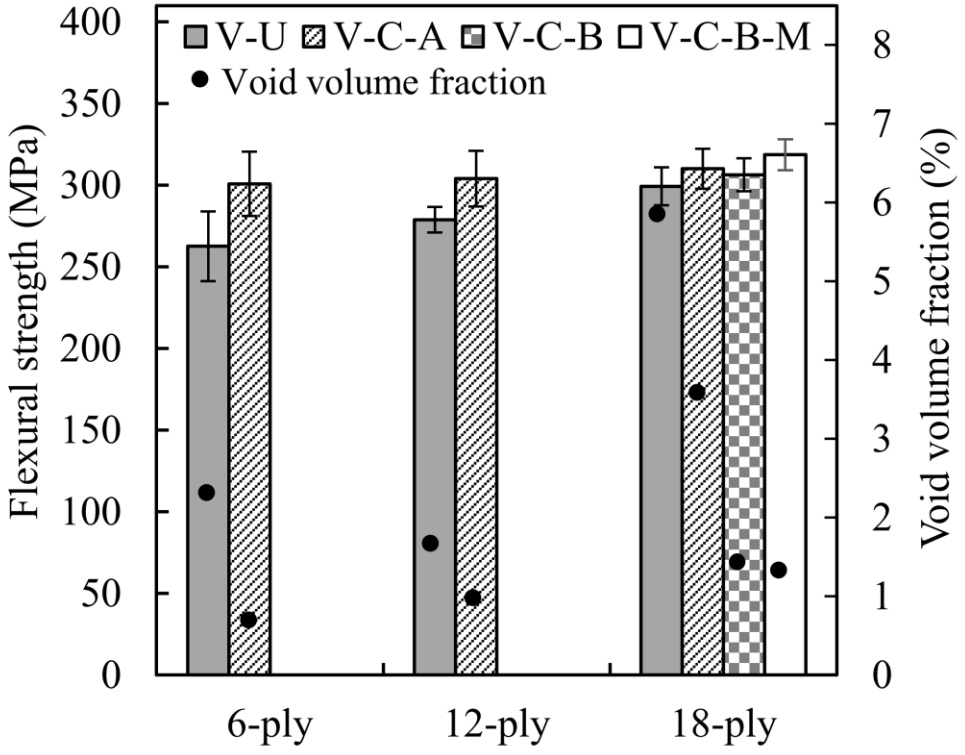

Figure 47. The flexural strength as a function of void volume fraction of the 6-, 12-, and 18-ply laminates fabricated under eight scenarios: (1) V-6-U, (2) V-6-C-A, (3) V-12-U, (4) V-12-C-A, (5) V-18-U, (6) V-18-C-A, (7) V-18-C-B, and (8) V-18-C-B-M. Note: Error bars indicate the 95% confidence interval for 14 samples.

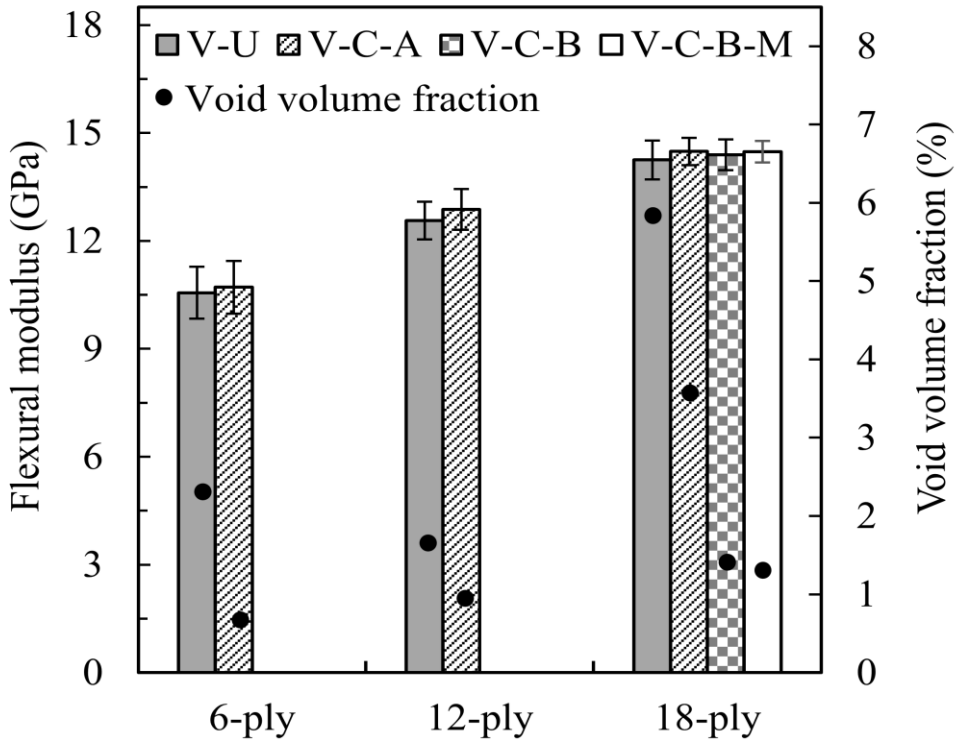

Figure 48. The flexural modulus as a function of void volume fraction of the 6-, 12-, and 18-ply laminates fabricated under eight scenarios: (1) V-6-U, (2) V-6-C-A, (3) V-12-U, (4) V-12-C-A, (5) V-18-U, (6) V-18-C-A, (7) V-18-C-B, and (8) V-18-C-B-M. Note: Error bars indicate the 95% confidence interval for 14 sample.

4.4. Concluding Remarks

In this chapter, a new method was introduced that reduces or eliminates the process-induced voids in VARTM laminates by compacting the preforms before infusion. This compaction was achieved by applying pressure on the lay-up using either stationary or moving magnets, thus covering a much larger lay-up size. Also, different levels of compaction pressure were applied using two different sets of magnets as well as different number of plies. The main conclusions are:

- Compaction of preforms decreased their permeability and pore spaces, thus led to a more uniform and slower resin flow compared to the resin flow observed in uncompacted laminates.
- Appling compaction pressure of 0.2 MPa or higher using either stationary or moving magnets was found to be very effective in reducing the void content by 65-95% to 0.1-0.8% in all laminates.
- Moving magnets with a smaller footprint over the larger vacuum bag surface proved to be a feasible approach for manufacturing larger parts provided that a suitable lubricant was used between the magnets and the vacuum bag to reduce the friction.
- The final thicknesses of the laminates made with compacted and uncompacted fabrics were almost the same because the compacted mat relaxed and recovered its initial thickness as the resin flow front progressed along the lay-up. This feature allows one to locally compact the preform for the local improvement of part quality while maintaining a uniform thickness throughout the whole part.
- The flexural strength of the laminates made by compacted preforms was improved by 6-14% to 301-319 MPa, possibly due to considerable reduction of void content.

Although not demonstrated here, the void-free parts made by the proposed method can also lead to additional improvements in the part quality such as increased fatigue life, enhanced resistance to crack initiation and growth, and decreased moisture absorption.

CHAPTER 5. Conclusion and Future Perspective

5.1. Conclusion

Liquid composite molding processes that involve a vacuum bag, such as wet lay-up vacuum bagging (WLVB) and vacuum assisted resin transfer molding (VARTM), are widely used in the fabrication of small to large composite parts due to their cost efficiency, ease of processing, and ability to manufacture complex parts. However, there are a number of processing drawbacks in vacuum bag lay-up processes such as limited consolidation pressure (i.e. 0.1 MPa) resulting in the parts with low fiber content, high process-induced defects, and low interlaminar consolidation. Accordingly, the focus of this dissertation is to develop novel manufacturing techniques to tackle the important problems encountered with the molding of composite materials. The common ground of all these novel manufacturing techniques is the use of high-power, permanent magnets in developing high compaction pressures during the molding of composite laminates.

In this dissertation, a novel composite manufacturing technique, magnet assisted composite manufacturing (MACM), is introduced to improve the quality of wet lay-up vacuum bag laminates. This new technique utilizes the Neodymium Iron Boron (NdFeB) magnets, the strongest permanent magnets commercially available, to apply sufficiently high consolidation pressure transverse to the composite laminate during cure. The results show that by MACM, 0.2-0.3 MPa (~30-45 psi) consolidation pressure can be applied on the lay-up, resulting in:

- Significant reduction in void content to less than 2%
- Considerable increase in the fiber content by more than 55% to above 27%

- Substantial improvement in flexural properties by more than 50%, primarily due to the increase in fiber volume fraction and decrease in process-induced voids.

The results also suggest that this technique gives the flexibility of applying consolidation pressure at different processing stages (e.g. when the resin viscosity is minimum, or the resin is gelled) with different time span. For example, applying magnetic pressure only for 15 minutes after resin gelation was shown to considerably enhance the flexural properties by 16-29%.

The effectiveness of applying additional external pressure by MACM to improve the overall quality of VARTM laminates is investigated and a new transient consolidation model for MACM is introduced in this dissertation. Considering that the applied magnetic pressure will decrease as the lay-up thickness is increased, the capability of this method to improve the quality of thin (i.e. 6-ply), as well as moderately thick (i.e. 12- and 18-ply) VARTM laminates is investigated. The experimental results lead to the following conclusions:

- Applying magnets either before or after the resin infusion yielded a similar level of increase in the fiber content of the 6-, 12-, and 18-ply laminates from 43-47% to 51-53%.
- The MACM method is shown to yield remarkable improvements in flexural properties (i.e. > 11-41%).
- Interestingly, applying the magnets before infusion minimized the risk of void entrapment, thus significantly reduced the void content of the laminates from 6% to less than 1%.

In addition, the results of the transient magnetic consolidation model were shown to accurately predict the final fiber volume fraction and thickness of all fabricated VARTM laminates. This model can be used to further investigate the magnetic compaction behavior for various process parameters, and help identify the appropriate combinations of magnets, fabric types, and resin systems to achieve the desired level of compaction and flexural properties.

Finally, in this dissertation, a novel processing technique of enhancing flow in VARTM process is introduced to substantially reduce or completely eliminate process induced voids in VARTM laminates. In this technique, the dry fibrous preforms are compacted prior to the resin infusion using either stationary or moving magnets to control the resin flow rate, thus enhancing the quality of VARTM laminates. The compaction of dry fiber preforms decreases the pore spaces, and thus reduces the preform permeability. Lower permeability corresponds to the more uniform and slower resin flow, preventing the void formation during the filling of the part. In this work, some of the main observations are:

- Applying 0.2 MPa or higher compaction pressure prior to infusion leads to the VARTM laminates with less than 1% voids.
- Sliding magnets with a smaller footprint on a larger surface is a viable technique in the fabrication of much larger VARTM parts with no process induced voids. However, it is important to note that the sliding of the magnets over the vacuum bag would be possible only if a proper lubricant is used between magnets and lay-up surface.
- The final thickness of VARTM laminates made by compacted and uncompacted preforms are almost the same due to the spring-back behavior

of the fabrics. This gives the possibility of local manipulation of the preform permeability to improve the laminate quality at critical locations while having a uniform final thickness throughout the part.

5.2. Future Perspective

At present, autoclave curing is the “gold standard” for the fabrication of FRP composites. However, this technique has a relatively high cost per cured part, which is an important inhibitor to the wider use of composite materials. In this regard, there is a growing interest in out-of-autoclave (OoA) techniques; however, the absence of sufficiently high compaction pressure is of major concern. In addition, with autoclave and common OoA techniques, the application of local as well as non-uniform pressure is not feasible for most applications. For instance, fabricating complex shape (e.g. L-shaped) composites either by autoclave or common OoA techniques yields high thickness variation and process-induced defects such as corner thinning in convex tooling, corner thickening in concave tooling, and voids at the corners. To address this problem one can benefit from the application of nonuniform magnetic pressure across the composite laminate, tailoring the mechanical properties at critical locations (e.g. the corner of L-shaped parts) with relatively low cost. The novel MACM technique along with detailed characterization techniques introduced in this dissertation can be a roadmap for fabricating high-quality complex composite parts.

In liquid composite molding (LCM) processes the fibrous reinforcement is impregnated by liquid resin. Thus, the fiber preform permeability and its spatial variation determine the filling pattern, dictating whether or not defects such as voids or dry spots are present in the final composite part. Therefore, customization of fiber

preform permeability that ensures the filling without voids or dry spots is of interest in industries that rely on composite materials, such as the aerospace and automotive industries. To address the abovementioned challenges in the filling of a complex composite part, the novel processing techniques introduced in this dissertation can be utilized to manipulate the permeability of a dry fiber preform using magnetic compaction. In this regard, permanent magnets can be used to compact the regions with higher permeability with high pressure and the zones that are more difficult to impregnate with lower pressure. Removing the compaction pressure prior to infusion will lead to the high-quality composite part with uniform thicknesses.

References

[1] Guermazi N, Tarjem AB, Ksouri I, Ayedi HF. On the durability of FRP composites for aircraft structures in hygrothermal conditioning. Composites Part B: Engineering, 2016;**85**:294-304.

[2] Thawre MM, Verma KK, Jagannathan N, Peshwe DR, Paretkar RK, Manjunatha CM. Effect of ply-drop on fatigue life of a carbon fiber composite under a fighter aircraft spectrum load sequence. Composites Part B: Engineering, 2016;**86**:120-5.

[3] Mueller EM, Starnes S, Strickland N, Kenny P, Williams C. The detection, inspection, and failure analysis of a composite wing skin defect on a tactical aircraft. Composite Structures, 2016;**145**:186-93.

[4] Esnaola A, Tena I, Aurrekoetxea J, Gallego I, Ulacia I. Effect of fibre volume fraction on energy absorption capabilities of E-glass/polyester automotive crash structures. Composites Part B: Engineering, 2016;**85**:1-7.

[5] Panaitescu I, Koch T, Archodoulaki V-M. Accelerated aging of a glass fiber/polyurethane composite for automotive applications. Polymer Testing, 2019;**74**:245-56.

[6] Pil L, Bensadoun F, Pariset J, Verpoest I. Why are designers fascinated by flax and hemp fibre composites? Composites Part A: Applied Science and Manufacturing, 2016;**83**:193-205.

[7] Hallonet A, Ferrier E, Michel L, Benmokrane B. Durability and tensile characterization of wet lay-up flax/epoxy composites used for external strengthening of RC structures. Construction and Building Materials,

2019;**205**:679-98.

[8] Hadigheh SA, Kashi S. Effectiveness of vacuum consolidation in bonding fibre reinforced polymer (FRP) composites onto concrete surfaces. Construction and Building Materials, 2018;**187**:854-64.

[9] Tahir M, Wang Z, Ali KM. Axial compressive behavior of square concrete columns confined with CFRP strip ties using wet lay-up technique. Construction and Building Materials, 2019;**200**:282-92.

[10] Ma R, Chang X, Zhang X, Fang P, Long B, Liu W. Effect of curing method on mechanical and morphological properties of carbon fiber epoxy composites for solid rocket motor. Polymer Composites, 2015;**36**(9):1703-11.

[11] Marouani S, Curtil L, Hamelin P. Composites realized by hand lay-up process in a civil engineering environment: initial properties and durability. Materials and structures, 2008;**41**(5):831-51.

[12] Justo J, París F. Experimental mechanical characterization of composite-concrete joints. Composites Part B: Engineering, 2018;**154**:148-56.

[13] Sciolti MS, Frigione M, Aiello MA. Wet lay-up manufactured FRPs for concrete and masonry repair: influence of water on the properties of composites and on their epoxy components. Journal of Composites for Construction, 2010;**14**(6):823-33.

[14] Karbhari VM, Abanilla MA. Design factors, reliability, and durability prediction of wet layup carbon/epoxy used in external strengthening. Composites Part B: Engineering, 2007;**38**(1):10-23.

[15] Al-Shawaf A. Influence of fibres' stiffness on wet lay-up CFRP/steel joints'

behaviour under subzero exposures. Composites Part B: Engineering, 2015;**73**:61-71.

[16] Abanilla MA, Karbhari VM, Li Y. Interlaminar and intralaminar durability characterization of wet layup carbon/epoxy used in external strengthening. Composites Part B: Engineering, 2006;**37**(7-8):650-61.

[17] Fragassa C. Marine applications of natural fibre-reinforced composites: A manufacturing case study. Advances in Applications of Industrial Biomaterials: Springer, 2017, pp. 21-47.

[18] Abraham D, Matthews S, Mcllhagger R. A comparison of physical properties of glass fibre epoxy composites produced by wet lay-up with autoclave consolidation and resin transfer moulding. Composites Part A: Applied Science and Manufacturing, 1998;**29**(7):795-801.

[19] Francucci G, Palmer S, Hall W. External compaction pressure over vacuum-bagged composite parts: Effect on the quality of flax fiber/epoxy laminates. Journal of Composite Materials, 2018;**52**(1):3-15.

[20] Hota GVS, Hota SRV. Advances in fibre-reinforced polymer composite bridge decks. Progress in Structural Engineering and Materials, 2002;**4**(2):161-8.

[21] Brouwer WD, Van Herpt ECFC, Labordus M. Vacuum injection moulding for large structural applications. Composites Part A: Applied Science and Manufacturing, 2003;**34**(6):551-8.

[22] Critchfield MO, Judy TD, Kurzweil AD. Low-cost design and fabrication of composite ship structures. Marine Structures, 1994;**7**(2-5):475-94.

[23] Lee C-L, Wei K-H. Effect of material and process variables on the performance

of resin-transfer-molded epoxy fabric composites. Journal of Applied Polymer Science, 2000;**77**(10):2149-55.

[24] Tackitt KD, Walsh SM. Experimental study of thickness gradient formation in the VARTM process. Materials and Manufacturing Processes, 2005;**20**(4):607-27.

[25] Yenilmez B, Senan M, Sozer EM. Variation of part thickness and compaction pressure in vacuum infusion process. Composites Science and Technology, 2009;**69**(11-12):1710-19.

[26] Yalcinkaya MA, Caglar B, Sozer EM. Effect of permeability characterization at different boundary and flow conditions on vacuum infusion process modeling. Journal of Reinforced Plastics and Composites, 2017;**36**(7):491-504.

[27] Mathuw R, Advani SG, Heider D, Hoffmann C, Gillespie Jr. JW, Fink BK. Flow front measurements and model validation in the vacuum assisted resin transfer molding process. Polymer Composites, 2001;**22**(4):477-90.

[28] Yalcinkaya MA, Sozer EM. Effect of part thickness variation on the mold filling time in vacuum infusion process. Journal of Reinforced Plastics and Composites, 2014;**33**(23):2136-50.

[29] Alms JB, Advani SG. Simulation and experimental validation of flow flooding chamber method of resin delivery in liquid composite molding. Composites Part A: Applied Science and Manufacturing, 2007;**38**(10):2131-41.

[30] Chang C-Y. Experimental analysis of mold filling in vacuum assisted compression resin transfer molding. Journal of Reinforced Plastics and Composites, 2012;**31**(23):1630-7.

[31] Yalcinkaya MA, Sozer EM, Altan MC. Dynamic pressure control in VARTM: Rapid fabrication of laminates with high fiber volume fraction and improved dimensional uniformity. Polymer Composites, 2018. DOI: 10.1002/pc.25130.

[32] Markicevic B, Litchfield D, Heider D, Advani SG. Role of flow enhancement network during filling of fibrous porous media. Journal of Porous Media, 2005;**8**(3):281-97.

[33] Seemann III WH. Plastic transfer molding techniques for the production of fiber reinforced plastic structures. Google Patents, 1990.

[34] Allende M, Mohan RV, Walsh SM. Experimental and numerical analysis of flow behavior in the FASTRAC liquid composite manufacturing process. Polymer Composites, 2004;**25**(4):384-96.

[35] Verma KK, Dinesh BL, Singh K, Gaddikeri KM, Srinivasa V, Kumar R, Sundaram R. Development of vacuum enhanced resin infusion technology (VERITy) process for manufacturing of primary aircraft structures. Journal of the Indian Institute of Science, 2013;**93**(4):621-34.

[36] Garofalo J, Walczyk D, Kuppers J. Rapid consolidation and curing of vacuum-infused thermoset composite parts. Journal of Manufacturing Science and Engineering, 2016;**139**(2):021010.

[37] Yalcinkaya MA, Sozer EM, Altan MC. Fabrication of high quality composite laminates by pressurized and heated-VARTM. Composites Part A: Applied Science and Manufacturing, 2017;**102**:336-46.

[38] Yalcinkaya MA, Guloglu GE, Pishvar M, Amirkhosravi M, Sozer EM, Altan MC. Pressurized Infusion: A New and Improved Liquid Composite Molding

Process. Journal of Manufacturing Science and Engineering, 2019;**141**(1):011007.

[39] Simacek P, Heider D, Gillespie Jr. JW, Advani SG. Post-filling flow in vacuum assisted resin transfer molding processes: Theoretical analysis. Composites Part A: Applied Science and Manufacturing, 2009;**40**(6):913-24.

[40] Acheson JA, Simacek P, Advani SG. The implications of fiber compaction and saturation on fully coupled VARTM simulation. Composites Part A: Applied Science and Manufacturing, 2004;**35**(2):159-69.

[41] Song YS, Youn JR. Modeling of resin infusion in vacuum assisted resin transfer molding. Polymer Composites, 2008;**29**(4):390-5.

[42] Simacek P, Advani SG. A numerical model to predict fiber tow saturation during liquid composite molding. Composites Science and Technology, 2003;**63**(12):1725-36.

[43] Lopatnikov S, Simacek P, Gillespie Jr. JW, Advani SG. A closed form solution to describe infusion of resin under vacuum in deformable fibrous porous media. Modelling and Simulation in Materials Science and Engineering, 2004;**12**(3):S191-204.

[44] Loudad R, Saouab A, Beauchene P, Agogue R, Desjoyeaux B. Numerical modeling of vacuum-assisted resin transfer molding using multilayer approach. Journal of Composite Materials, 2017;**51**(24):3441-52.

[45] Lawrence JM, Frey P, Obaid AA, Yarlagadda S, Advani SG. Simulation and validation of resin flow during manufacturing of composite panels containing embedded impermeable inserts with the VARTM process. Polymer Composites,

2007;**28**(4):442-50.

[46] Phelan Jr. FR. Simulation of the injection process in resin transfer molding. Polymer Composites, 1997;**18**(4):460-76.

[47] Bruschke MV, Advani SG. A finite element/control volume approach to mold filling in anisotropic porous media. Polymer Composites, 1990;**11**(6):398-405.

[48] Tang J-M, Lee WI, Springer GS. Effects of cure pressure on resin flow, voids, and mechanical properties. Journal of Composite Materials, 1987;**21**(5):421-40.

[49] Loos AC, Springer GS. Curing of epoxy matrix composites. Journal of Composite Materials, 1983;**17**(2):135-69.

[50] Gutowski TG, Morigaki T, Cai Z. The consolidation of laminate composites. Journal of Composite Materials, 1987;**21**(2):172-88.

[51] Dave R, Kardos JL, Duduković MP. A model for resin flow during composite processing part 2: numerical analysis for unidirectional graphite/epoxy laminates. Polymer Composites, 1987;**8**(2):123-32.

[52] Terzaghi K. Principles of soil mechanics, IV—Settlement and consolidation of clay. Engineering News-Record, 1925;**95**(3):874-8.

[53] Lindt JT. Engineering principles of the formation of epoxy resin composites. SAMPE Quarterly, 1982, pp. 14-19.

[54] Halpin JC, Kardos JL, Dudukovic MP. Processing science: an approach for prepreg composite systems. Pure and Applied Chemistry, 1983;**55**(5):893-906.

[55] Mehdikhani M, Gorbatikh L, Verpoest I, Lomov SV. Voids in fiber-reinforced polymer composites: a review on their formation, characteristics, and effects on mechanical performance. Journal of Composite Materials, 2019;**53**(12):1579-

669.

[56] Kosmann N, Karsten JM, Schuett M, Schulte K, Fiedler B. Determining the effect of voids in GFRP on the damage behaviour under compression loading using acoustic emission. Composites Part B: Engineering, 2015;**70**:184-8.

[57] Sisodia S, Gamstedt EK, Edgren F, Varna J. Effects of voids on quasi-static and tension fatigue behaviour of carbon-fibre composite laminates. Journal of Composite Materials, 2015;**49**(17):2137-48.

[58] Maragoni L, Carraro PA, Peron M, Quaresimin M. Fatigue behaviour of glass/epoxy laminates in the presence of voids. International Journal of Fatigue, 2017;**95**:18-28.

[59] Yoshida H, Ogasa T, Hayashi R. Statistical approach to the relationship between ILSS and void content of CFRP. Composites Science and Technology, 1986;**25**(1):3-18.

[60] Ledru Y, Bernhart G, Piquet R, Schmidt F, Michel L. Coupled visco-mechanical and diffusion void growth modelling during composite curing. Composites Science and Technology, 2010;**70**(15):2139-45.

[61] Varna J, Joffe R, Berglund LA, Lundström T. Effect of voids on failure mechanisms in RTM laminates. Composites Science and Technology, 1995;**53**(2):241-9.

[62] Talreja R. Defect damage mechanics: broader strategy for performance evaluation of composites. Plastics, Rubber and Composites, 2009;**38**(2-4):49-54.

[63] Yalcinkaya MA, Sozer EM, Altan MC. Effect of external pressure and resin flushing on reduction of process-induced voids and enhancement of laminate

quality in heated-VARTM. Composites Part A: Applied Science and Manufacturing, 2019;**121**:353-64.

[64] Naganuma T, Naito K, Kyono J, Kagawa Y. Influence of prepreg conditions on the void occurrence and tensile properties of woven glass fiber-reinforced polyimide composites. Composites Science and Technology, 2009;**69**(14):2428-33.

[65] Xu K, Qian X. An FEM analysis with consideration of random void defects for predicting the mechanical properties of 3D braided composites. Advances in Materials Science and Engineering, 2014;**2014**:1-12.

[66] Lee J, Soutis C. A study on the compressive strength of thick carbon fibre-epoxy laminates. Composites Science and Technology, 2007;**67**(10):2015-26.

[67] Bazhenov SL, Kuperman AM, Zelenskii ES, Berlin AA. Compression failure of unidirectional glass-fibre-reinforced plastics. Composites Science and Technology, 1992;**45**(3):201-8.

[68] Hernández S, Sket F, González C, LLorca J. Optimization of curing cycle in carbon fiber-reinforced laminates: Void distribution and mechanical properties. Composites Science and Technology, 2013;**85**:73-82.

[69] Liebig WV, Leopold C, Schulte K. Photoelastic study of stresses in the vicinity of a unique void in a fibre-reinforced model composite under compression. Composites Science and Technology, 2013;**84**:72-7.

[70] Zhang A, Lu H, Zhang D. Research on the mechanical properties prediction of carbon/epoxy composite laminates with different void contents. Polymer Composites, 2016;**37**(1):14-20.

[71] Stone DEW, Clarke B. Ultrasonic attenuation as a measure of void content in carbon-fibre reinforced plastics. Non-Destructive Testing, 1975;**8**(3):137-45.

[72] Uhl KM, Lucht B, Jeong H, Hsu DK. Mechanical strength degradation of graphite fiber reinforced thermoset composites due to porosity. Review of progress in quantitative nondestructive evaluation: Springer, 1988, pp. 1075-82.

[73] Ghiorse S. Effect of void content on the mechanical properties of carbon/epoxy laminates. SAMPE Quarterly, 1993, pp. 54-9.

[74] Davies LW, Day RJ, Bond D, Nesbitt A, Ellis J, Gardon E. Effect of cure cycle heat transfer rates on the physical and mechanical properties of an epoxy matrix composite. Composites Science and Technology, 2007;**67**(9):1892-9.

[75] Nikishkov Y, Seon G, Makeev A. Structural analysis of composites with porosity defects based on X-ray computed tomography. Journal of Composite Materials, 2014;**48**(17):2131-44.

[76] Prakash R. Significance of defects in the fatigue failure of carbon fibre reinforced plastics. Fibre Science and Technology, 1981;**14**(3):171-81.

[77] Lambert J, Chambers AR, Sinclair I, Spearing SM. 3D damage characterisation and the role of voids in the fatigue of wind turbine blade materials. Composites Science and Technology, 2012;**72**(2):337-43.

[78] Schmidt F, Rheinfurth M, Horst P, Busse G. Multiaxial fatigue behaviour of GFRP with evenly distributed or accumulated voids monitored by various NDT methodologies. International Journal of Fatigue, 2012;**43**:207-16.

[79] Liu L, Zhang B-M, Wang D-F, Wu Z-J. Effects of cure cycles on void content and mechanical properties of composite laminates. Composite Structures,

2006;**73**(3):303-9.

[80] Li Y, Li Q, Ma H. The voids formation mechanisms and their effects on the mechanical properties of flax fiber reinforced epoxy composites. Composites Part A: Applied Science and Manufacturing, 2015;**72**:40-8.

[81] Harper BD, Staab GH, Chen RS. A note on the effects of voids upon the hygral and mechanical properties of AS4/3502 graphite/epoxy. Journal of Composite Materials, 1987;**21**(3):280-89.

[82] Thomason JL. The interface region in glass fibre-reinforced epoxy resin composites: 2. Water absorption, voids and the interface. Composites, 1995;**26**(7):477-85.

[83] Selzer R, Friedrich K. Mechanical properties and failure behaviour of carbon fibre-reinforced polymer composites under the influence of moisture. Composites Part A: Applied Science and Manufacturing, 1997;**28**(6):595-604.

[84] Costa ML, Rezende MC, De Almeida SFM. Strength of hygrothermally conditioned polymer composites with voids. Journal of Composite Materials, 2005;**39**(21):1943-61.

[85] Pérez-Pacheco E, Cauich-Cupul JI, Valadez-González A, Herrera-Franco PJ. Effect of moisture absorption on the mechanical behavior of carbon fiber/epoxy matrix composites. Journal of Materials Science, 2013;**48**(5):1873-82.

[86] Allred RE. The effect of temperature and moisture content on the flexural response of Kevlar/epoxy laminates: Part I. [0/90] filament orientation. Journal of Composite Materials, 1981;**15**(2):100-16.

[87] Park CH, Woo L. Modeling void formation and unsaturated flow in liquid

composite molding processes: a survey and review. Journal of Reinforced Plastics and Composites, 2011;**30**(11):957-77.

[88] Park CH, Lebel A, Saouab A, Bréard J, Lee WI. Modeling and simulation of voids and saturation in liquid composite molding processes. Composites Part A: Applied Science and Manufacturing, 2011;**42**(6):658-68.

[89] Hayward JS, Harris B. The effect of vacuum assistance in resin transfer moulding. Composites Manufacturing, 1990;**1**(3):161-6.

[90] Barraza HJ, Hamidi YK, Aktas L, O'Rear EA, Altan MC. Porosity reduction in the high-speed processing of glass-fiber composites by resin transfer molding (RTM). Journal of Composite Materials, 2004;**38**(3):195-226.

[91] Amirkhosravi M, Pishvar M, Altan MC. Void reduction in VARTM composites by compaction of dry fiber preforms with stationary and moving magnets. Journal of Composite Materials, 2019;**53**(6):769-82.

[92] Amirkhosravi M, Pishvar M, Altan MC. Reduction of voids in VARTM composites by magnetic compaction of preforms before infusion. Proceedings of the American Society of Composites-32nd Technical Conference, West Lafayette, Indiana, USA, 2017.

[93] Kuentzer N, Simacek P, Advani SG, Walsh S. Correlation of void distribution to VARTM manufacturing techniques. Composites Part A: Applied Science and Manufacturing, 2007;**38**(3):802-13.

[94] Patel N, Rohatgi V, Lee LJ. Micro scale flow behavior and void formation mechanism during impregnation through a unidirectional stitched fiberglass mat. Polymer Engineering and Science, 1995;**35**(10):837-51.

[95] Rohatgi V, Patel N, Lee LJ. Experimental investigation of flow-induced microvoids during impregnation of unidirectional stitched fiberglass mat. Polymer Composites, 1996;**17**(2):161-70.

[96] Ruiz E, Achim V, Soukane S, Trochu F, Bréard J. Optimization of injection flow rate to minimize micro/macro-voids formation in resin transfer molded composites. Composites Science and Technology, 2006;**66**(3-4):475-86.

[97] Lee DH, Lee WI, Kang MK. Analysis and minimization of void formation during resin transfer molding process. Composites Science and Technology, 2006;**66**(16):3281-9.

[98] Johnson RJ, Pitchumani R. Enhancement of flow in VARTM using localized induction heating. Composites Science and Technology, 2003;**63**(15):2201-15.

[99] Johnson RJ, Pitchumani R. Flow control using localized induction heating in a VARTM process. Composites Science and Technology, 2007;**67**(3-4):669-84.

[100] Johnson RJ, Pitchumani R. Simulation of active flow control based on localized preform heating in a VARTM process. Composites Part A: Applied Science and Manufacturing, 2006;**37**(10):1815-30.

[101] Johnson RJ, Pitchumani R. Active flow control in a VARTM process using localized induction heating. Proceedings of the 7th International Conference on Flow Processes in Composite Materials. Delaware, 2004, pp. 247-52.

[102] Matsuzaki R, Kobayashi S, Todoroki A, Mizutani Y. Flow control by progressive forecasting using numerical simulation during vacuum-assisted resin transfer molding. Composites Part A: Applied Science and Manufacturing, 2013;**45**:79-87.

[103] Alms JB, Glancey JL, Advani SG. Mechanical properties of composite structures fabricated with the vacuum induced preform relaxation process. Composite Structures, 2010;**92**(12):2811-6.

[104] Alms JB, Advani SG, Glancey JL. Liquid composite molding control methodologies using vacuum induced preform relaxation. Composites Part A: Applied Science and Manufacturing, 2011;**42**(1):57-65.

[105] Bender D, Schuster J, Heider D. Flow rate control during vacuum-assisted resin transfer molding (VARTM) processing. Composites Science and Technology, 2006;**66**(13):2265-71.

[106] Kedari VR, Farah BI, Hsiao K-T. Effects of vacuum pressure, inlet pressure, and mold temperature on the void content, volume fraction of polyester/e-glass fiber composites manufactured with VARTM process. Journal of Composite Materials, 2011;**45**(26):2727-42.

[107] Davies P, Petton D. An experimental study of scale effects in marine composites. Composites Part A: Applied Science and Manufacturing, 1999;**30**(3):267-75.

[108] Kolat K, Neşer G, Özes Ç. The effect of sea water exposure on the interfacial fracture of some sandwich systems in marine use. Composite Structures, 2007;**78**(1):11-7.

[109] Sutherland LS, Soares CG. Impact behaviour of typical marine composite laminates. Composites Part B: Engineering, 2006;**37**(2):89-100.

[110] Beardmore P, Johnson CF. The potential for composites in structural automotive applications. Composites Science and Technology, 1986;**26**(4):251-81.

[111] Zhang J, Chaisombat K, He S, Wang CH. Hybrid composite laminates reinforced

with glass/carbon woven fabrics for lightweight load bearing structures. Materials and Design, 2012;**36**:75-80.

[112] Atas C, Akgun Y, Dagdelen O, Icten BM, Sarikanat M. An experimental investigation on the low velocity impact response of composite plates repaired by VARIM and hand lay-up processes. Composite Structures, 2011;**93**(3):1178-86.

[113] Found MS, Friend MJ. Evaluation of CFRP panels with scarf repair patches. Composite Structures, 1995;**32**(1-4):115-22.

[114] Hollaway LC. The evolution of and the way forward for advanced polymer composites in the civil infrastructure. Construction and Building Materials, 2003;**17**(6-7):365-78.

[115] Hollaway LC. A review of the present and future utilisation of FRP composites in the civil infrastructure with reference to their important in-service properties. Construction and Building Materials. 2010;**24**(12):2419-45.

[116] White DM, Daniell WE, Maxwell JK, Townes BD. Psychosis following styrene exposure: a case report of neuropsychological sequelae. Journal of Clinical and Experimental Neuropsychology, 1990;**12**(5):798-806.

[117] Castillo L, Baldwin M, Sassine MP, Mergler D. Cumulative exposure to styrene and visual functions. American Journal of Industrial Medicine, 2001;**39**(4):351-60.

[118] Jeong H. Effect of void on the mechanical strength and ultrasonic attenuation of laminated composites. Journal of Composite Materials, 1997;**31**(3):276-92.

[119] Bowles KJ, Frimpong S. Void effects on the interlaminar shear strength of unidirectional graphite-fiber-reinforced composites. Journal of Composite

Materials, 1992;**26**(10):1487-509.

[120] Graham-Jones J, Summerscales J. Marine applications of advanced fibre-reinforced composites. Cambridge: Woodhead, 2015.

[121] Robson JE, Matthews FL, Kinloch AJ. The strength of composite repair patches: a laminate analysis approach. Journal of Reinforced Plastics and Composites, 1992;**11**(7):729-42.

[122] Strong AB. Fundamentals of composites manufacturing: materials, methods, and applications. 2nd ed. Dearborn: Society of Manufacturing Engineers, 2008.

[123] Stringer LG. Optimization of the wet lay-up/vacuum bag process for the fabrication of carbon fibre epoxy composites with high fibre fraction and low void content. Composites, 1989;**20**(5):441-52.

[124] Wang Y, Li J. Properties of composites reinforced with E-glass nonwoven fabrics. Journal of Advanced Materials, 1995;**26**(3):28-34.

[125] Wang Y. Effect of consolidation method on the mechanical properties of nonwoven fabric reinforced composites. Applied Composite Materials, 1999;**6**(1):19-34.

[126] Grunenfelder LK, Nutt SR. Void formation in composite prepregs - Effect of dissolved moisture. Composites Science and Technology, 2010;**70**(16):2304-9.

[127] Campbell FC. Manufacturing technology for aerospace structural materials. London: Elsevier, 2006.

[128] Ziegenbein JM, Colton JS. Magnetic-clamping structures for the consolidation of composite laminates. Polymer Composites, 2012;**33**(6):951-60.

[129] Pallapa M, Yeow JTW. A review of the hybrid techniques for the fabrication of

hard magnetic microactuators based on bonded magnetic powders. Smart Materials and Structures, 2014;**24**(2):025007.

[130] Phani KK, Bose NR. Temperature dependence of hydrothermal ageing of CSM-laminate during water immersion. Composites Science and Technology, 1987;**29**(2):79-87.

[131] Little JE, Yuan X, Jones MI. Characterisation of voids in fibre reinforced composite materials. NDT and E International, 2012;**46**:122-7.

[132] Ferry JD. Viscoelastic properties of polymers. New York: John Wiley & Sons, 1980.

[133] Anderson JP, Altan MC. Properties of composite cylinders fabricated by bladder assisted composite manufacturing. Journal of Engineering Materials and Technology, 2012;**134**(4):044501.

[134] Merle G, Allemand J, Camino G, Luda MP, Revellino M, Blancon R. Morphology analysis of microvoids in SMC: ageing effects. Composites Part A: Applied Science and Manufacturing, 1998;**29**(12):1535-43.

[135] Hamidi YK, Dharmavaram S, Aktas L, Altan MC. Effect of fiber content on void morphology in resin transfer molded e-glass/epoxy composites. Journal of Engineering Materials and Technology, 2009;**131**(2):021014_1-_11.

[136] Zhu HY, Li DH, Zhang DX, Wu BC, Chen YY. Influence of voids on interlaminar shear strength of carbon/epoxy fabric lamiantes. Transactions of Nonferrous Metals Society of China, 2009;**19**:470-5.

[137] Liebig WV, Viets C, Schulte K, Fiedler B. Influence of voids on the compressive failure behaviour of fibre-reinforced composites. Composites Science and

Technology, 2015;**117**:225-33.

[138] Hagstrand P-O, Bonjour F, Månson J-A. The influence of void content on the structural flexural performance of unidirectional glass fibre reinforced polypropylene composites. Composites Part A: Applied Science and Manufacturing, 2005;**36**(5):705-14.

[139] Chang X, Ren M, Li T, Guo X. Evaluation of mechanical behaviour of unidirectional fibre-reinforced composites considering the void morphology. Journal of Reinforced Plastics and Composites. 2017;**36**(24):1817-28.

[140] Wisnom MR, Reynolds T, Gwilliam N. Reduction in interlaminar shear strength by discrete and distributed voids. Composites Science and Technology, 1996;**56**(1):93-101.

[141] Meraghni F, Desrumaux F, Benzeggagh ML. Implementation of a constitutive micromechanical model for damage analysis in glass mat reinforced composites structures. Composites Science and Technology, 2002;**62**(16):2087-97.

[142] Chen Y-T, Macosko CW, Davis HT. Wetting of fiber mats for composites manufacturing: II. Air entrapment model. AIChE Journal, 1995;**41**(10):2274-81.

[143] Chambers AR, Earl JS, Squires CA, Suhot MA. The effect of voids on the flexural fatigue performance of unidirectional carbon fibre composites developed for wind turbine applications. International Journal of Fatigue, 2006;**28**(10):1389-98.

[144] Bayldon JM, Daniel IM. Flow modeling of the VARTM process including progressive saturation effects. Composites Part A: Applied Science and Manufacturing, 2009;**40**(8):1044-52.

[145] Parnas RS, Howard JG, Luce TL, Advani SG. Permeability characterization. Part 1: A proposed standard reference fabric for permeability. Polymer Composites, 1995;**16**(6):429-45.

[146] Zhou F, Kuentzer N, Simacek P, Advani SG, Walsh S. Analytic characterization of the permeability of dual-scale fibrous porous media. Composites Science and Technology, 2006;**66**(15):2795-803.

[147] Gebart BR. Permeability of unidirectional reinforcements for RTM. Journal of Composite Materials, 1992;**26**(8):1100-33.

[148] Nabovati A, Llewellin EW, Sousa ACM. Through-thickness permeability prediction of three-dimensional multifilament woven fabrics. Composites Part A: Applied Science and Manufacturing, 2010;**41**(4):453-63.

[149] Binetruy C, Hilaire B, Pabiot J. Tow impregnation model and void formation mechanisms during RTM. Journal of Composite Materials, 1998;**32**(3):223-45.

[150] Jinlian H, Yi L, Xueming S. Study on void formation in multi-layer woven fabrics. Composites Part A: Applied Science and Manufacturing, 2004;**35**(5):595-603.

[151] Bickerton S, Advani SG. Characterization and modeling of race-tracking in liquid composite molding processes. Composites Science and Technology, 1999;**59**(15):2215-29.

[152] Kang MK, Lee WI, Hahn HT. Formation of microvoids during resin-transfer molding process. Composites Science and Technology, 2000;**60**(12-13):2427-34.

[153] Judd NCW, Wright WW. Voids and their effects on the mechanical properties of composites-an appraisal. SAMPE Journal, 1978;**14**:10-4.

[154] Olivier P, Cottu JP, Ferret B. Effects of cure cycle pressure and voids on some mechanical properties of carbon/epoxy laminates. Composites, 1995;**26**(7):509-15.

[155] Huang H, Talreja R. Effects of void geometry on elastic properties of unidirectional fiber reinforced composites. Composites Science and Technology, 2005;**65**(13):1964-81.

[156] Gupta N, Sundaram R. Fiber optic sensors for monitoring flow in vacuum enhanced resin infusion technology (VERITy) process. Composites Part A: Applied Science and Manufacturing, 2009;**40**(8):1065-70.

[157] Verma KK, Dinesh BL, Singh K, Gaddikeri K, Sundaram R. Challenges in processing of a cocured wing test box using vacuum enhanced resin infusion technology (VERITy). Procedia Materials Science, 2014;**6**:331-40.

[158] Walczyk D, Kuppers J, Hoffman C. Curing and consolidation of advanced thermoset composite laminate parts by pressing between a heated mold and customized rubber-faced mold. Journal of Manufacturing Science and Engineering, 2011;**133**(1):011002.

[159] Walczyk D, Kuppers J. Thermal press curing of advanced thermoset composite laminate parts. Composites Part A: Applied Science and Manufacturing, 2012;**43**(4):635-46.

[160] Amirkhosravi M, Pishvar M, Altan MC. Improving laminate quality in wet lay-up/vacuum bag processes by magnet assisted composite manufacturing (MACM). Composites Part A: Applied Science and Manufacturing, 2017;**98**:227-37.

[161] Sussmann M, Amirkhosravi M, Pishvar M, Altan MC. Fabrication of high quality, large wet lay-up/vacuum bag laminates by sliding a magnetic tool. Polymers, 2018;**10**(9):992.

[162] Pishvar M, Amirkhosravi M, Altan MC. Magnet assisted composite manufacturing: A flexible new technique for achieving high consolidation pressure in vacuum bag/lay-up processes. JoVE (Journal of Visualized Experiments), 2018(135):e57254.

[163] Rodriguez E, Giacomelli F, Vazquez A. Permeability-porosity relationship in RTM for different fiberglass and natural reinforcements. Journal of Composite Materials, 2004;**38**(3):259-68.

[164] Pishvar M, Amirkhosravi M, Altan MC. Magnet assisted composite manufacturing: A novel fabrication technique for high-quality composite laminates. Polymer Composites, 2019;**40**(1):159-69.

[165] Pavlidou S, Papaspyrides CD. The effect of hygrothermal history on water sorption and interlaminar shear strength of glass/polyester composites with different interfacial strength. Composites Part A: Applied Science and Manufacturing, 2003;**34**(11):1117-24.

[166] Keller T, Tirelli T, Zhou A. Tensile fatigue performance of pultruded glass fiber reinforced polymer profiles. Composite Structures, 2005;**68**(2):235-45.

[167] Hamidi YK, Aktas L, Altan MC. Three-dimensional features of void morphology in resin transfer molded composites. Composites Science and Technology, 2005;**65**(7-8):1306-20.

[168] Olivero KA, Barraza HJ, O'Rear EA, Altan MC. Effect of injection rate and

post-fill cure pressure on properties of resin transfer molded disks. Journal of Composite Materials, 2002;**36**(16):2011-28.

[169] Bodaghi M, Cristóvão C, Gomes R, Correia NC. Experimental characterization of voids in high fibre volume fraction composites processed by high injection pressure RTM. Composites Part A: Applied Science and Manufacturing, 2016;**82**:88-99.

[170] Hamidi YK, Aktas L, Altan MC. Effect of packing on void morphology in resin transfer molded E-glass/epoxy composites. Polymer Composites, 2005;**26**(5):614-27.

[171] Guo Z-S, Liu L, Zhang B-M, Du S. Critical void content for thermoset composite laminates. Journal of Composite Materials, 2009;**43**(17):1775-90.

[172] Gutowski TG, Cai Z, Bauer S, Boucher D, Kingery J, Wineman S. Consolidation experiments for laminate composites. Journal of Composite Materials, 1987;**21**(7):650-69.

[173] Bickerton S, Abdullah MZ. Modeling and evaluation of the filling stage of injection/compression moulding. Composites Science and Technology, 2003;**63**(10):1359-75.

[174] Bickerton S, Buntain MJ. Modeling forces generated within rigid liquid composite molding tools. Part B: Numerical analysis. Composites Part A: Applied Science and Manufacturing, 2007;**38**(7):1742-54.

[175] Gu Y, Li M, Zhang Z, Sun Z. Numerical simulation and experimental study on consolidation of toughened epoxy resin composite laminates. Journal of Composite Materials, 2006;**40**(24):2257-77.

[176] Patel N, Rohatgi V, Lee LJ. Influence of processing and material variables on resin-fiber interface in liquid composite molding. Polymer Composites, 1993;**14**(2):161-72.

[177] Chen Z-R, Ye L. A micromechanical compaction model for woven fabric preforms. Part II: Multilayer. Composites Science and Technology, 2006;**66**(16):3263-72.

[178] Blackmore B, Li D, Gao J. Detachment of bubbles in slit microchannels by shearing flow. Journal of Colloid and Interface Science, 2001;**241**(2):514-20.

[179] Kardos JL, Dudukovic MP, Dave R. Void growth and resin transport during processing of thermosetting-matrix composites-epoxy resins and composites. In: Dušek K. (eds) Epoxy Resins and Composites IV. Advances in Polymer Science, Berlin: Springer, 1986, pp. 101-123.

[180] Pillai KM. Modeling the Unsaturated Flow in Liquid Composite Molding Processes: A Review and Some Thoughts. Journal of Composite Materials, 2004;**38**(23):2097-118.

[181] Patel N, Lee LJ. Effects of fiber mat architecture on void formation and removal in liquid composite molding. Polymer Composites, 1995;**16**(5):386-99.

[182] Liu X, Chen F. A review of void formation and its effects on the mechanical performance of carbon fiber reinforced plastic. Engineering Transactions, 2016;**64**(1):33-51.

[183] Chen D, Arakawa K, Xu C. Reduction of void content of vacuum-assisted resin transfer molded composites by infusion pressure control. Polymer Composites, 2015;**36**(9):1629-37.

[184] Suarez JC, Molleda F, Güemes A. Void content in carbon fibre/epoxy resin composites and its effects on compressive properties. Proceedings of ICCM-9 Composites: Properties and Applications, Madrid, Spain, 1993, pp. 589-96.

[185] De Almeida SFM, Neto ZdSN. Effect of void content on the strength of composite laminates. Composite Structures, 1994;**28**(2):139-48.

[186] Costa ML, De Almeida SFM, Rezende MC. The influence of porosity on the interlaminar shear strength of carbon/epoxy and carbon/bismaleimide fabric laminates. Composites Science and Technology, 2001;**61**(14):2101-08.

[187] De Almeida SFM, Santacreu ACM. Environmental effects in composite laminates with voids. Polymers and Polymer Composites, 1995;**3**(3):193-204.

[188] Costa ML, Rezende MC, De Almeida SFM. Effect of void content on the moisture absorption in polymeric composites. Polymer-Plastics Technology and Engineering, 2006;**45**(6):691-98.

[189] Aktas L, Hamidi YK, Altan MC. Effect of Moisture on the Mechanical Properties of Resin Transfer Molded Composites-Part I: Absorption. Journal of Materials Processing and Manufacturing Science, 2002;**10**:239-54.

[190] Amirkhosravi M, Pishvar M, Altan MC. Fabricating high-quality VARTM laminates by magnetic consolidation: experiments and process model. Composites Part A: Applied Science and Manufacturing, 2018;**114**:398-406.

[191] Hapke J, Gehrig F, Huber N, Schulte K, Lilleodden ET. Compressive failure of UD-CFRP containing void defects: in situ SEM microanalysis. Composites Science and Technology, 2011;**71**(9):1242-49.

[192] Zhu H, Wu B, Li D, Zhang D, Chen Y. Influence of voids on the tensile

performance of carbon/epoxy fabric laminates. Journal of Materials Science and Technology, 2011;**27**(1):69-73.

[193] Shih C-H, Lee LJ. Analysis of void removal in liquid composite molding using microflow models. Polymer Composites, 2002;**23**(1):120-31.

[194] Lundström TS. Bubble transport through constricted capillary tubes with application to resin transfer molding. Polymer Composites, 1996;**17**(6):770-79.

[195] Yang J, Xiao J, Zeng J, Jiang D, Peng C. Compaction behavior and part thickness variation in vacuum infusion molding process. Applied Composite Materials, 2012;**19**(3-4):443-58.

[196] Niggemann C, Song YS, Gillespie Jr. JW, Heider D. Experimental investigation of the controlled atmospheric pressure resin infusion (CAPRI) process. Journal of Composite Materials, 2008;**42**(11):1049-61.

[197] Goodwin AA, Howe CA, Paton RJ. The role of voids in reducing the interlaminar shear strength in RTM laminates. Proceedings of ICCM-11 Composites: Composite Processing and Microstructure, Gold Coast, Australia, 1997.

[198] Ricotta M, Quaresimin M, Talreja R. Mode I strain energy release rate in composite laminates in the presence of voids. Composites Science and Technology, 2008;**68**(13):2616-23.

[199] Scott AE, Sinclair I, Spearing SM, Mavrogordato MN, Hepples W. Influence of voids on damage mechanisms in carbon/epoxy composites determined via high resolution computed tomography. Composites Science and Technology, 2014;**90**:147-53.

[200] Zhang AY, Li DH, Zhang DX, Lu HB, Xiao HY, Jia J. Qualitative separation of the effect of voids on the static mechanical properties of hygrothermally conditioned carbon/epoxy composites. Express Polymer Letters, 2011;**5**(8):708-16.

[201] Zhang AY, Li DH, Lu HB, Zhang DX. Qualitative separation of the effect of voids on the bending fatigue performance of hygrothermal conditioned carbon/epoxy composites. Materials and Design, 2011;**32**(10):4803-09.